LECTURE NOTES

IN

PHYSICAL OCEANOGRAPHY

ODD HENRIK SÆLEN
EYVIND AAS

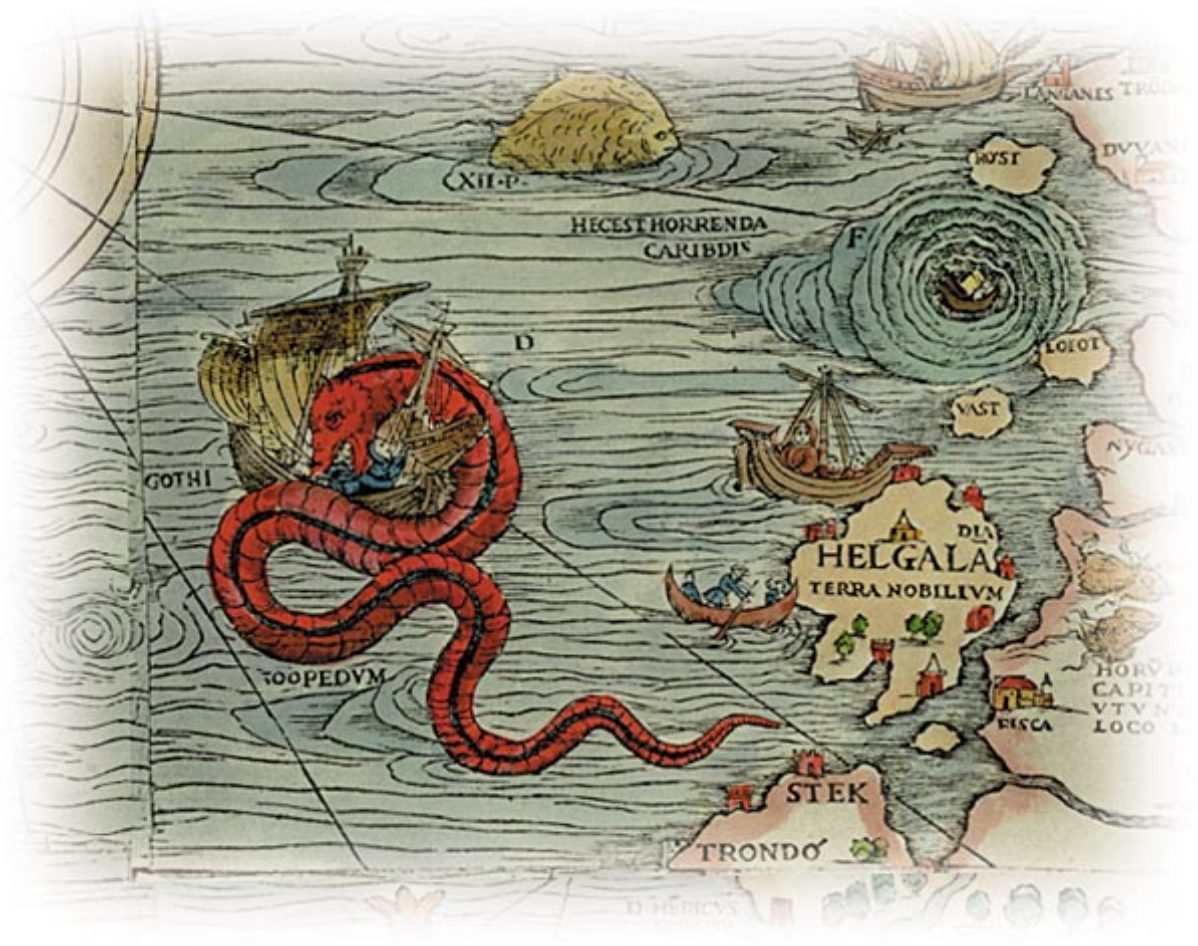

1976

2012

CONTENTS

FOREWORD

INTRODUCTION

1 EXTENT OF THE OCEANS AND THEIR DIVISIONS

1.1 Distribution of Water and Land.....1

1.2 Depth Measurements.....3

1.3 General Features of the Ocean Floor.....5

2 CHEMICAL PROPERTIES OF SEAWATER

2.1 Chemical Composition.....1

2.2 Gases in Seawater.....4

3 PHYSICAL PROPERTIES OF SEAWATER

3.1 Density and Freezing Point.....1

3.2 Temperature.....3

3.3 Compressibility.....5

3.4 Specific and Latent Heats.....5

3.5 Light in the Sea.....6

3.6 Sound in the Sea.....11

4 INFLUENCE OF ATMOSPHERE ON THE SEA

4.1 Major Wind and Pressure Systems.....1

4.2 Heat Budget.....2

4.3 Volume Budget.....6

4.4 Salt Budget.....6

5 GLOBAL DISTRIBUTION OF *T*, *S* AND ρ

5.1 Temperature Distribution.....1

5.2 Salinity Distribution.....4

5.3 Density Distribution.....4

6 EQUATIONS AND MODELS FOR MOTION IN THE SEA

6.1 Transformation of Newton's Second Law.....1

6.2 Hydrostatic Equilibrium.....4

6.3 Geostrophic Currents.....6

6.3 Wind Currents.....7

7 CIRCULATION OF THE OCEANS

7.1 Oceanic Gyres (***Atlantic Ocean, Pacific Ocean, Indian Ocean)***.....1

7.2 Surface Currents in Other Areas (*Southern Ocean, Mediterranean Sea, Norwegian Sea, Baltic Sea, Norwegian Coastal Current, North Sea, Barents Sea, Arctic Sea)*.....8

7.3 Upwelling.....22

7.4 Vertical Circulation.....24

8 WAVES

8.1 Generation of Waves.....1

8.2 Wave Theory.....2

8.3 Wave Observations.....6

8.4 Internal Waves.....6

9 TIDES

9.1 Tidal Force.....1

9.2 Equilibrium Theory.....2

9.3 Presentation of Observed Tides.....6

9.4 Tidal Types.....8

9.5 Tidal Currents.....9

10 FJORDS AND ESTUARIES

10.1 Characteristics of Estuaries and Fjords.....1

10.2 Seasonal Changes.....1

10.3 Estuarine Circulation.....2

10.4 Deeper Layers in the Fjord.....5

11 ICE IN THE SEA

References

FOREWORD

These notes were originally written in 1976 for the course "Gf 0 - Basic Course in Geophysics". The course offered an introduction to the different fields covered by the Department of Geophysics: physics of the solid earth, meteorology, hydrology, and physical oceanography. The notes in oceanography were written by professor Odd Henrik Sælen and scientific assistant Eyvind Aas. Through the years the course changed name to Gf 100 and Gf 001, and at some point a single textbook was chosen to cover all the fields. Finally, in 1995, the course was closed down.

In later years the notes have been found to provide a brief and useful introduction to the more descriptive parts of physical oceanography, which is why they have come to new use in GEF2610. During the 30 years that have passed, only the methods of measurement have changed significantly, and accordingly most of the text remains in its original form. The translation to English was made in 2007 with support from the Faculty of Mathematics and Natural Sciences.

E. Aas

INTRODUCTION

When we use the term *oceanography*, it should be noted that it is a term that can mean different things. Many people like to use *oceanography* as a collective term for all marine sciences, for example: marine biology, marine chemistry, marine geology and physical oceanography. This last branch mentioned is to be the topic of these lectures. The subject *physical oceanography* includes many sciences, and is supported by basics sciences such as mathematics, mechanics, physics and to a certain extent also chemistry. It collects everything that has to do with the physical condition, movements, etc. in the ocean. *Descriptive physical oceanography*, which is often called *hydrography*, describes the condition, for example: the distribution of temperature, salt content, currents, etc. Physcial qualities such as sound propagation, light conditions, and compressibility are investigated. Dynamical oceanography is concerned with motions, both on a practical and theoretical level. Tidal research is its own branch of physical oceanography. We will give a short overview of this in these lectures.

1 EXTENT OF THE OCEANS AND THEIR DIVISIONS

1.1 Distribution of Water and Land

Water covers 70.8% of the surface of the earth. The earth's surface is 510 million km^2, and of this 361 million km^2 is water. There is comparatively more water in the southern hemisphere than there is in the northern. Figure 1.1 shows the distribution of land and sea at various latitudes. Only around the Antarctic continent is there an uninterrupted ring of water, and all the way up in the north we also have a water cap in the Arctic Ocean. Otherwise the oceans are divided by the continents.

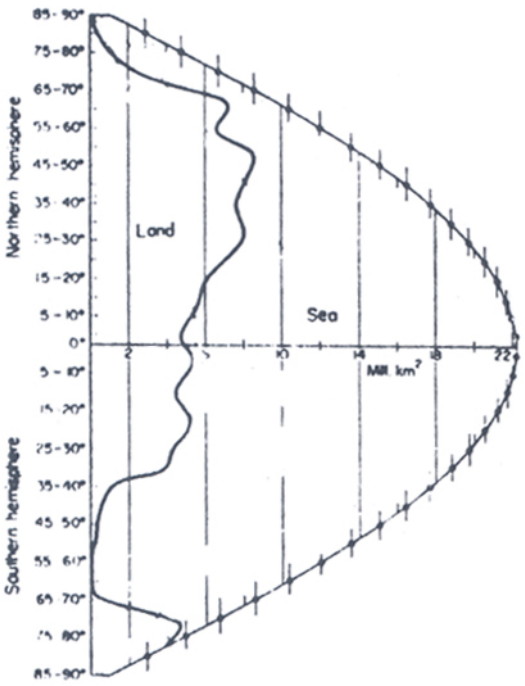

Distribution of water and land between parallels of latitude.

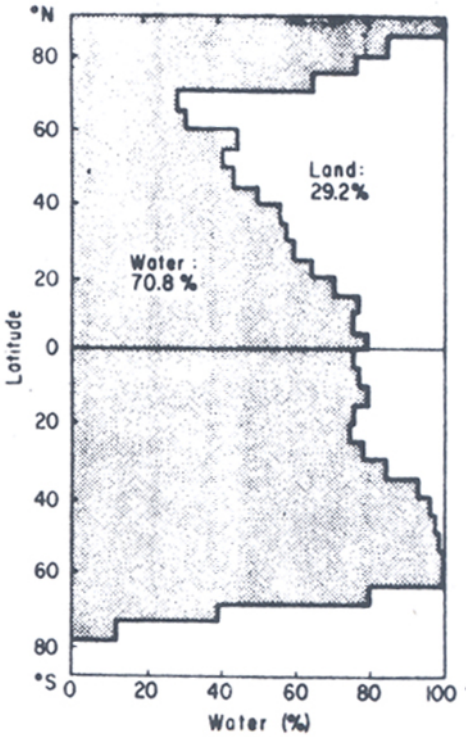

Percentage distribution of water and land areas in five degree zones.

Fig.1.1

In this way the world's oceans have been divided into three major *oceans*. The Pacific Ocean, with its 165 million km^2, is larger than the other two together (the Atlantic Ocean and the Indian Ocean). Earlier the Antarctic Ocean was considered an independent ocean; now it is most common to divide it among the three major oceans. In addition to the three world oceans, there are several types of smaller seas. A sea is considered a *mediterranean sea* if it is for the most part enclosed by land, with one or more narrow openings to the oceans. An

intercontinental sea lies between continents, while an *intracontinental sea* lies within a single continent. In addition there also *adjacent seas*, which lie relatively open to the oceans. (For examples see Table 1.1)

Table 1.1

		Area of the sea surface in 10^6 km^2	**Sum**
Oceans, without mediterranean and adjacent seas	Atlantic	82.2	
	Indian	73.4	
	Pacific	165.3	320.9
Intercontinental mediterranean seas	Arctic	14.3	
	European	3.0	
	Australasian	8.1	25.2
Intracontinental mediterranean seas	American	4.3	
	Baltic Sea	0.4	
	Hudson Bay	1.2	
	Red Sea	0.5	
	Persian Gulf	0.2	6.6
Adjacent seas	North Sea	0.6	
	Gulf of St. Lawrence	0.2	
	Bering Sea	2.3	
	Others	5.0	8.1
	All seas	360.0	360.9
	Earth's surface	510.1	

Area of all seas in percent of earth's surface is 70.8 %, where depths between 0 and 200 m constitute 5.5 %, and depths above 3000 m 54.6 %

Mean depth of all seas is 3790 m
Mean depth is 0.0006 times earth's radius
Greatest depth is 0.002 times earth's radius

Volume of all seas is $1370 \cdot 10^6$ km^3.

1.2 Depth Measurements

The most obvious method of measuring depth, which has been used throughout history, is to lower a weight down at the end of a rope. This works fine as long as the sea is not too deep. However, when the depth is great, this method will lead to numerous practical difficulties. It is difficult to notice when the weight hits the bottom, and the current can also cause the hemp rope (which was used for a long time) to move away from the desired vertical line. A classic example is the so called "Swedish depth" of 4850 meter between Spitsbergen and Greenland, which was measured in 1868 with ropes; this depth was assumed most likely not to exist, until it was confirmed in the 1970ties by more modern methods.

Later people began to use piano string with an automatic stop when the weight reached the bottom (*e.g*. the Lucas sounding machine). This was more precise and worked faster. Still, with this mechanical method the number of possible soundings was much too few in relation to the great size of the world's oceans.

It was therefore a radical improvement, both in quality and quantity, when the *echo-sounder* was introduced after the First World War. The idea was old (Aragon 1807) but the technical necessities were first in place 100 years later. The principle of the echo-sounder is very simple. An acoustic signal from the surface is sent into the water. This reflects off the bottom and is received again at the surface (Fig. 1.2) after t seconds. If the depth is D meter, then the signal has gone $2D$ meters in t seconds and we have the formula

$$2D = \bar{v}t\,, \tag{1.1}$$

where $\bar{v}$ is the average speed of sound between the surface and the bottom. The time difference t is small, but with modern technology it can be measured very accurately. The speed of sound in saltwater is now very well known. It varies with temperature, salinity and pressure. Because the salinity in the open sea does not vary much, variations in v are most often due to variations in temperature and depth (pressure).

Numerical example: If $\bar{v}$ = 1500 m s^{-1}, and the depth D is 1500 m, then t = 2 s. Since $2\mathrm{d}D/\mathrm{d}t$ = 1500 m s^{-1}, we see that $\mathrm{d}D$ = 1 meter corresponds to a time difference $\mathrm{d}t$ of 1/750 seconds, which can be recorded. When measuring depth, one must take into consideration variations in the speed of sound. There are tables and computer programs that can be used for this in connection to the different ocean and sea areas.

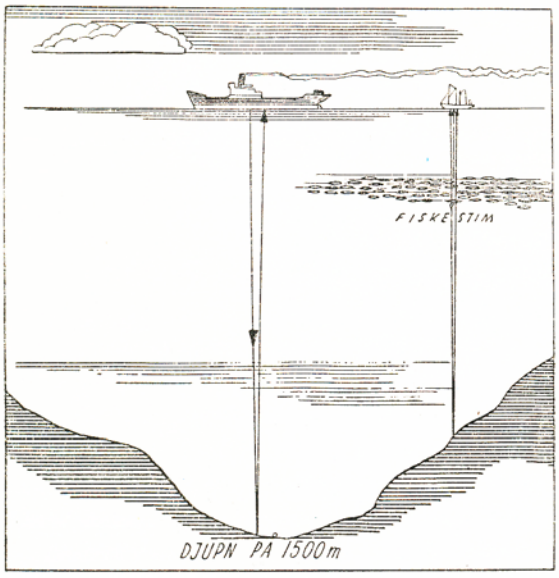

Fig. 1.2 With the echo-sounder we may find the depth to the bottom, or the depth of a shoal

The echo-sounder consists of a sending, a receiving and a recording instrument. In the sender, electric oscillations are converted to mechanical oscillations which are producing sound waves. Certain ferromagnetic materials change dimensions in a varying magnetic field. The effect is reversible, so the same instrument may be used as both the sender and the receiver. The echo goes through an amplifier to a printer which draws a profile showing the bottom depth. We are not going to go into detail as to how this works, or the corrections one must apply. An echogram is shown in Fig. 1.3. The echo-sounder does not only receive echoes from the ocean floor, it will also receive echoes from objects in the water. This has made the echo-sounder very useful to the fisheries. More and more refined uses are being found for this method. With a modern echo-sounder, one can see each and every fish. Sound in seawater will be discussed in more detail in Chapter 3.1c.

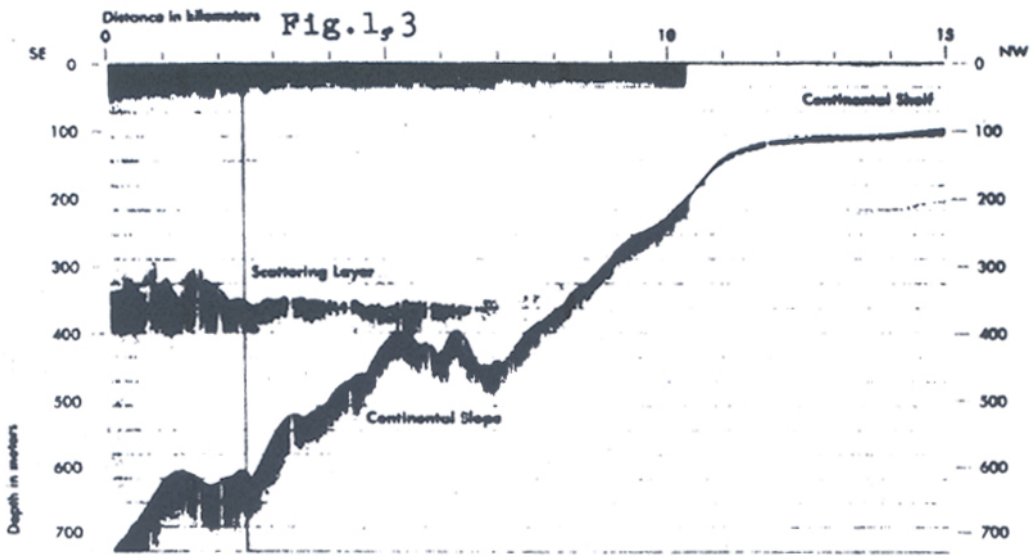

Fig.1.3

Precision echo sounding across the continental margin off Virginia.

1.3 General Features of the Ocean Floor

The principal features of the ocean floor are shown in Fig. 1.4. The *shelf* or *continental shelf* can be considered an extension of the earth's surface. It occupies approximately 7% of the ocean floor. The width varies greatly, from almost nothing to over 1000 km (outside of Siberia). It is difficult to define an

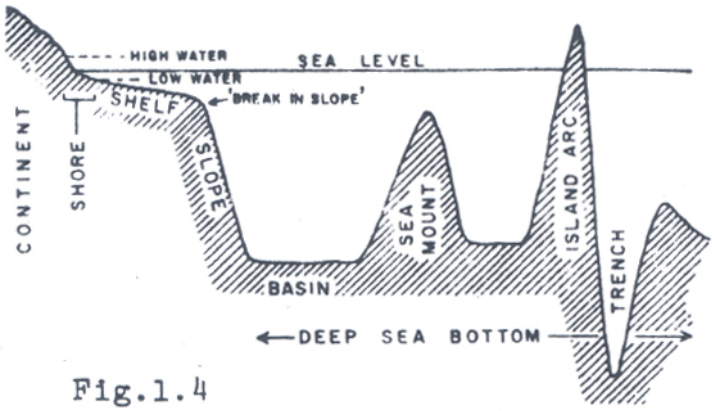

Fig.1.4

Section through ocean floor to show principal features schematically.

exact depth for the end of the shelf; one has to look for where the slope becomes steeper in such a way that the ocean floor becomes the *continental slope*. Approximately 200 m can be used as an average value for the shelf depth.

The under-water valleys (canyons) are a much debated characteristic, as they cut

through the shelf in many places across the coast. Some of them appear to be a continuation of rivers on land (for example, the Hudson, Kongo, Ganges) and others do not. Sediment is often transported through these canyons out to greater depths. From the continental slope, one goes over to the *deep-sea basin*.

The deep sea is divided between larger and smaller basins with more or less defined under-water ridges. These basins have a relatively flat floor, and can be as deep as 6000 meters. One also finds *island arcs* and individual under-water mountains, – *seamounts*. A particularly striking characteristic are the *deep-sea trenches*. They look like long drawn out fissures on the ocean floor, and they are most often found outside of and parallel to the island arcs. They are especially numerous on the west side of the Pacific Ocean but are also found in the Pacific outside of South America as well as a few in the Atlantic and Indian Oceans. In these trenches we have the greatest ocean depths. In the Pacific Ocean, there is the depth of 11000 meters in the Marianer trench. The deepest trench in the Atlantic Ocean is found in a trench outside of Puerto Rico with a depth of 9200 meters.

If we make a frequency distribution of height levels for the earth's surface we end up with a figure such as Fig. 1.5 Here we see two typical levels, one between +1000 and -1000 m and one between -4000 and -6000 meters. One third of the ocean's floor lies between 4000 and 5000 m depth.

If we integrate the curve in Fig. 1.5, we obtain the *hypsographic curve*, Fig. 1.6. Here the abscissa indicates how many km^2 of the earth's surface which lie at a higher level than

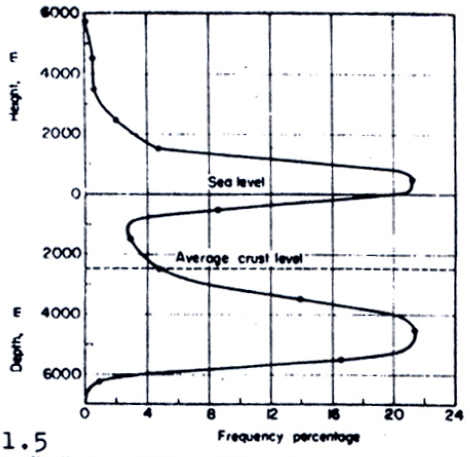

Fig.1.5
Frequency distribution of different height and depth intervals over the entire surface of the Earth.

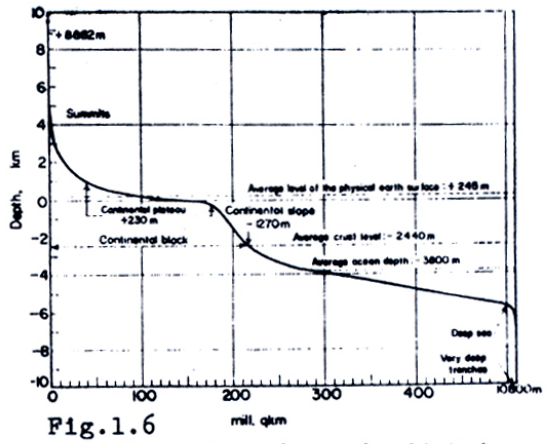

Fig.1.6
Hypsographic curve for the surface of the Earth.

indicated by the ordinate. The curve can roughly be seen as a description of the average depths of the earth's surface. We can clearly see a division between two "step levels."

The average depth of all seas is calculated to be 3790 m, and the volume of all the water in the seas is then 1370 million km^3, that is 13 times the volume of land over sea level. But the vertical extent of the seas is still quite small in comparison to the horizontal dimensions.

An important characteristic in the ocean floor's topography is the main system of sub-sea mountain ridges (Fig. 1.7). This is a continuous system of ridges which rise 2- 4000 meters over the ocean floor in the basins. They play an

The major oceanic ridge systems. Because in the Atlantic Ocean the ridge system is almost exactly in the middle of the ocean the system is also called the "Mid-Oceanic" ridge system. The transverse faults are probably the result of differential movement of the ridge areas on either side of the faults due to ocean-floor spreading
(After Heezen, 1963, in The Sea, *ed. by Hill.)*

Fig.1.7

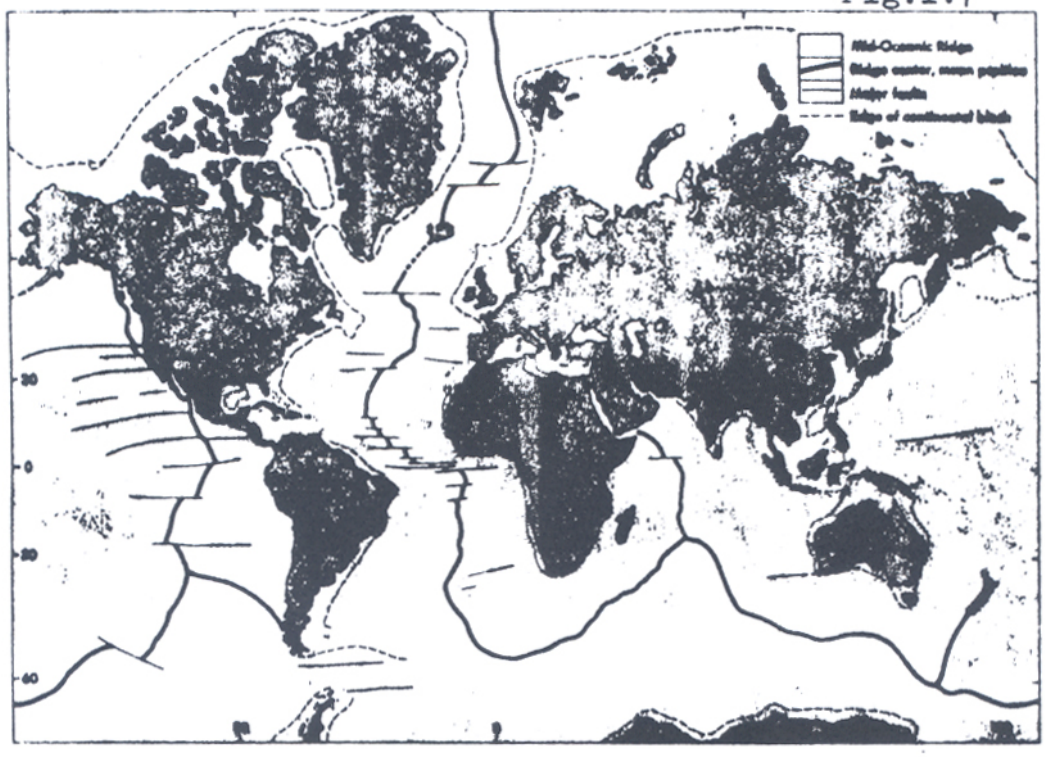

important role in modern theories of how the ocean became as it is today. For a long time it was believed that the oceans were a very old characteristic of the earth's crust. Wegener (1922) was the first to cast doubt on this belief with his *continental drift theory*. In the last 10 – 20 years a great deal of facts concerning the ocean floor have been joined together and created a logical wholeness for the *plate tectonics theory*. The earth's crust is seen as being divided into a number of "plates" which move relative to one another. A ridge is a border between two plates which are moving away from each other. Here the lava rises up, hardens after some time and creates a new ocean floor which pushes the old ocean floor to the side.

Look, for example, at the Atlantic Ocean in Fig. 1.8. Only 100 -200 million years ago, America and Europe-Asia were side by side. Then they began to sail away from each other,

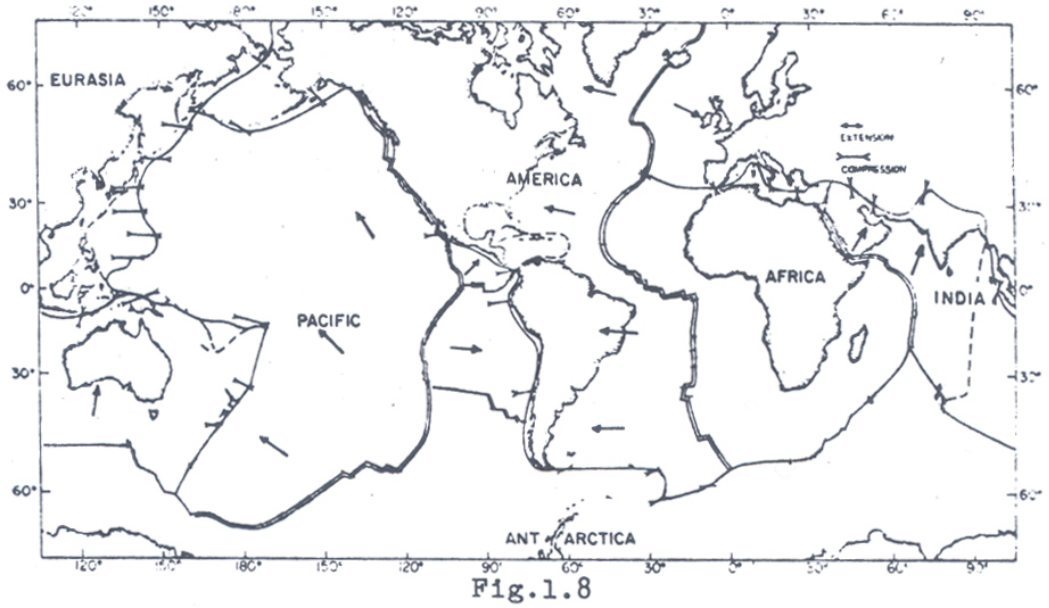

Fig.1.8

each on their side of the fracture zone, which with time became the *Mid-Atlantic Ridge*. This indicates an average speed for the two plates of a few cm per year. The earlier mentioned deep-sea trenches are also connected to this plate movement. This is where two plates hit against one another, the one goes under the other and melts when it has gone deep enough (Fig. 1.9). During this process the deep sea trenches come into existence as long, narrow ditches in the earth's crust. This process has been especially active on the west side of the Pacific Ocean. Because of this, the Pacific is getting smaller while the Atlantic Ocean is becoming larger. (3-5 cm per year).

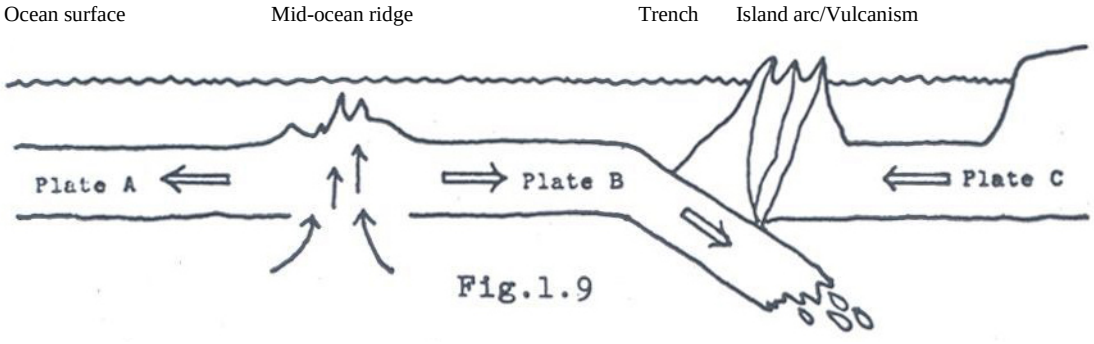

Fig.1.9

2 CHEMICAL PROPERTIES OF SEAWATER

2.1 Chemical Composition

On average 1 kg of seawater consists of 96.5 % water and 3.5 % dissolved material. Most likely all known materials can be found dissolved in seawater, some of them in such small concentrations that they still have not been determined with certainty. The great ability of water to dissolve other materials, as well as its other "unusual" characteristics, is due to the fact that the water molecule is built asymmetrically; the two hydrogen atoms do not lie symmetrically on each side of the oxygen atom but instead lie at an angle of 105° (Fig. 2.1).

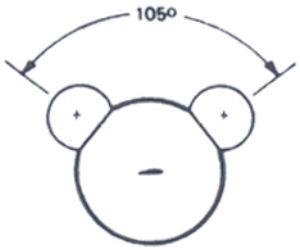

Fig.2.1

As a result the water molecule has the properties of an electric dipole and the water molecules have a strong interactive effect with one another and combine in larger entities. Because of the dipole effect, the dissolved material will dissociate almost completely and appear as seawater a good conductor of electricity. The contents of the most common compounds and elements are found in Table 2.1. The relative amounts of these main constituents are practically the same in all oceans and seas. Only with the most detailed analysis can one find some very small variations. (This conclusion was drawn already by Forchhammer in 1865, based on surface samples collected from all of the world's oceans and seas. The famous "Challenger" expedition concluded 20 years later that the same was true for the deeper layers.) The rest of the constituents appears in such small concentrations that they hardly influence the total salinity (this term is defined below).

Some examples of these materials that are only found in small traces are given in Table 2.1. For many of these materials the rule mentioned above about the relatively constant composition does not apply. One often hears talk about the "salt" in the saltwater. As was explained earlier, seawater contains iones and not salts. Salt only appears after the water has been evaporated away from a seawater sample (Table 2.1). Some of the trace elements are

essential for life in the oceans and seas. This is particularly true of nitrogen and phosphorus combinations which are the main fertilizing ingredient for marine plants. At times these are completely used up by the algae in the surface layer and are replaced by the decomposition of dead organisms and plants and by the supply from deeper layers or from land. Other trace elements are also necessary, for example selenium for the creation of shells. Only a few of the dissolved elements in seawater are produced and sold for economical purposes. Cooking salt is produced through evaporation, otherwise is magnesium the only other material that is extracted from seawater in large amounts.

Table 2.1. Chemical composition of seawater

Principal constituents of 1 kg seawater at salinity 35.00

	cationes	**gram**	**%**		**aniones**	**gram**	**%**
Sodium	Na^{+}	10.75	30.6	Chlorine	Cl^{-}	19.35	55.3
Magnesium	Mg^{++}	1.3	3.7	Sulphate	SO_4^{--}	2.7	7.7
Calcium	Ca^{++}	0.42	1.2	Bicarbonate	NCO_3^{-}	0.14	0.4
Potassium	K^{+}	0.39	1.1	Bromine	Br^{-}	0.066	0.2
Strontium	Sr^{++}	0.01	0.04	Borate	BO_3^{---}	0.027	0.08

Salts obtained after 1 kg of seawater has evaporated

		gram	**%**
Sodium chloride	NaCl	27.213	77.758
Magnesium chloride	MgCl	1.3807	10.878
Magnesium sulphate	$MgSO_4$	1.658	4.737
Calcium sulphate	$CaSO_4$	1.26	3.600
Potassium sulphate	K_2SO_4	0.863	2.465
Calcium carbonate	$CaCO_2$	0.123	0.345
Magnesium bromide	$MgBr_2$	0.0766	0.217
Total		35.000	100.000

Examples of concentrations of other elements in seawater in mg m^{-3} (the numbers can vary strongly)

Fluorine	1400	Copper	5
Silica	1000	Manganese	5
Nitrogen	1000	Zinc	5
Rubidium	200	Selenium	4
Aluminium	120	Uranium	2
Lithium	70	Caesium	2
Phosphorus	60	Silver	0.3
Barium	54	Nickel	0.1
Iron	50	Mercury	0.03
Iodine	50	Gold	0.005
Arsenic	15	Radium	1.0×10^{-10}

Although trace elements appears in very small concentrations, their collected mass in the ocean can be quite large due to the ocean's colossal volume (1370 mill. km^3). For example there is approximately 8 million tons of gold in the oceans. The collected mass of dissolved material in the oceans is about 5×10^{15} tons. If this was dried and spread evenly over the entire earth, it would create a layer of salt 45 meter thick!

Salinity is one of the most basic concepts in oceanography. Its definition is burdened with a few practical difficulties. Apparently it is simple enough: one only needs to isolate, one way or another, all of the dissolved material in 1 kg of seawater, weigh them and define the salinity as the salt content in gram per kilogram of seawater. In this way we obtain a salinity expressed in dimensionless units of per mille. However, in praxis this "ideal" definition is much too difficult and laborious.

Since the beginning of the century scientists therefore used a detour by finding a quantity that was both easy to determine precisely and which was also exact and clearly related to the ideal salt content term. The *chlorinity* was chosen, after thorough studies done primarily by Danish researchers. Their work was based on the earlier mentioned principle of the constant relative composition of seawater. If we are able to determine the amount of one of the elements, then the total salt content should be known as well. The material that is most abundant in saltwater is chlorine, and its amounts can be calculated exactly by titration using the Mohr-Knudsen method. In this way the salinity S could be determined through a very simple formula,

$$S = 1.80655\, Cl \ ,$$

where Cl was the chlorinity in units of per thousand (per mille). This was the established practical determination of salinity until the 1980ies. The error of chlorine titration during routine investigations would seldom be greater than 0.02 per mille in salinity, and with precision determination this error could be brought even lower.

Since the beginning of the 1960ies there was another method that was used more and more, and in 1978 the oceanographic community decided that this new method and definition should replace the older one as the standard definition of salinity. This is a physical method where the seawater's *electrical conductivity* is determined, and from this the salinity is calculated. The accuracy of the conductivity measurements is better than for the chlorine titration.

2.2 Gases in Seawater

In addition to the iones which are found dissolved in saltwater, one also finds dissolved gasses. All of the earth's seawater will one day or another come in contact with the atmosphere. The gasses found in the atmosphere at that time will be able to be absorbed in accordance with the laws for the absorption of gasses in a liquid. Oxygen, nitrogen, argon, etc., and all gasses that do not react chemically with seawater or change their molecular size when they dissolve, will follow these laws which have been presented by Boyle, Dalton, and Henry. At a certain temperature, salt content, and normal air pressure, seawater is able to absorb a certain amount of gas. This amount is called the *solubility*. We know that the atmosphere contains approximately 20% oxygen and 80% nitrogen. The solubility for oxygen is about 8 ml l^{-1} and for nitrogen about 15ml l^{-1}. Because of this there can be a relatively greater amount of oxygen in the water than in the atmosphere. However, the opposite can also be true. For example if we look at a figure where there is a negative oxygen concentration, this means that the O_2 concentration is zero, and instead we have hydrogen sulphide, H_2S.

Oxygen is often the most interesting gas in the sea, and its concentration is determined by chemical as well as by other methods. Its solubility varies with the temperature and salinity, and Table 2.2 shows the variability.

Table 2.2 Solubility of oxygen in seawater in ml l^{-1}

	S	
T	0	35
0 °C	10.3	8.4
20 °C	6.6	5.4

Seawater has two oxygen sources: (1) the atmosphere and (2) plants that produce oxygen during photosynthesis. Both of these sources exist in the top layer of the sea. At greater depths there is too little light. However, oxygen is used everywhere; animals breathe it and it is used in the decomposition of organic material and by bacteria. Oxygen is found at the bottom of the sea at great depths, this is due to the fact that water is always renewed through a slow circulation. In some areas the oxygen-rich water sinks vertically and at greater depths spreads outwards horizontally. This happens for example in the Antarctic and in northern parts of the Atlantic Ocean. In other areas there is a slow rising of the water from the deep areas. Because of this we can often find more oxygen between 3000 and 4000 m depth than at 1000 m (Fig. 2.2).

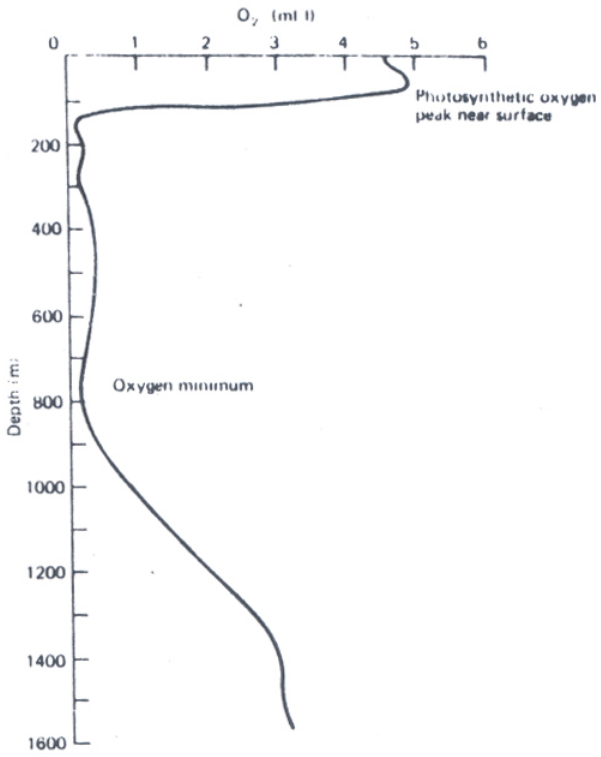

Fig.2.2
Typical profile of dissolved oxygen in the sea (from Eastern Tropical Pacific Ocean).

In some areas, closed basins and fjords for example, the circulation can be so weak or even nonexistent that the oxygen that is used in the deeper layers is not replaced. This results in oxygen deficiency (*anoxia*), sometimes with the development of hydrogen sulphide. The classic example of this is the Black Sea. Here there is an oxygen deficiency below 200 m, and it is replaced with hydrogen sulphide. Similar conditions can also be found in some Norwegian fjords. In some (for example Framvaren at Lista Fig. 10.5) this is the result of the topography (shallow sill) and layering (freshwater above more saline water). In the Oslofjord where there is every once in awhile an oxygen deficiency and hydrogen sulphide in the Inner Fjord, this is a result of human activity (pollution) combined with the fjord's topography.

Carbon dioxide, CO_2, is a necessary gas for all organic production. This production occurs in the sea in relatively greater amounts than it does outside the sea. Seawater also has a CO_2 reserve in carbonate and bicarbonate, which produces CO_2 when the use of CO_2 becomes too great. Here we see a complicated balancing system that is extremely important for all life in the sea.

3 PHYSICAL PROPERTIES OF SEAWATER

3.1 Density and Freezing Point

The density ρ is defined as mass per volume unit, and it is a function of temperature T, salinity S, and pressure p. If one knows T, S and p then the density can be determined from tables or from formulas. Density differences have a great influence on the movements of the sea. Usually seawater density will increase when the salinity and the pressure increase, and decrease when the temperature increases (Fig. 3.1). However, this is not the case when the salinity is lower than 24.7. Then the water will have its maximum density at a temperature that is higher than the freezing point of the water (Fig. 3.2). The line of the freezing point at atmospheric pressure can be described by

$$T_f = -0.0543\,S \ , \tag{3.1}$$

and the line for the temperature of the maximum density by

$$T_{\rho\max} = 3.98 - 0.215S \ , \tag{3.2}$$

where T_f and $T_{\rho max}$ are in °C. This means that if a vertical water column has a constant salinity less than 24.7 from top to bottom and a constant density equal to the maximum density for this salinity, then a cooling of the surface water will make it lighter than the water below and it will stay still. It can then be cooled even more until the water freezes and ice is produced. However, if the constant salinity is above 24.7, and the top of the column is cooled to the freezing point, it will become heavier than the water below it and sink, which will start a vertical convection, and this can continue until the entire water mass, from top to bottom, is near freezing. This difference between brackish water and seawater is of great importance for the mixing processes in the ocean, and it is also important for the forming of sea ice and the climate. According to equation (3.1) the freezing point at salinity 35.00 is -1.9°C, but seawater can also be found in a supercooled state.

The variations in $\rho(S, T, p)$ normally lie in the third decimal. For example, surface values of ρ at the open sea are mostly between 1024 and 1030 kg m^{-3}. In order to get rid of the first two digits, which are always the same, the quantity σ_t has been introduced. σ_t is defined as $\sigma_t = \rho(S,T,0)$-1000 where ρ is the numerical value in units of kg m^{-3}. Note that σ_t is a dimensionless quantity and that σ_t is based on the density the water would have had at surface pressure, because p=0 means that we are at the surface. (In oceanography the pressure of the atmosphere is usually disregarded. The pressure of a standard atmosphere is otherwise 101.325 kPa.) Seawater with salinity 35.00 and temperature 20.00°C will at surface pressure have a density of 1024.78 kg m^{-3}, and it follows that σ_t = 24.78.

Instead of the density, the specific volume α, defined as volume per mass unit, is often used. The relationship between α and ρ is

$$\alpha \equiv 1/\rho\,. \tag{3.3}$$

DENSITY OF SEAWATER

Fig. 3.1

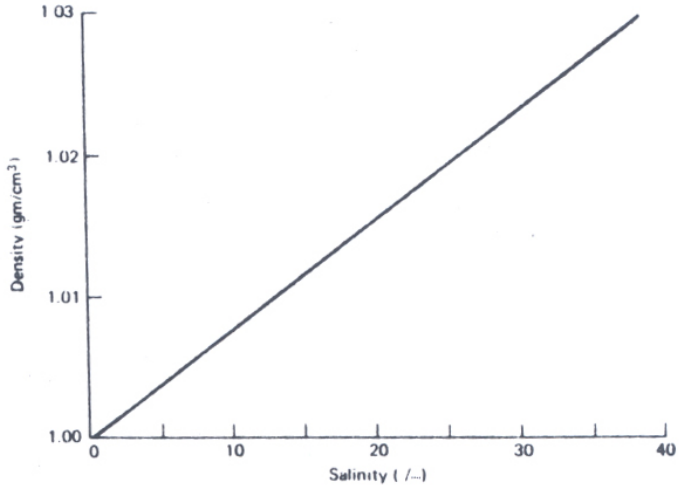

Curve showing the variation of density with salinity for water of 10° C.

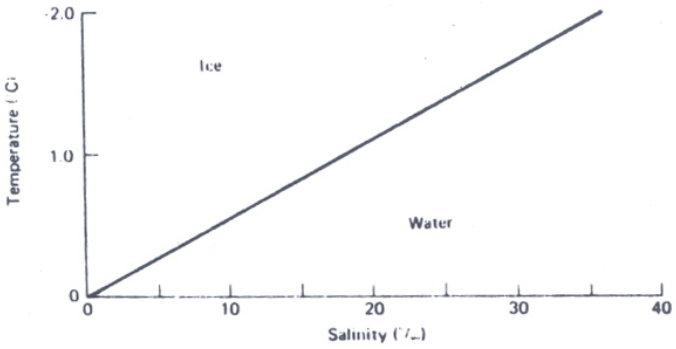

Curve showing the variation of freezing point of water as a function of salinity.

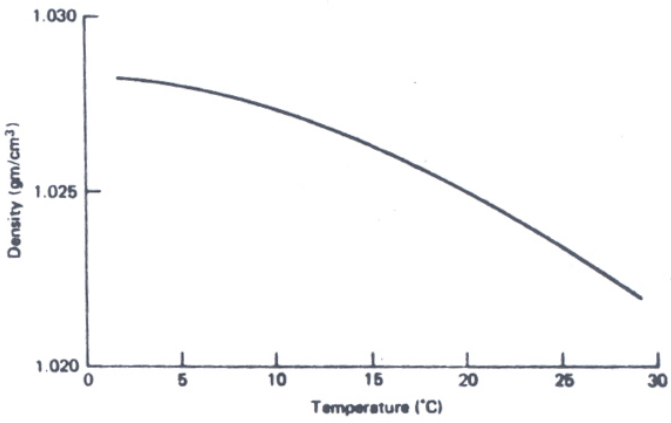

Variation of density of sea water (35 ‰) with temperature.

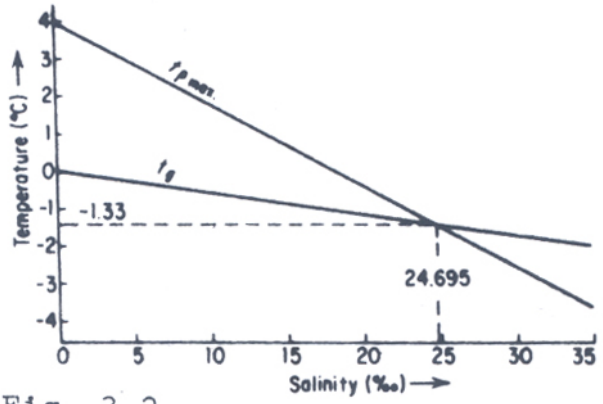

Fig. 3.2 Temperature of the density maximum, $t_{\rho max}$, and temperature of the freezing point, t_f, for sea water of different salinities.

3.2 Temperature

Besides the salinity, the temperature is the most important parameter in descriptive oceanography. Knowledge of the temperature is necessary in order to calculate the density, and the temperature at some distance from the surface can also be regarded as a conservative property and used to determine the origin of the water mass.

In order to measure the temperature of the ocean surface, the old method was to throw a bucket connected to a rope out into the water and pull it in, and put a thermometer showing the temperature to the nearest tenth of a degree into the bucket. One just had to be careful that the bucket was not standing in the sun and that the temperature was read within a couple of minutes. The reason the accuracy is not so important here is that there is already so much variation of temperature in the top half meter of the sea that greater accuracy becomes meaningless.

However, at greater depths greater accuracy is not only expedient but is also necessary. When oceanography was still a young science, researchers tried to haul up a closed water sample from the desired depth as fast as possible and then immediately take the temperature. This method was not very good because the temperature of the water sample was affected by the water layers it went through on its way to the surface. Things improved with the introduction of thermo-isolated water samplers, where the temperature was taken on deck and an adiabatic temperature correction was applied. When the water sample was lifted to the surface, the pressure would decrease, and the sample would expand and perform work on its

surroundings. Because of this the temperature would sink somewhat, and if heat was not exchanged with the surroundings, these changes would occur *adiabatically*.

However, a satisfactory method for measuring water temperature was first available after the construction of the *reversing thermometer* (Fig. 3.3). An improved construction was designed by Nansen, and the thermometer was used for the first time with satisfactory results in 1900. The measuring principle is that when the thermometer is turned upside down at the desired depth, the mercury string will be broken off, and its length will show the

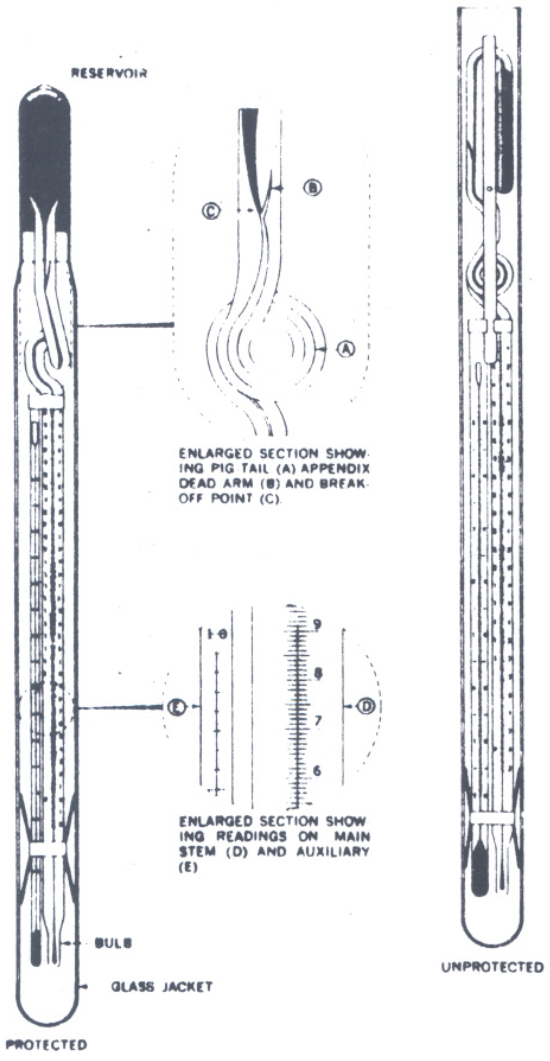

Fig. 3.3 Details of the construction of oceanographic thermometers. [Courtesy of U.S. Naval Oceanographic Office, Washington, D.C.]

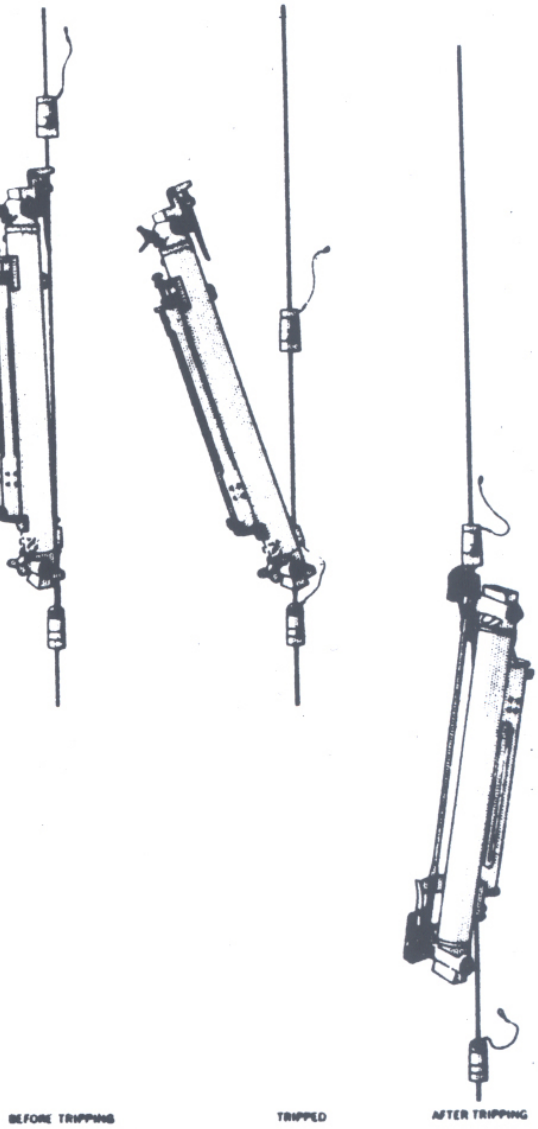

Fig. 3.4 A Nansen bottle being released by a messenger: before tripping, during tripping, and after tripping. [Courtesy of U.S. Naval Oceanographic Office, Washington, D.C.]

temperature when the instrument was turned (Fig. 3.4). The length of the string can be determined on deck. This method, which gave the temperature to the nearest 0.02°C, was considered the standard method within oceanography until the 1970ies, but by then it was being replaced by *CTD instruments*. CTD sensors (conductivity, temperature, depth) are connected to a deck unit by an electrical cable or wire, and will provide the temperature, the depth (from pressure), the salinity (from conductivity) and the density (from temperature, salinity and pressure).

3.3 Compressibility

The relative change in volume per pressure unit is termed the *compressibility K*. It is defined as

$$K = -\frac{1}{\alpha}\frac{\partial \alpha}{\partial p} \ . \tag{3.4}$$

A vertical water column of 10 000 meters has actually sunk 200 m due to the increasing pressure that occurs at increasing depths. If seawater was incompressible, the average surface of all oceans would be 30 m higher than it is today. Still, water is much less compressible than is air.

3.4 Specific and Latent Heats

The specific heat for seawater of salinity 35 is 4.0 kJ kg^{-1} K^{-1}. Consequently the ocean currents carry great amounts of energy. If the Norwegian Atlantic Current transports 6 Sv (1 Sv = 10^6 m^3 s^{-1}) with an average temperature of 5°C into the Norwegian Sea, this represents a potential effect, if the current is cooled to 0°C, of $1 \cdot 10^{14}$ W (= 100 teraW). In 2001 Norway's total energy consumption corresponded to $3 \cdot 10^{10}$ W, implying that the current carries more than 1000 times this consumption.

The heat capacity of the entire atmosphere corresponds to the capacity of the 2 upper meters of the ocean. Consequently the ocean can in principle store infinitely more heat than the atmosphere.

On a cloud-free day, the daylight can provide approximately 750 W to 1 m^2 of the surface in the Norwegian Sea. If half of this effect is absorbed in the top meter without any heat loss to the environments, it will take about 3 hours for the temperature to rise one degree.

The latent heat of evaporation decreases with increasing salinity and increasing temperature in the sea. For $S = 0$ and $T = 0°C$ it will be 2494 kJ kg^{-1}. Thus the heat required to evaporate 1 kg of water corresponds to the heating of more than 500 kg of water by 1 °C.

The latent heat of melting decreases with increasing salinity. For fresh ice ($S = 0$) it is 335 kJ kg^{-1}. The specific heat of fresh ice is approximately 2.0 kJ kg^{-1} K^{-1}.

3.5 Light in the Sea

The energy of the direct sunlight and the diffuse skylight that hits the surface of the sea lies between the wavelengths 300 and 3000 nm. The amount of light that is reflected off the surface depends on the solar altitude, the cloudiness, the roughness of the sea surface, as well as the wavelength. However, one can estimate an average reflection of 3 – 7 %. The *infrared part* of the spectrum (wavelengths above 750 nm), which contribute half of the energy, is absorbed in the top meter. The *visible part* (wavelengths between 350 and 750nm, what we usually call *daylight*) will be attenuated as depth increases, and the attenuation depends strongly on the wavelength (Fig. 3.5).

Fig. 3.5

Schematic representation of the energy spectrum of the radiation from the sun and the sky that penetrates the sea surface, and of the energy spectra in pure water at depths of 0.1, 1, 10, and 100 meters. Inset: percentages of total energy and of energy in the visible part of the spectrum reaching different depths. [From Sverdrup, *et al.*, (1942).]

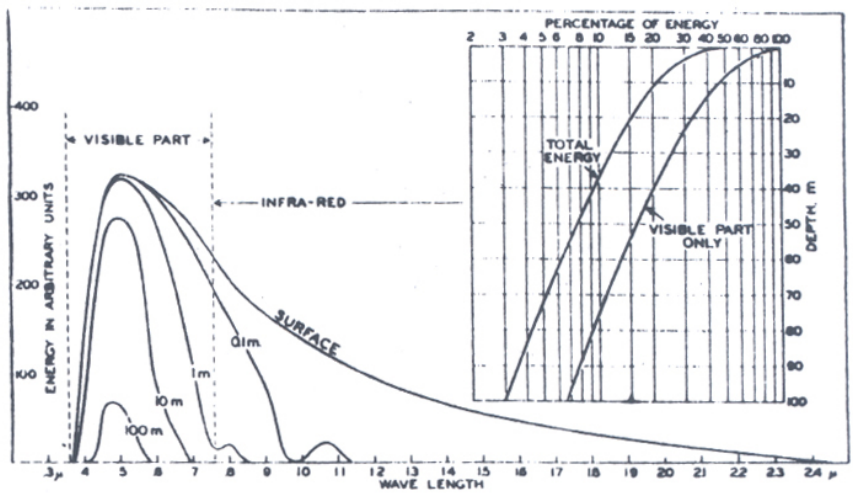

Fig. 3.6 shows that in clear ocean water the vertical transmission of blue light will be greatest, for green light somewhat less, and for red light even less. Because blue light is attenuated the least, the light that is scattered upward towards the surface will also be mainly blue light, and the ocean will look blue.

Turbid fjord and coastal waters are often supplied with large amounts of yellow-brown decomposed material, which is usually named by the collective term *yellow substance*. In the

US the term *CDOM* (*coloured dissolved organic material*) is more often used. In such waters the blue light will be attenuated more quickly with depth than the green light, and the green almost as much as the red (Fig. 3.6). The colour of the water will then seem green or maybe even brown. Large amounts of algae can also colour the sea.

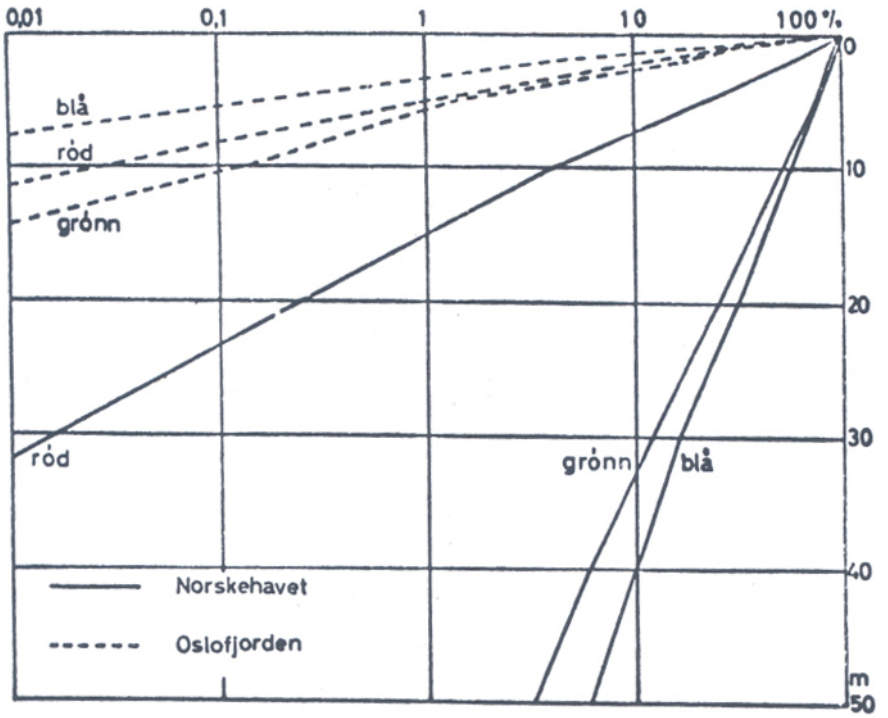

Fig. 3.6

Irradiance in percent of the surface value (blå=blue=465 nm; grønn =green=530 nm; rød=red=620 nm)

Usually at least half of the total energy from the sun (300 – 3000 nm) is absorbed within the first meter of the sea, and at least three fourths are absorbed within the top 10 meters. The spectral parts corresponding to the observed colour of the sea will be less absorbed. In clear oceanic water half of the blue light can penetrate down to 30 m and 1% down to 140 m, and this is of great importance for photosynthesis in marine plants and algae. The absorbed radiation is mainly converted to heat, while a very small part may be transformed into chemical energy by photosynthesis.

The refractive index of seawater relative to the index of air varies with wavelength, temperature and salinity, but the average value can be set at 4/3. Snell's Law of Refraction for a ray of light entering the sea from above can then be written

$$\sin i = \frac{4}{3}\sin j \ . \qquad (3.5)$$

Here *i* is the angle (of incidence) in air and *j* is the angle (of refraction) in water, both angles relative to the vertical direction. It should be noted that Snell's Law works both ways, meaning that a ray passing from water to air still follows equation (3.4), with *i* and *j* being the angles in air and water, respectively. If i = 90° then *j* = 48.6° according to equation (3.4). Light rays in water with an angle of incidence larger than 48.6° up against a flat sea will then not be refracted into air but will be completely reflected (Fig. 3.7). For angles *j* in the range 0-48.6° the amount of light reflected can be calculated by the *Fresnel Equations*. These will not be discussed here.

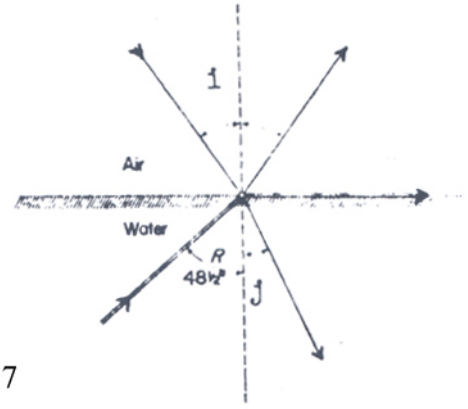

Fig. 3.7

Reflection and refraction of radiation at the interface between air and water.

The simplest instrument for determining the clarity or transparency of seawater has gotten its name from the Italian frater Pietro Angelo Secchi, who in 1866 described a number of experiments done with a white disk which was lowered into the sea until it was out of sight. The average between the depth where it disappears from sight and the depth where it again becomes visible is today called the *Secchi disk depth*. In the Oslofjord during summer the Secchi depth can vary between 0.5 and 10 m, while in wintertime it can extend to 20 m. The world record was set up in the Weddel Sea in 1986 when the Secchi depth was observed to be 79.5 m. The Secchi depth depends on the optical properties of the water, but it is also to some extent influenced by waves, sun glitter, and the observer's eyesight. Still it is a very useful and practical quantity. Other optical properties of the seawater are usually determined by special electronic instruments using photodiodes and other types of sensors, but we are not going to discuss these here.

The attenuation of a parallel beam of monochromatic light follows the *Bouguer-Lambert Law*

$$d\phi = -c\,\phi\,dx \ , \qquad (3.6)$$

where ϕ is the energy flux of the beam, that is the energy per time and area units (W m^{-2}), $d\phi$ is the attenuated part of this flux along the distance *dx* of the beam, *x* being the coordinate in the beam's direction, and *c* is a constant of proportionality; *the attenuation coefficient*. This coefficient will be expressed per length unit (m^{-1}). The integrated form of the Bouguer-Lambert Law becomes

$$\phi(x) = \phi_0 \, e^{-c\,x} \ , \tag{3.7}$$

where ϕ_0 is the beam flux at $x = 0$. The coefficient *c* can then be determined from measurements of the flux at two different points with a distance *x* along the beam.

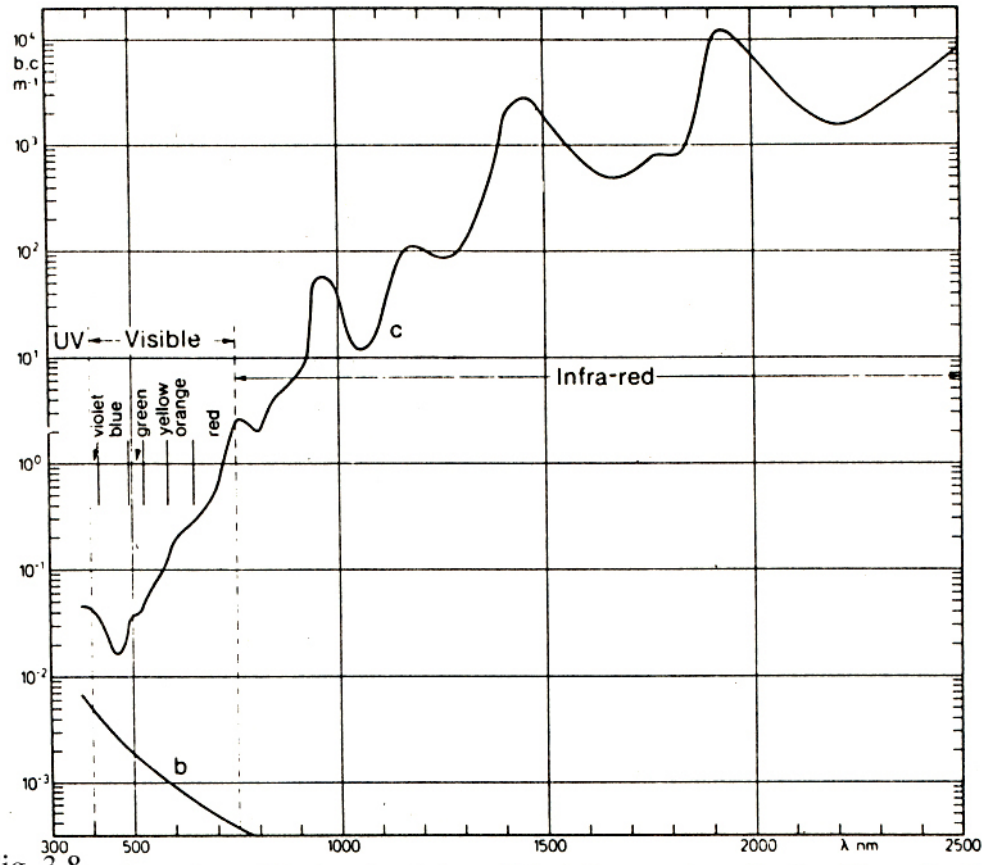

Fig. 3.8 **Attenuation coefficient c and scattering coefficient b for pure water as a function of the wavelength λ of the radiation.**

Energy is lost from the beam by two processes: *absorption* where the light disappears and is mainly converted to heat, and *scattering* where the light only changes direction. The contributions to the attenuation from the two processes can be quantified by two corresponding coefficients: the absorption coefficient *a* and the scattering coefficient *b*, so that

$$a + b = c \ . \tag{3.8}$$

Fig. 3.8 shows *c* and *b* as functions of the wavelength for pure water. Since $a = c - b$ we see that the absorption always is greater than the scattering for pure water. In natural seawater, however, conditions may be different, and we often have that $b > a$.

The scattering in seawater is mainly caused by particles. Even if the water molecules scatter light, their contribution to the total scattering is usually negligible. The particles consist of *mineral particles, phytoplankton* and different types of *detritus*, and in addition to the scattering they may also absorb light. Other important contributions to the absorption come from the water molecules and the yellow substance. In natural seawater we often find that *c* has its maximum in the UV and that it decreases monotonously towards the red, implying that particles and dissolved material are the dominant contributors to the attenuation.

The vertical attenuation of spectral daylight in the sea is usually described by an analogue to the Bouguer-Lambert Law:

$$E(z) = E_0 \, e^{-Kz} \tag{3.9}$$

Here $E(z)$ is the downward irradiance for a narrow wavelength band at the depth z, E_0 is the irradiance at $z = 0$, and K is the vertical attenuation coefficient for the chosen wavelength.

The vertical attenuation of irradiance differs from the attenuation of a beam of parallel rays since the downward irradiance receives rays in all possible directions from the upper hemisphere. The vertical attenuation of irradiance is only to a minor extent influenced by the scattering, since most of the scattered light will be scattered in forward directions. Even if the scattered light is lost from the original ray it is not necessarily lost from the irradiance. Theory and observations reveal that an approximate relationship between K, a and b is

$$K = (a + 0.02b)\frac{1}{\mu_d} \ , \tag{3.10}$$

where μ_d is the average cosine for the downward directed light. The angle used by the cosine is the angle relative to the vertical direction. In the sea $1/\mu_d$ is likely to obtain values between 1.0 and 1.7. If we choose the mean value 1.35, equation (3.10) becomes

$$K \approx 1.35\,a + 0.03b \ , \tag{3.11}$$

clearly demonstrating that the vertical attenuation coefficient of irradiance is dominated by the absorption coefficient. In many text-books there is a mix-up between c and K, but according to the equations (3.9)-(3.11) the two coefficients will only be equal when $b/a = (1-\mu_d)/(\mu_d-0.02) \approx 0.4$.

The irradiance *transmittance* τ per vertical meter, defined by

$$\tau = \frac{E(1m)}{E(0)} = e^{-K \cdot 1m} \ , \tag{3.12}$$

is presented for different water types according to Jerlov's classification in Fig. 3.9. The transmittance is a dimensionless quantity. It is seen that the transmittance of clear blue ocean waters depends strongly on wavelength in the UV and red parts of the spectrum, while the transmittance of the greener and more turbid coastal waters also has a significant spectral dependence in the blue part.

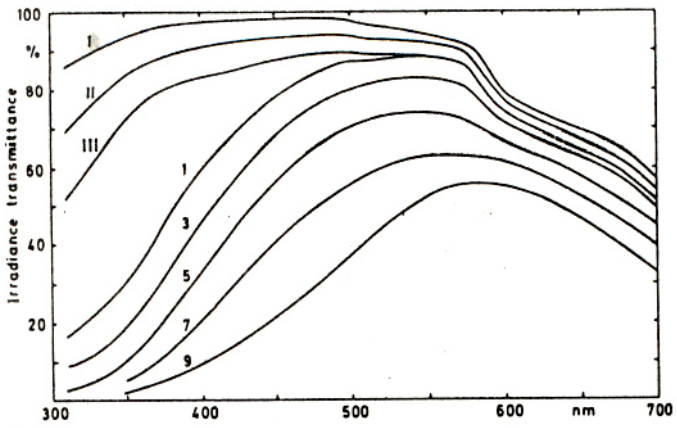

Fig. 3.9 **Transmittance per meter of downward irradiance in the surface layer for optical water types. Oceanic types *I*, *II*, *III* and coastal types *1*, *3*, *5*, *7*, *9*.**

3.6 Sound in the Sea

Sound is a wave-phenomenon just like light, and therefore follows many of the same laws, like for instance Snell's Law of Refraction and the Bouguer-Lambert Law. Otherwise the results for the light and sound waves are in many ways completely different, as shown in Table 3.1.

Because seawater is much less compressible than air, the speed of sound is much higher in water; about 1.5 km per second in water and about 300 m per second in air. The speed of sound increases with salinity, temperature, and pressure (Fig. 3.10 and 3.11). A simplified empirical formula is

Table 3.1 Properties of light and sound

	Light	Sound
Reflectance at normal incidence from air to water	2%	99.8%
Speed in air	300 000 km s^{-1}	300 m s^{-1}
Speed in water	225 000 km s^{-1}	1500 m s^{-1}
Refractive index of water relative to air	1.33	0.2
Angel in air of total reflection	90°	12°
Angel in water of total reflection	48°	90°
Smallest attenuation coefficient of pure water	0.02 m^{-1}	0
Typical attenuation coefficients of natural waters	0.1-2.0 m^{-1}	10^{-4}-10^{-2} m^{-1}

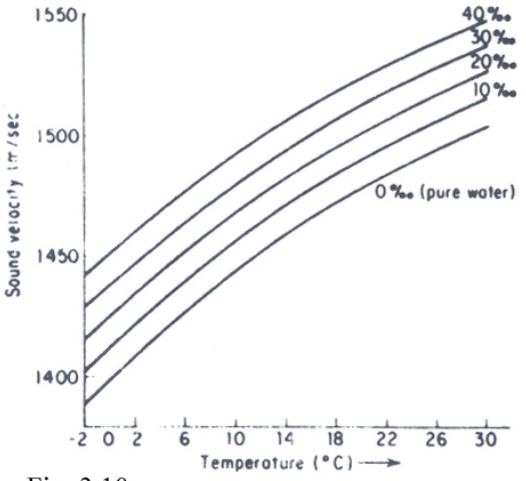

Fig. 3.10 Velocity of sound (m/sec) in pure water and sea water of different salinity (‰) at atmospheric pressure as a function of temperature (°C).

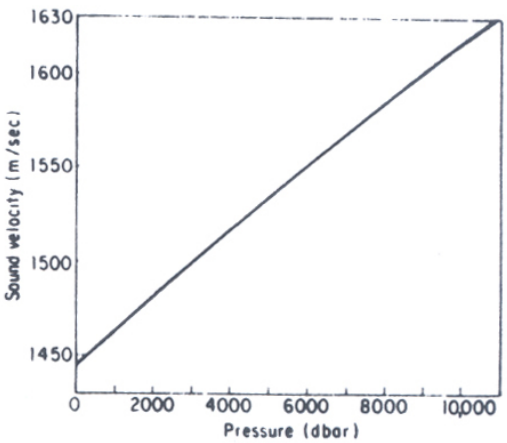

Fig. 3.11 Sound velocity in sea water of 35‰ salinity at 0°C as a function of pressure.

$$v = 1449 + 4.6\,T + 1.3\,(S - 35) + 0.18\,Z \text{ (m s}^{-1}\text{)} \qquad (3.13)$$

where pressure has been substituted by depth Z, and v = speed, T = temperature, S = salinity.

When a ray of sound goes from one layer of water to another having a different speed, it will be refracted according to Snell's Law of Refraction, which can be written on the form

$$\frac{\sin i}{v_i} = \frac{\sin j}{v_j}\ , \qquad (3.14)$$

where i is the angle of incidence (relative to the normal of the layer), j is the angle of refraction, and v_i and v_j are the speeds of sound in the two layers of water.

The layers having the same speed of sound in the sea will for the most part lie horizontally, and when rays of sound propagates through these at an angle, they will be refracted towards the layer with the minimum speed. If the speed of sound decreases with increasing depth, as in Fig. 3.12, then all sound rays, except the horizontal and vertical ones, will curve downwards as shown in the figure. However, if the speed of sound increases with increasing depth as in Fig. 3.13, the sound rays will curve upwards and are almost trapped by the surface layer.

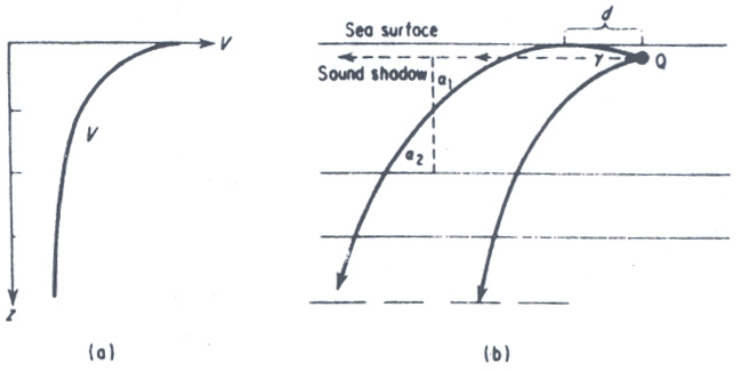

Fig. 3.12 Schematic representation of sound refraction in water where the sound velocity, V, decreases with depth. (a) The decrease of sound velocity with depth. (b) The limiting sound rays emitted at the source, Q, for a beam angle γ.

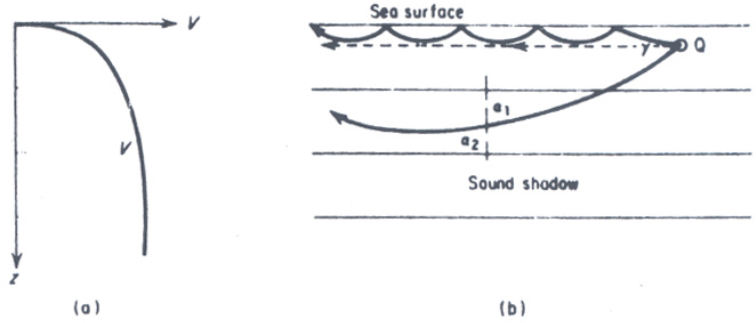

Fig. 3.13 Schematic representation of sound refraction in water where the sound velocity increases with depth. (a) The increase of sound velocity, V. (b) The limiting sound rays emitted at the source, Q, for a beam angle γ.

The vertical division of layers within the sea is of little importance for the *echo-sounder* because the angle of incidence for the sound rays will be perpendicular to the layers ($i = j = 0°$), and therefore they will not change direction. In contrast, with the *sonar* (*sound navigation ranging*) the angle of incidence may be closer to 90°, and the rays of sound can become quite curved. In principle the sonar is an echo-sounder where the transducer is mounted in such a way that the sound signal can be sent out in an approximately horizontal direction. The transducer can be turned in both the horizontal and vertical planes. In this way we are able to search a larger area and locate sound-reflecting objects to the side of the ship and not only directly under it. This has made searching for shoals of fish more effective and the instrument is also used by the military. The case of Fig. 3.13 is typical of our fjords, where

it is very difficult for a surface ship to find a submarine by sonar, unless the ship is directly over the submarine.

The attenuation of a sound ray in the sea is due to the absorption by the water and the dissolved substances in the water. When the temperature, salinity and pressure are constant, the attenuation coefficient will be approximately proportional to the square of the frequency. For frequencies f less than 30 kHz (1 Hz = 1 s^{-1}) and $p = S = 0$ and $T = 7°C$ the attenuation coefficient c can be described by

$$c \approx c_0 \frac{f^2}{f_0^2} \ , \tag{3.15}$$

where $c_0 = 2 \cdot 10^{-6}$ m^{-1} and $f_0 = 1$ kHz.

For a parallel beam of sound the attenuation will follow the Bouguer-Lambert Law, but if the source is emitting the sound waves as spherical shells moving outwards, the energy will be distributed over areas increasing with the square of the spherical radius. The energy per area unit of such a spherical sound wave will follow a modified form of the Bouguer-Lambert Law:

$$\phi(R) = \phi_0 \frac{R_0^2}{R^2} e^{-c(R-R_0)} \ . \tag{3.16}$$

An important point when the frequency shall be chosen, is the size of the target one intends to "see" with the sound. As a rule of thumb the ratio between the wavelength and the size of the target should be of the order of magnitude 1 or less. The relationship between frequency f, wavelength L and the speed of sound v is

$$f = \frac{v}{L} \ . \tag{3.17}$$

Since v is a function of temperature, salinity and pressure (equation (1.1)), f is determined once L is chosen. The higher the frequency, the shorter will be the wavelength, and the better the power of resolution. On the other hand c will increase as f^2, and in practical work a compromise between signal strength and resolution has to be chosen.

3.7 Ice in the Sea

There are two types of ice in the sea: *sea-ice* and *land-ice*. Sea-ice is created when the ocean water freezes, land-ice comes from glaciers when they break off, and is called *icebergs*. In the Antarctic the glaciers extending out into the ocean is called *shelf ice*.

In order for freshwater to freeze, the entire water mass has to cool down to 4°C before the lighter surface water can freeze. In homogeneous seawater with a salinity above 25 the entire water mass must cool down to the freezing point before ice can be formed. That is why sea-ice is more likely to be found in shallow areas or where there is a more brackish layer on the top.

The salt in the ice will not be evenly distributed, but collected in small pores with concentrated brine. Only at -55°C or colder will all of the brine freeze. At higher temperatures the brine will melt again and with time melt through the ice and into the water. In the Arctic Sea, the sea-ice can be 2-6 years old before it is carried out with the East Greenland Current or the Labrador Current. That is why old sea-ice often has been melted by hunters and sailors in the Arctic in order to provide drinking water.

If the surface is calm, a thin clear ice can form, but if there are any waves, then *ice-slush* or *grease ice* will form which will later freeze into a layer of ice. This layer can also be broken up by the wind, and the small ice flakes will then lie and rub against each other until they become rounded and after awhile develop up-turned edges. These flakes are called *pancake ice*. If the ice is continually broken up and packed together again, then we end up with what we call *pack ice*. If it is twisted and compressed together even more it is called a *pressure ridge* or a *hummock*, and this can become up to 8 meters high.

A strange type of ice that resembles the pancake ice, but instead of being formed on the surface is formed below it, is observed outside of the Swedish West Coast. After a period with extremely cold temperatures, round pieces of ice can suddenly shoot up through the surface with its edge first and land on the surface with a splash. It has been reported to be quite a strange sight when this happens over the course of a couple of hours as far as the eye can see, but a less pleasant experience for the small boats that are suddenly locked in by the ice. This ice forms between the surface water, which has a temperature close to the freezing point, and a deeper layer which is more saline and has a temperature near its own freezing point, but which is also colder than the freezing point of the surface water. In the transition zone between the two layers conditions for freezing can be created.

The icebergs at Newfoundland, which led to the sinking of the Titanic, come from glaciers on Greenland or around the Baffin Island. Since fresh ice has a density of 900 kg m^{-3} or less, only 1/9 of the volume will stick out above the surface (Fig. 11.1). The form is very irregular. The International Ice Patrol (under the U.S. Coastguard) watches for and sends out warnings about icebergs. The icebergs in the Southern Ocean are formed when the *ice front* or *shelf ice*, which is an extension out in the sea of the enormous glaciers on land, breaks off. They will therefore be flat and regular in their form with heights of up to 40 m above the surface.

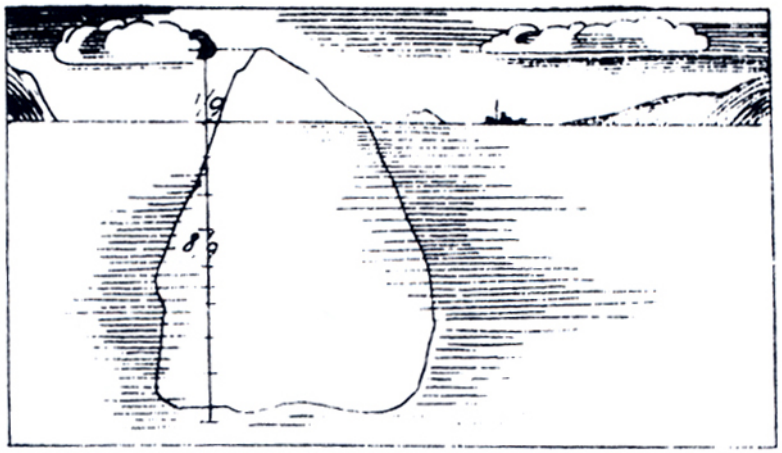

Fig. 3.14 Only 1/9 of the ice volume lies above the sea surface.

4 INFLUENCE OF ATMOSPHERE ON THE SEA

4.1 Major Wind and Pressure Systems

The sun is the direct or indirect force behind all movement in the sea, the lunar tide being an exception. Directly the sun influences the sea by warming it and indirectly it affects the sea through processes in the atmosphere. There is an interaction between the sea and the air, such that the conditions in the sea influence the atmosphere and vice versa, but here we are only going to discussed how the sea is affected.

The most important way in which the atmosphere influences the sea is through the large-scale distributions of wind and high and low pressures. The wind and the pressure systems transfer kinetic energy from the atmosphere to the sea, and they contribute to the climatic conditions by clouds, precipitation, evaporation, heat transfer and ice freezing, and all of this influences the large-scale circulations of the sea.

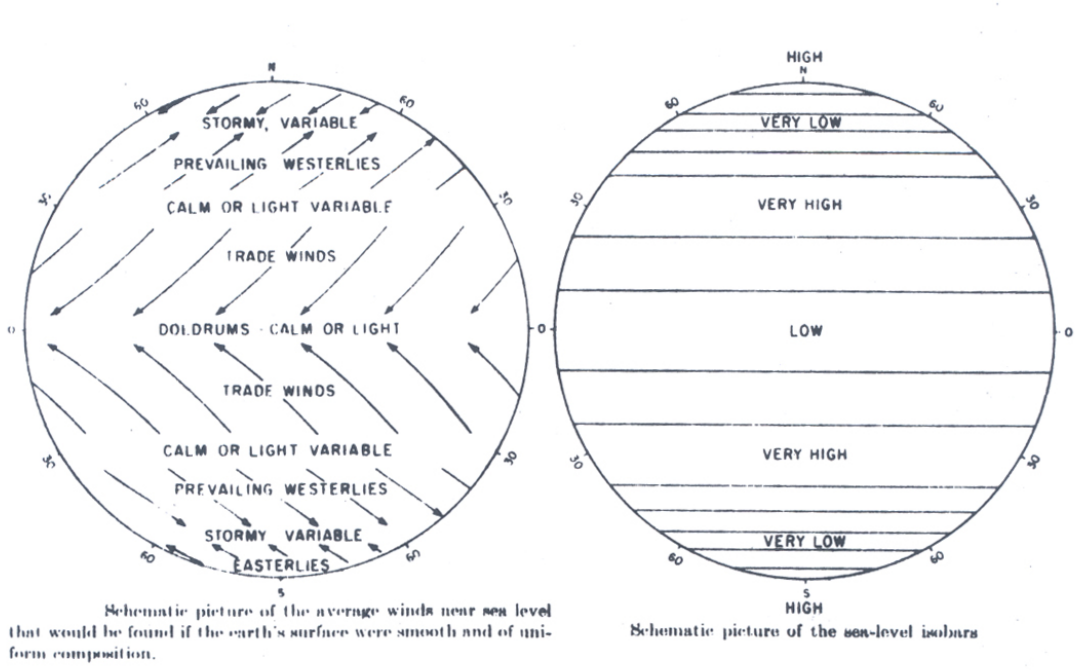

Schematic picture of the average winds near sea level that would be found if the earth's surface were smooth and of uniform composition.

Schematic picture of the sea-level isobars

Fig.4.1

Idealized wind and pressure systems are shown in Fig. 4.1. At 30° north and south (the *horse latitudes*) there lies a high pressure system that creates light wind belts. From these high pressure zones the wind blows in two directions: the *trade winds* are blowing west towards the equator, while the prevailing *westerlies* are blowing in the opposite direction and transporting low pressures with precipitation up to our latitudes. Along the equator it is another calm wind belt, sometimes called the *doldrums*.

However, in nature the conditions are not as orderly as in the figure; for one thing the distribution of land and sea influences the pressure and wind systems. These are also shifted somewhat, for example the equatorial calm wind belt lies not exactly at the equator but at 10°N. In the following and in later sections, we will look closer at the effect of these systems.

4.2 Heat Budget

In the ocean the temperature varies with time and location. The balance between the change in temperature and the losses and gains of heat is called the heat budget. Here we will give the amount of heat (or the amount of energy) the symbol Q. The flux of heat per surface unit will be given the symbol q. We will specify the different terms with indexes. Q_s is the net amount of solar energy that passes through the surface of the ocean, Q_v is the net advective supply of heat (transported by ocean currents), and Q_h describes the amount of heat gained (or lost) by conduction between ocean and atmosphere. Q_b is the net transfer of infrared (heat) radiation from atmosphere to ocean, Q_e is usually a negative term describing the heat loss due to evaporation. If we call the total heat gain Q_t, we have an equation for the heat budget:

$$Q_t = Q_s + Q_v + Q_h + Q_b + Q_e \tag{4.1}$$

A positive Q_t corresponds to an increase in temperature. Other factors such as heat conduction through the ocean bottom, heat production from friction in the water or from chemical processes are so small in comparison to the other terms in the equation that they are omitted.

If we let equation (4.1) represent the World Ocean, then Q_v must be 0, and if we average over many years, then Q_t =0 (that is to say that the average temperature in the ocean is constant). We are then left with

$$Q_s = -Q_h - Q_b - Q_e \tag{4.2}$$

This equation must also apply on average per surface unit and time unit, and we then obtain for the heat fluxes

$$q_s = -q_h - q_b - q_e \tag{4.3}$$

Mosby has calculated these terms to be 150 = 10 + 60 + 80 in units of W m^{-2}. This means that one m^2 of ocean surface will absorb on average 150 W sun and sky radiation, it will emit a net value of 60 W of infrared radiation, and it will lose 10 W to the air by conduction and 80 W as latent heat due to evaporation. It should be noted that q_s is a gain from the sun and not from the atmosphere, while q_h and q_e are direct losses to the atmosphere and q_b is mostly a loss to

the atmosphere (some infrared radiation will be lost to space). On average it is therefore the atmosphere that receives heat from the sea and not the other way around.

The above numbers give an idea of the average values of the different terms in the heat budget, but here it must be pointed out that these quantities can vary greatly with time and space. Q_s varies with the latitude and with the seasons of the year. Q_h and Q_e also vary with latitude and season and can change sign. Q_b is the only part of the equation that is almost constant. We will now look more closely at the different terms and to the reasons for their variation.

Q_b expresses the balance between the infrared radiation emitted by the ocean surface to the atmosphere and the infrared radiation from the atmosphere absorbed by the sea. It depends on air and water temperatures, humidity and cloudiness. The combined effect is a surprisingly constant Q_b (Fig. 4.2).

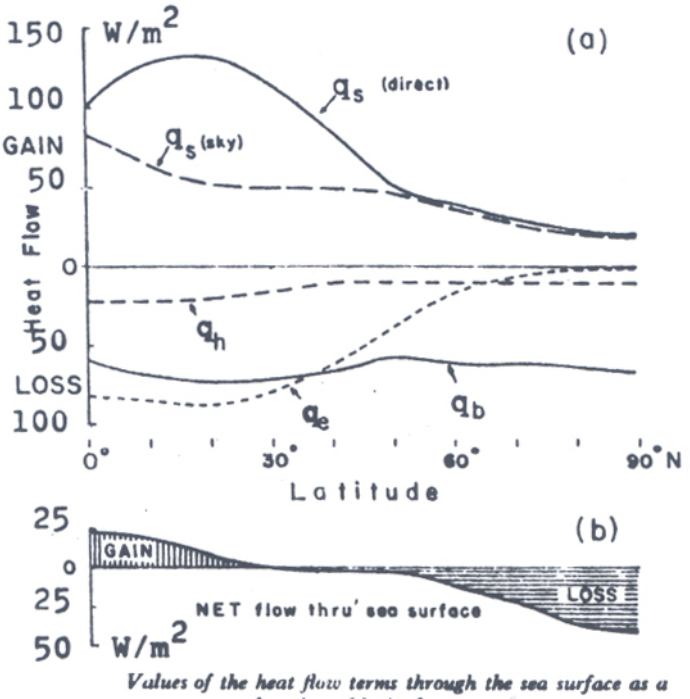

Values of the heat flow terms through the sea surface as a function of latitude.

Fig.4.2

Q_s actually consists of two types of solar radiation: the direct solar rays and the more diffuse light from the sky which is scattered sunlight. Despite the fact that half of Q_s is invisible infrared radiation, as mentioned in section 3.1d, it is normally termed *short-wave* radiation, in contrast to Q_b which is described as *long-wave* radiation, because the

.

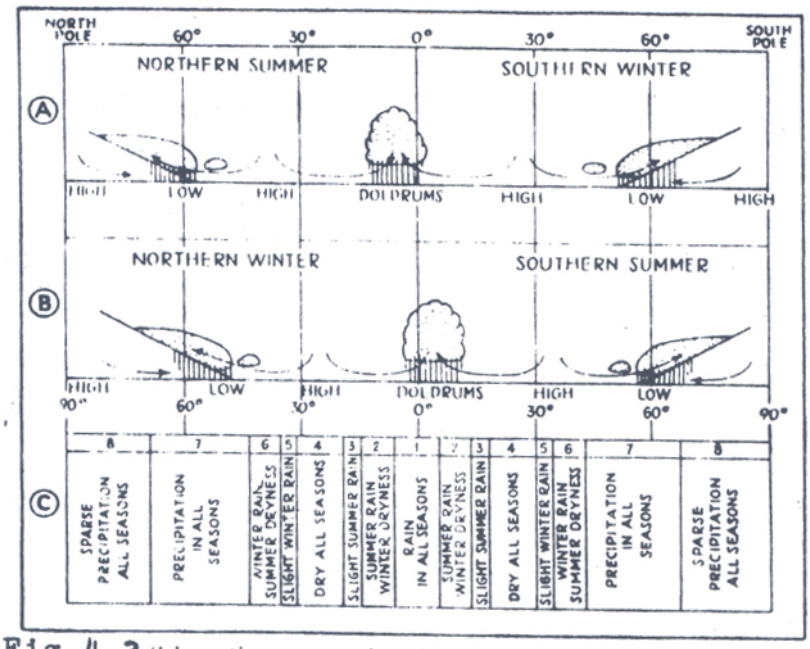

Fig. 4.3 Schematic cross section through the atmosphere showing the main zones of ascending and descending motion: (*a*) during the northern summer; (*b*) during the northern winter; (*c*) the main zones of precipitation.

wavelengths of Q_b are 10 times as long as those of the infrared solar radiation. Q_s is the net solar radiation that the sea receives from sun and sky. If we look at Fig. 4.3, or turn back to Fig 4.1, we would expect that q_s would have its greatest value in the high pressure zones at 30° N and S, where there is a lot of sun and not many clouds. As shown in Fig. 4.2, this is correct in regards to direct sunlight. Near the equator there is less direct sun due to the clouds that are formed there. On the other hand, the clouds increase the diffuse radiation coming from the sky, so that the total q_s only increases weakly from the equator to about 20° N.

As mentioned earlier, lower solar altitudes will lead to an increase in the reflection on the ocean surface, and to an increase in the albedo. At the same time the solar rays will be more attenuated because they have a longer distance to travel through the atmosphere. A third effect is that the vertical component of the radiative flux decreases when the sunlight becomes more horizontal. Together with the distribution of clouds, the combined effect becomes that q_s decreases from 20°N towards the pole as shown in Fig. 4.2.

Q_e depends on the amount of water that evaporates, E, and the specific latent heat, L, so that

$$Q_e = E\,L \tag{4.4}$$

L decreases somewhat when the temperature increases, and in seawater it is approximately 2.4 10^6 J kg^{-1}. E is usually given per time and surface unit, so we end up with

$$q_e = \rho h_e L \tag{4.5}$$

where ρ is the density of seawater and h_e is the height of the water evaporated per time unit. Fig. 5.5 shows how h_e, measured in cm year^{-1}, varies with the latitude. The variation of q_e with latitude has a form very similar to that of the total q_s: A weak increase from the equator towards 20°N and then a decrease towards the pole (Fig. 4.2).

q_h is almost always negative (a loss of heat from water to air), but in some areas the air just above the ocean surface is warmer than the water, and then q_h becomes positive, implying that the atmosphere is heating the ocean by conduction. Fig. 4.2 shows that q_h at the tropical and subtropical latitudes is significantly less than the other terms of the heat budget, while q_h at the polar latitudes can be of the same order of magnitude.

We will now return to equation (4.1). If we look at the oceanic area between two circles of latitude and presume that the average temperature does not vary from year to year ($Q_t = 0$), then the heat budget may be written on the form

$$Q_v = -(Q_s + Q_h + Q_b + Q_e) \tag{4.6}$$

This means that if the sum in parenthesis is positive, then Q_v will be negative, implying that ocean currents must transport a net amount of heat out of the area. The net *vertical* transport of heat to the sea, which is expressed by the parenthesis, is compensated for by a *horizontal* transport, Q_v. The lower part of Fig. 4.2 shows that from the equator to approximately 30°N the sea will receive a surplus of heat through the surface that it can only get rid of through a transport towards the poles. Between 30°N and 60°N there is almost a balance in the vertical transport, and this area can be interpreted as a transition zone for the poleward transport. From 60°N and up there is a continuously greater loss of heat through the surface to the atmosphere, and this is compensated for by the mentioned horizontal (advective) transport of heat. For the entire ocean surface the heat gain must equal the heat loss. On Fig. 4.2 it can look as if this is not true, but we need to take into consideration that the area of the sea between the latitude circles decreases towards the poles (Fig. 1.1).

4.3 Volume Budget

An important axiom in the old classic physics is the *principle of conservation of mass*. When this is applied to seawater, and if the density can be assumed to be practically constant in time, this becomes a *principle of the conservation of volume*, since mass is density multiplied by volume. For every fixed geometrical area we can set up a volume budget for water, where the volume of the water vapour is calculated as the volume the vapour would have had in a condensed state. If we call the volume of seawater flowing into the area V_i, the volume flowing out of the area V_o, the water volume supplied by rivers R, the evaporated volume E, and the precipitated volume P, then the volume budget is

$$V_i + R + P - V_o - E = F\,h \tag{4.7}$$

where F is the surface area and h is the average increase of the water level.

If there is no change of the water level ($h = 0$), we get

$$V_o - V_i = +R + P - E \tag{4.8}$$

This can be interpreted to mean that the net volume of seawater leaving an area must be the same as the net volume of freshwater entering it.

4.4 Salt Budget

As earlier mentioned, we can assume with a high degree of accuracy that the amount of salts in the oceans is constant. Salts are not created nor used. We will now look at the simplified case where neither the water level nor the average salinity changes with time in a specific area. An equal amount of salts must be brought into the area as taken out of it, and the salt budget for this special condition yields

$$S_i\,\rho_i\,V_i = S_o\,\rho_o\,V_o \tag{4.9}$$

where S_i and ρ_i are salinity and density of the entering volume of water, and S_o and ρ_o are the corresponding values for the leaving volume of water. Because there is usually little variation in ρ in comparison with S, we can reduce the equation by ρ and obtain

$$S_i\,V_i = S_o\,V_o \tag{4.10}$$

In some cases, when h=0 and we know R+P-E and have measured S_o and S_i, equations (4.8) and (4.10) can be combined to express V_o and V_i as functions of the known quantities. These are the so-called *Knudsen relations*, and they will be discussed in Chapter 10. Since it is easier to record salinity than volume transport, these are quite handy for estimating transports in areas where the inward and outward currents have clearly defined salinities.

5 GLOBAL DISTRIBUTION OF *T*, *S* AND ρ

5.1 Temperature Distribution

We have earlier seen how the solar energy obtained its highest values from the equator to 20°-30° and then began to weaken towards the poles. The same was true for the net heat flux down through the ocean surface. We should then expect to find the highest surface temperatures around the equator and the lowest at the poles.

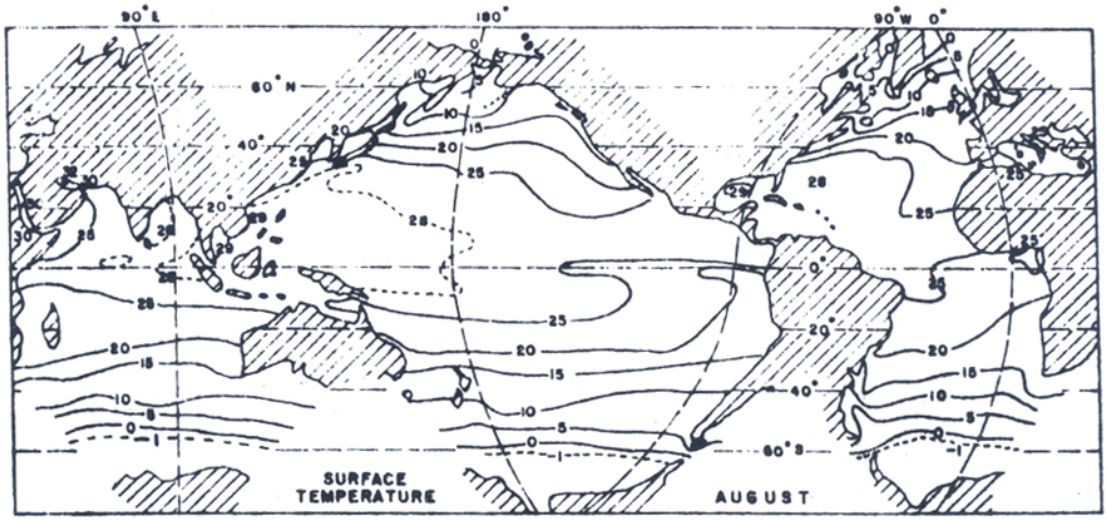

Fig.5.1 *Surface temperature of the oceans in August.*

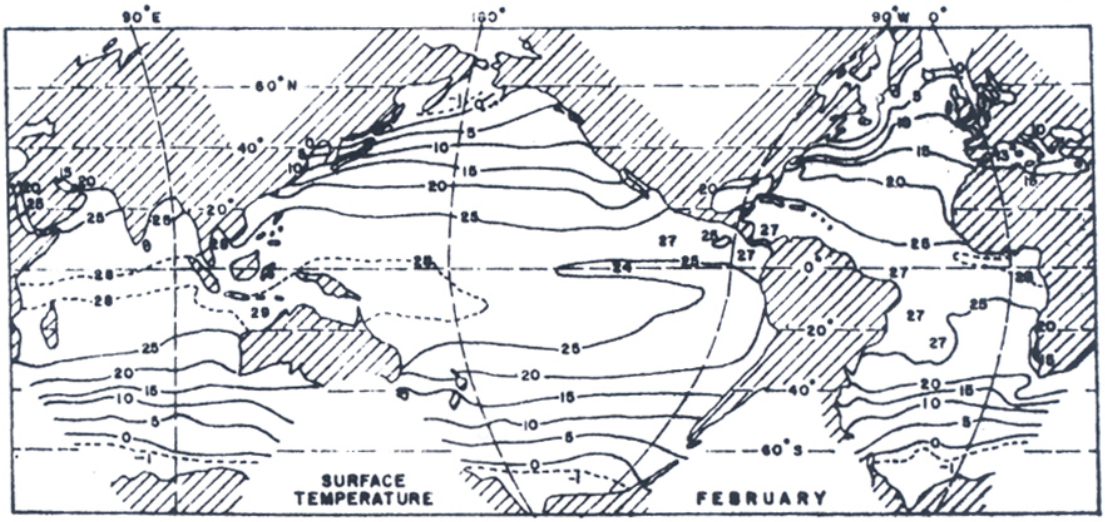

Fig.5.2 *Surface temperature of the oceans in February.*

Figs. 5.1 and 5.2 show that this is also the case; in a belt along the equator the temperature is higher than 25°C, near the poles the temperature sinks to the freezing point,

that is below -1°C. The belt of maximum temperature at the equator has its centre in the northern hemisphere when it is summer there (August), and in the southern hemisphere during the southern summer (February).

The presence of land increases the yearly temperature variations. For example, the water in the Red Sea, surrounded by desert land, is warmer in August than the water in the adjacent Indian Ocean, which is an open area. The average distribution of surface temperature for all oceans is shown in Fig. 5.3.

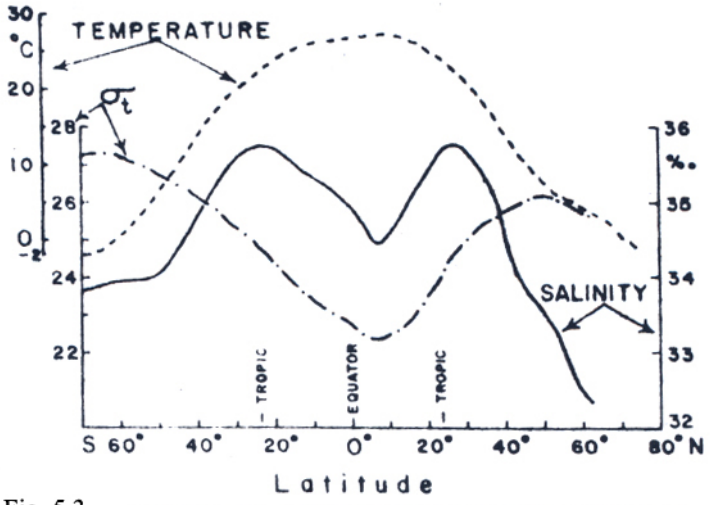

Fig. 5.3 *Variation with latitude of surface temperature, salinity and density (σ_t)—average for all oceans.*

The temperature at greater depths can be very different from the surface temperature. Ocean water can normally be divided into 3 layers: an *upper mixed layer* extending from the surface down to 50 - 200 m, a *transition layer* going down to somewhere between 500 and 1000 m, and a *deep layer* lying below the transition layer.

The upper mixed layer is characterized by having an almost constant temperature equal to the temperature at the surface, due to stirring and mixing induced by currents and waves. The transition layer, as the name implies, is a gradual transition between the temperatures above and below. This layer is therefore also called the *thermocline*. In the deep layer the temperature will only decrease slowly with increasing depth.

The shape and seasonal variation of the vertical temperature profile depend on the latitude (Fig. 5.4). Near the equator the surface temperature is high and varies little from summer to winter. Therefore, there will always be a big difference between the upper mixed layer and the deep layer. At middle latitudes the mixed layer will not be as warm, especially

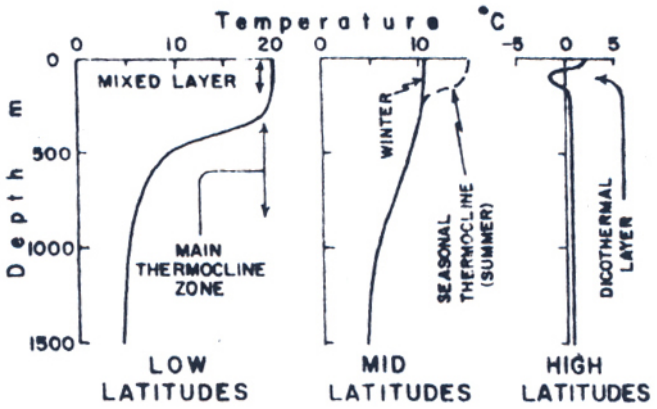

Fig. 5.4 *Typical mean temperature profiles in the open ocean.*

during the winter, so the difference between the two layers will be smaller and the thermocline less clearly defined. However, in the summer the mixed layer is heated by the sun, creating a seasonal thermocline. The same seasonal dependence is seen in the polar regions, but there the winter cooling can be down to the freezing point, resulting in a mixed layer being colder than the deep layer. Here the mixed layer is often called the *convection layer* because the process of vertical convection mixes the water. In the winter the temperature therefore will increase with increasing depth in the thermocline. In the summer there are two thermoclines, one on each side of a temperature minimum (Fig. 5.4).

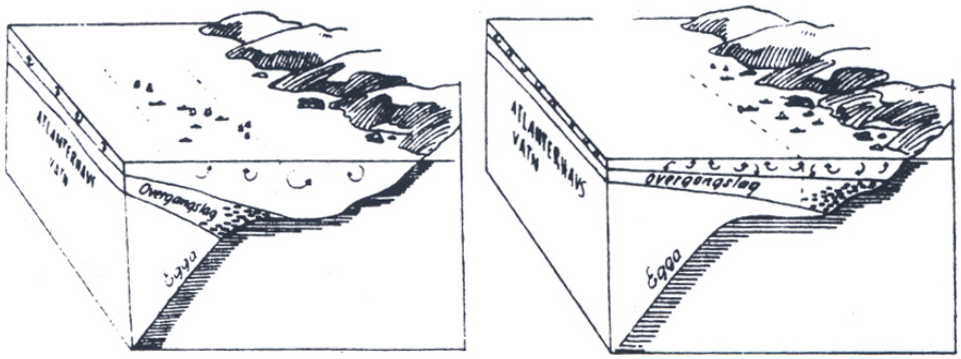

Fig. 5.5. (left) When the convection layer is thick, the transition layer is deeper down, and the cod is found far from land, that is closer to the continental slope. (right) When the convection layer is thin, the transition layer will be closer to the surface and the cod will thus be found closer to the land.

If the upper mixed layer is thin, then the amount of heat it receives in the summer will produce a higher temperature than if the same amount of heat should have been distributed over a thicker layer. For a thin upper layer there will also be a greater cooling during the winter. In the shallow Norwegian Coastal Current outside the West Coast of Norway, the

temperature is higher at the same latitude than in the deeper Norwegian Atlantic Current in the summer, while the opposite is the case in the winter.

The thickness of the convection layer that develops during the winter plays an important role for our fisheries (Fig. 5.5). In Lofoten, the pelagic cod will only stay in water with a temperature between 4° and 6°C, and in February this temperature is only found in the transition layer between the warmer Atlantic (7°C-8°C) and the colder coastal water. If the upper convection layer is thin, then the transition layer will reach the bottom closer to land and the cod will be easier to catch.

5.2 Salinity Distribution

The factors that can influence the surface salinity out at open sea at low and middle latitudes are *evaporation*, which increases the salinity since only water and not salt evaporates, and *precipitation*, which lowers the salinity. *Condensation* at the surface only happens on such a small scale that it can be ignored. Closer to the shore the supply of freshwater from *river runoff* may also have an effect on the salinity

At high latitudes an additional factor is the *freezing*. When seawater freezes, the ice will likely contain less salt than the water had originally, and the remaining salt in the ice will be separated out with time. In this way the freezing of ice leads to an increase of salinity in the surrounding water that has not yet frozen. This process is important for formation at the surface of deep and bottom water, but its effect on the surface salinity is so local that we will not discuss it here. The opposite process of freezing is the *melting* of ice, which reduces the salinity. The most significant influence on the surface salinity in the Arctic Sea is neither evaporation, precipitation nor freezing, but river runoff.

Precipitation has its maximum in the low at the equator (Fig. 5.6), it obtains minima in the high-pressure belts at 30°N and S, and it has lesser maxima near the beginnings of the low-pressure zones at 50° N and S. As mentioned earlier, evaporation has a minimum at the equator, maxima in the high pressure belts at 30°N and S, and then decreasing values as we move towards the poles. The difference between evaporation and precipitation gives the net water loss from the surface. In Fig. 5.6 we see that the surface receives up to 60 cm per year at the equator, while it loses up to 80 cm in the high-pressure belts. From about 40° to the poles, precipitation is greater than evaporation. Salinity, for the most part, follows the curve for evaporation minus precipitation. The influence of the river runoff in the Arctic Sea is evident.

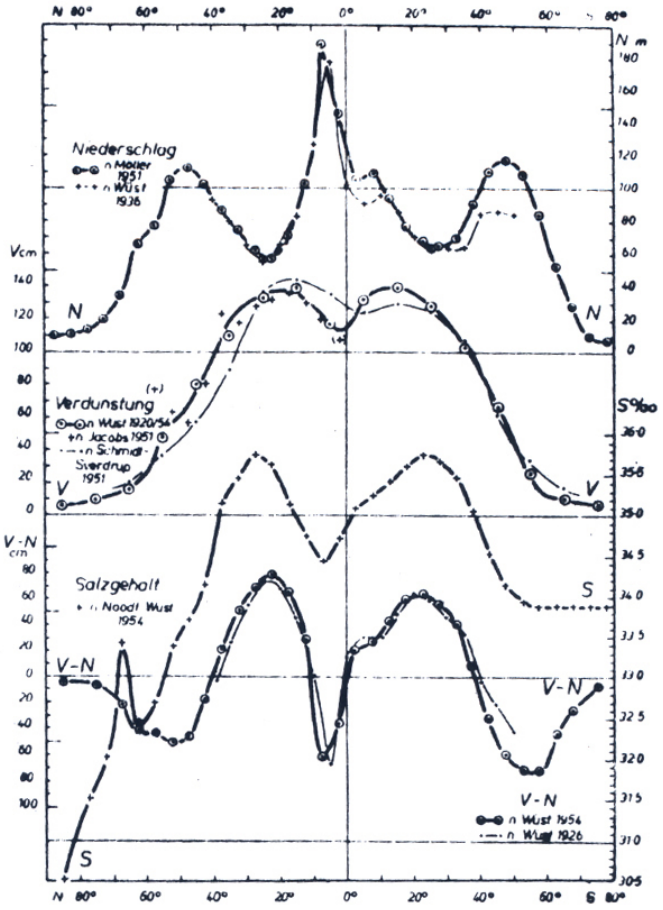

Fig. 5.6

Zonale Verteilung von Niederschlag N, Verdunstung V, $V-N$ und Oberflächensalzgehalt S im Weltmeer *einschließlich* der Nebenmeere (nach MÖLLER, JACOBS, SCHMIDT-SVERDRUP, NOODT und WÜST).

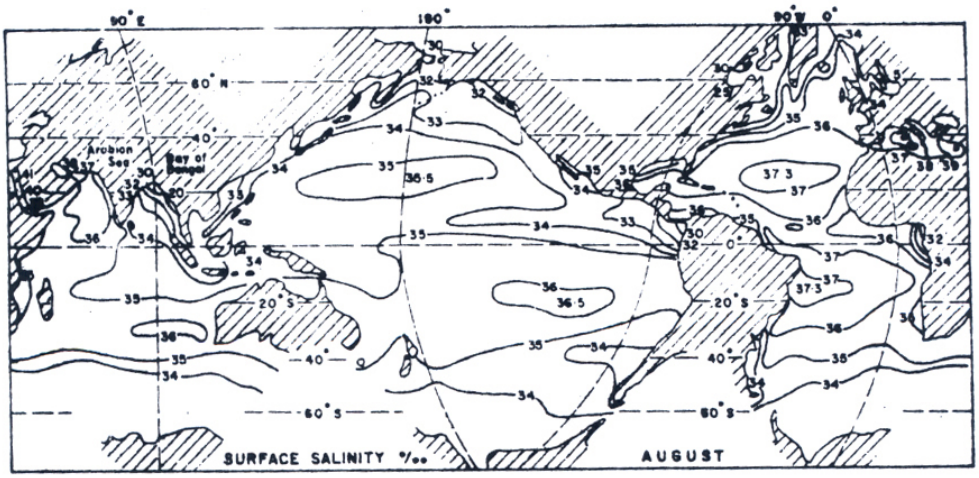

Surface salinity of the oceans in August.

Fig. 5.7

We can see the same in Fig. 5.7: a small minimum near the equator of 34-36, two maxima at 20°-30°N and S of 35-37, and then gradually decreasing salinity towards the poles. The maximum salinity is over 41 and is found in the Red Sea, where the surrounding dry and warm land leads to an extra high evaporation. Local minima can be seen at the mouths of the Ganges, Niger-Congo and the large Siberian rivers. Another reason for local minima is upwelling, a phenomenon that will be discussed in Chapter 7.2.

Fig. 5.8 provides examples of typical vertical salinity profiles at different latitudes. Except for the higher latitudes, where salinity increases with depth, salinity will usually decrease when depth increases.

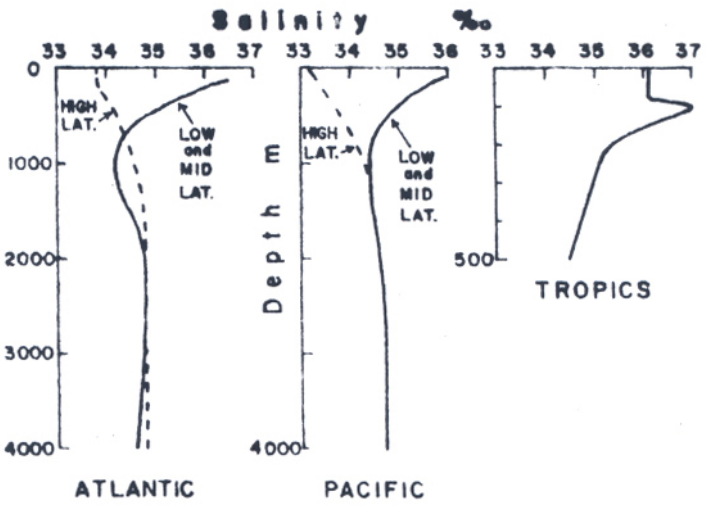

Fig. 5.8 *Typical mean salinity profiles in the open ocean.*

5.3 Density Distribution

The natural variations of the surface temperature out at open sea have a greater effect on the density than the variations of salinity. Because an increasing temperature reduces the density, the distribution of surface density over the various latitudes will almost mirror the corresponding temperature distribution (Fig.5.3). Surface density has a minimum at the equator and two maxima at 50°-60°N and S, and then it slowly decreases towards the poles.

Especially in the warmer latitudes, the surface water is light and the density increases strongly with increasing depth (Fig. 5.9). Down in the deep water, density is more constant. The sharp transition layer of density called the *pycnocline* is of great importance for many of the physical processes in the sea. The pycnocline functions as a barrier between the upper

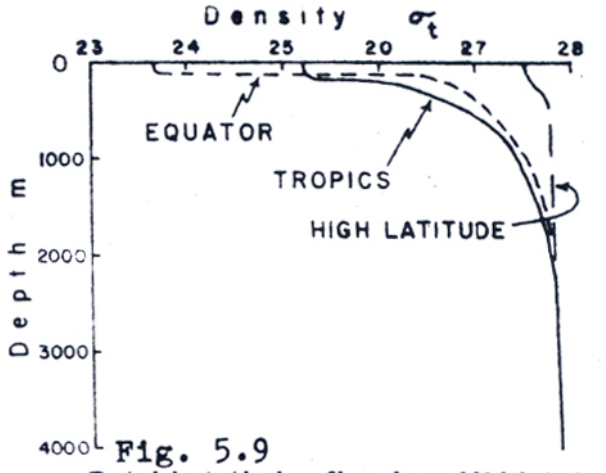

Fig. 5.9

Typical density/depth profiles at low and high latitudes.

light water and the deeper heavy water. The density difference makes it difficult for the upper layer to mix with the lower layer, and it prevents the transfer of kinetic energy from the surface to the deeper layers. That is why deep and bottom water can only be formed in areas where the surface water is so cold that the pycnocline becomes very weak. It should be noticed that out in the open sea where the temperature usually determines the density, the thermocline and the pycnocline are likely to mirror each other.

6. EQUATIONS AND MODELS FOR MOTION IN THE SEA

6.1 Transformation of Newton's Second Law

The motions in the sea have to follow the equation of continuity, which expresses that the mass is constant. As long as the density of the water particles does not change, there has to be the same amount of water flowing out of a volume unit as there is flowing in. We will not deduce the mathematical expression for this principle, but an integrated form of the equation has already been presented in Chapter 4.3 as the volume budget.

In addition to fulfilling the equation of continuity, the motions of the sea must also follow Newton's 2. Law:

$$\vec{a}_a = \frac{1}{m}\sum \vec{K} \tag{6.1}$$

where the term on the right side is the sum of the forces acting on the mass *m*, and $\vec{a}_a$ is the resulting *absolute acceleration*. By absolute acceleration we mean acceleration in a coordinate system that is fixed relative to space (an *inertial reference frame*). In such a system all acting forces will have opposite forces within the system of equal magnitude (Newton's 3. Law: *action equals reaction*), and all masses will follow Newton's 1. Law (the law of inertia). On the other hand the description of motions on our rotating earth will become very complicated in such a coordinate system, and it is more practical to use a local coordinate system where the *vertical* is always pointing towards the centre of the earth, and where the *horizontal* coordinates always are parallel to the surface of the earth. In this new coordinate system the absolute acceleration has to be substituted by four other terms:

$$\vec{a}_a = \vec{a}_o + \vec{a}_{ce} + \vec{a} + \vec{a}_v \ . \tag{6.2}$$

The new terms are

$\vec{a}_o$: the acceleration of the earth's centre in the absolute coordinate system.

$\vec{a}_{ce}$: the centripetal acceleration that all points on the earth are experiencing due to the earth's rotation.

$\vec{a}$: the acceleration relative to our new coordinate system.

$\vec{a}_v$: a correction term due to mass points moving with a velocity in our new coordinate system.

The right side of equation (6.1) contains the forces that can act on a mass of water in the sea:

$$\frac{1}{m}\sum \vec{K} = \vec{b} + \vec{F} + \vec{G}_e + \vec{G}_m + \vec{G}_s \tag{6.3}$$

These are

$\vec{b}$: pressure force per mass unit.

$\vec{F}$: frictional force per mass unit.

$\vec{G}_e$: gravitational force from the earth per mass unit.

$\vec{G}_m$: gravitational force from the moon per mass unit.

$\vec{G}_s$: gravitational force from the moon per mass unit.

Substitution from (6.2) and (6.3) in (6.1) results in

$$\vec{a}_o + \vec{a}_{ce} + \vec{a} + \vec{a}_v = \vec{b} + \vec{F} + \vec{G}_e + \vec{G}_m + \vec{G}_s \tag{6.4}$$

which may be sorted and written as

$$\vec{a} = \vec{b} - \vec{a}_v + \vec{F} + (\vec{G}_e - \vec{a}_{ce}) + (\vec{G}_m + \vec{G}_s - \vec{a}_o) \tag{6.5}$$

The negative accelerations $-\vec{a}_v$, $-\vec{a}_{ce}$ and $-\vec{a}_o$ may be interpreted as *fictional forces* (*inertial forces*). They are not real forces because they create no corresponding forces of equal magnitude and opposite direction in our coordinate system.

The acceleration $-\vec{a}_v$ is proportional to the velocity of the mass we are studying. It is called the *Coriolis force*, named after the French mathematician and engineer Gustave Gaspard Coriolis who in the beginning of the 18th century presented the mathematical expression for the force. Here we will simplify its notation by

$$\vec{c} = -\vec{a}_v \quad . \tag{6.6}$$

The Coriolis force is characterized by being proportional to the velocity, and its horizontal component is directed 90° to the right of the velocity on the northern hemisphere, and 90° to the left on the southern hemisphere. The magnitude of the horizontal component is usually written as *fv*, where *v* is the velocity and *f* is the Coriolis parameter, defined as

$$f = 2\Omega \sin\phi \tag{6.7}$$

Here Ω is the angular velocity of the earth and ϕ is the latitude. The value of Ω is $\Omega = 2\pi / 24 hours = 7.27 \cdot 10^{-5} s^{-1}$.

The negative value $-\vec{a}_{ce}$ of the centripetal acceleration is the centrifugal force (inertial force) that seems to be acting. When added to the gravitational force $\vec{G}_e$ of the earth, the resultant force vector becomes the observed gravity $\vec{g}$,

$$\vec{g} = \vec{G}_e - \vec{a}_{ce}. \tag{6.8}$$

The centrifugal force will have its maximum value at the equator and will be zero at the poles, and consequently $\vec{g}$ obtains its maximum at the poles and minimum at the equator. An added effect is caused by the slightly elliptic shape of the earth. Due to the rotation of the earth the equatorial radius is a little longer than the radius to the poles. The resulting effect on $\vec{g}$ is small, since $\vec{g}$ is only 0.5 % greater at the poles (9.83 m s^{-2}) than at the equator (9.78 m s^{-2}). The direction of $\vec{g}$ defines the vertical in our coordinate system.

In equation (6.5) the negative acceleration $-\vec{a}_o$ of the earth's centre was added to the gravitational forces from the moon and sun. The earth centre moves around the sun once a year, and it also completes a small closed orbit once a month due to the moon's circulation around the earth. The sum of the vectors is what we call the tidal force $\vec{T}$:

$$\vec{T} = \vec{G}_m + \vec{G}_s - \vec{a}_o \tag{6.9}$$

The absolute value of $\vec{T}$ is of the order of magnitude $\leq 10^{-7}g$. The tide will be discussed in Chapter 9.

Equation (6.5), representing the hydrodynamic equation of motion in oceanography, can now be written

$$\vec{a} = \vec{b} + \vec{c} + \vec{F} + \vec{g} + \vec{T} \tag{6.10}$$

It can be deduced that the pressure force is proportional to the gradient of the pressure. In other words; if the pressure is constant everywhere, there will be no force. Similarly the frictional force can be expressed as proportional to the second derivative of the velocity field. The friction term still represents an unsolved problem in all geophysical models where friction has a significant influence on the motion.

Equation (6.8) can with some approximations and simplifications be solved by advanced numerical models. In order to obtain analytical solutions, however, it is necessary to reduce the number of terms. In this way we can find analytic models describing idealized conditions in the sea. Some of these simplified models are:

Hydrostatic equilibrium: $0 = \vec{b} + \vec{g}$

Ekman spiral: $0 = \vec{c} + \vec{F}$

Geostrophic current: $0 = \vec{b} + \vec{c} + \vec{g}$

Equilibrium tide: $0 = \vec{b} + \vec{g} + \vec{T}$

Wind waves: $\vec{a} = \vec{b} + \vec{g}$

Inertial oscillations: $\vec{a} = \vec{c}$

The three first models will be briefly discussed in this chapter, and the fourth model in Chapter 9.

6.2 Hydrostatic Equilibrium

The simplest hydrodynamic state is the static one, where the velocity is zero everywhere. The acceleration as well as the Coriolis and friction force will then be zero, and if we can ignore the tidal force, then the equation of motion will express equilibrium between the gravity and the pressure force (Fig. 6.1).:

$$0 = \vec{b} + \vec{g} \ . \tag{6.11}$$

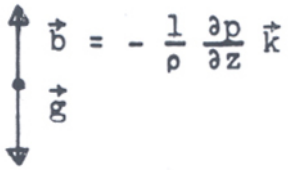

Fig. 6.1

Because gravity does not have any horizontal components, the pressure force cannot have it either, and the equation of motion will only have vertical components. We have already stated in Chapter 3.3 that an integrated form of the *hydrostatic equation* is

$$p(z) = g\int_{z}^{h} \rho(z)\, dz = g\,\overline{\rho}\,(h - z) \tag{6.12}$$

Here $p(z)$ is the pressure at depth z (z-axis positive upwards), h is the vertical coordinate of the surface where p=0, $\rho(z)$ is the density at depth z and $\overline{\rho}$ is the mean density between z and h. Equation (6.9) expresses that the *hydrostatic pressure* at depth z is equal to the weight of the

water column above *z*. The hydrostatic pressure is one of the most used simplifications in physical oceanography, and it may be a satisfactory approximation of the pressure even if there are velocities present.

We will now look at how horizontal pressure forces may originate in the sea when the pressure is hydrostatic. Let us assume that the density is the same everywhere and that equation (6.9) applies. The only way that the pressure at the two different points *A* and *B* in the same horizontal plane (Fig. 6.2) could be different would be if the surface was at different heights over the two points, or in other words that the surface was sloping from *C* to *E*. In Fig. 6.2 the pressure at *B* is greater than the pressure at *A*, and we then have a pressure force directed from *B* towards *A*.

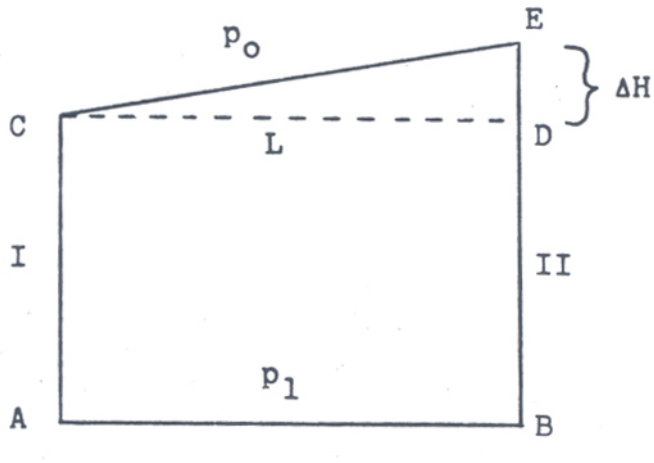

Fig. 6.2

However, if the density is not constant, this is not necessarily the case. If the ratio BE/AC between the verticals is not too great, then the density in the water column over *A* could be so much greater than in the water column over *B* that the hydrostatic pressure in *A* became equal to or greater than the pressure in *B*. In general, if we know the density field in the sea and the slope of the surface, then we are able to calculate the resulting hydrostatic pressure forces in all directions.

6.3 Geostrophic Currents

In the large-scale circulation of the world's oceans the accelerations are normally small. If we ignore these, as well as the tidal and frictional forces, the equation of motion will be reduced to

$$0 = \vec{b} + \vec{c} + \vec{g} \tag{6.13}$$

Because the Coriolis force $\vec{c}$ is a horizontal vector, it is only the vertical component $\vec{b}_v$ of the pressure force that balances the gravity $\vec{g}$ along the *z*-axis (: hydrostatic equilibrium). The horizontal pressure force $\vec{b}_h$ needs to be directed opposite to the Coriolis force, and due to this the two forces stand at right angles to the velocity vector (Fig. 6.3).

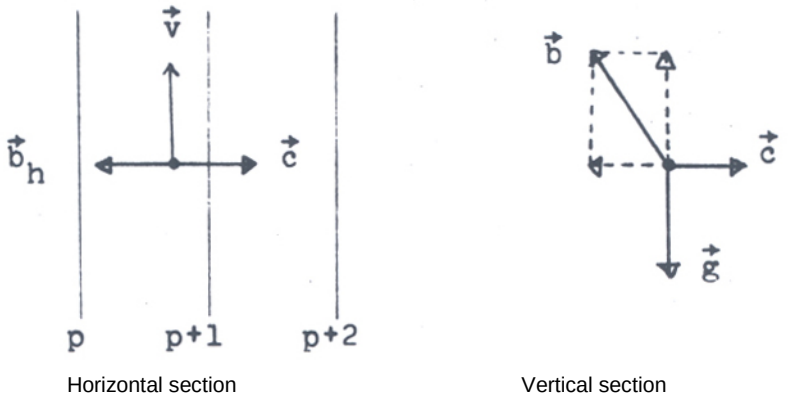

Fig. 6.3

As we have mentioned earlier, in the northern hemisphere the Coriolis force will be directed at right angles to the velocity vector. The horizontal pressure force goes from higher to lower pressure, at a right angle with the isobars, from the right towards the lower pressure. This implies that with *geostrophic equilibrium* (equilibrium between the Coriolis and pressure forces) the *geostrophic current* will follow the isobars, with the higher pressure on the right side (the northern hemisphere).

We can further conclude that if the isobaric surface is horizontal in a point, then the horizontal pressure force $\vec{b}_h$ will equal zero; so that no geostrophic current can be set up. Similarly it may be concluded that when there is no geostrophic current in a point, then the isobaric plane through that point is horizontal. When the surface of the sea can be considered as an isobaric plane, then it follows that if we have a geostrophic current, the surface will slant up towards the right, seen in the direction of the current. If the slope of the surface is φ, then the component of the Coriolis force in this plane, $c\cos(\varphi) = fv\cos(\varphi)$, must balance the component of the gravity, $g\sin(\varphi)$ (Fig. 6.4):

$$fv\cos(\varphi) = g\sin(\varphi) \tag{6.14}$$

or

$$v = \frac{g}{f}\tan(\varphi) \tag{6.15}$$

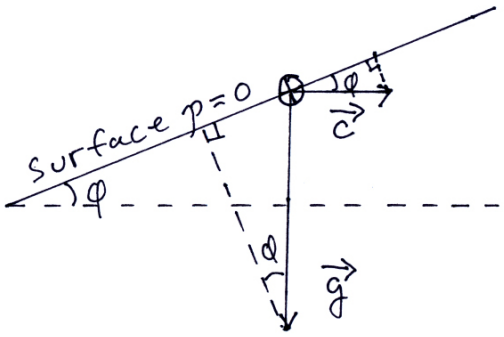

Fig. 6.4

Equation (6.15) implies that in all areas where we know the slope of the oceans from remote sensing by satellites, we can in principle calculate the corresponding geostrophic currents.

6.3 Wind Currents

The simple model for geostrophic currents assumes a balance between the Coriolis force and the horizontal pressure force, and that the friction is so small compared to them that it can be ignored. However, it seems reasonable that if the wind shall be able to generate any significant current in the water mass, frictional forces between the wind and the ocean surface and within the water mass itself have to be included in the model. If the frictional force is going in the opposite direction of the velocity (this is not necessarily the case), then the velocity will no longer follow the isobars, but will turn an angle towards the lower pressure (Fig. 6.5).

We can assume that we have the simplified case where there are neither any accelerations, tides, or horizontal pressure forces, implying a balance between the Coriolis force and the frictional force. The frictional force will then have to be perpendicular to the velocity (Fig. 6.6), which can seem to be both unnatural and impossible since we normally think of the frictional force as directed opposite to the movement. In most cases this is also correct, but if the velocity changes direction with increasing depth, then the frictional forces at the top and bottom of a water volume will not be completely opposite one another but deviate

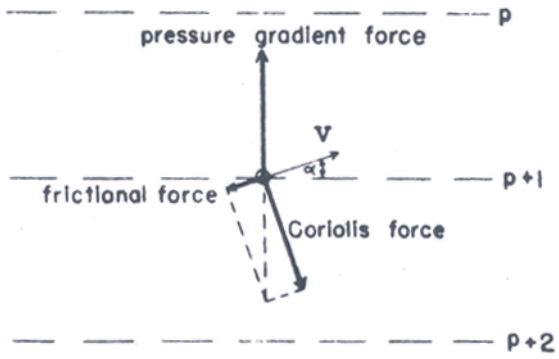

Fig.6.5 Balance among pressure-gradient, Coriolis, and frictional forces

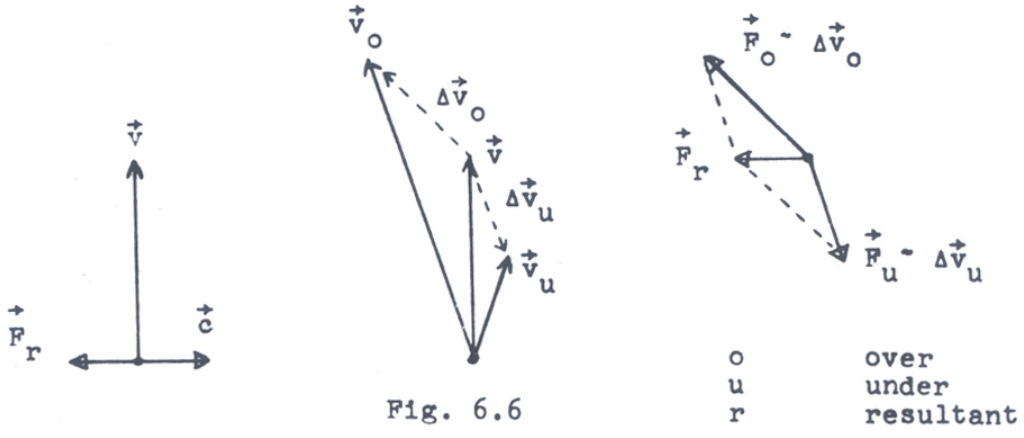

Fig. 6.6

from a 180° angle. The resultant of these two forces may be a net force that stands perpendicular to the average velocity of the water volume (Fig.6.6). Here we will not go into the mathematical solution of the problem, but only mention that the result is a rotation to the right and an exponential decrease of the velocity with increasing depth in the northern hemisphere. The velocity of the surface water will be directed 45° to the right of the wind direction, and the net volume transport will be directed 90° to the right of the wind.

Nansen observed how the ice in the Polar Sea did not drift exactly in the direction of the wind, but rather to the right of it. He assumed that this was caused by the earth's rotation, but because he was not a mathematician, he gave the problem to Valfrid W. Ekman, who in 1905 came up with the solution that is now called the *Ekman spiral* (Fig. 6.7).

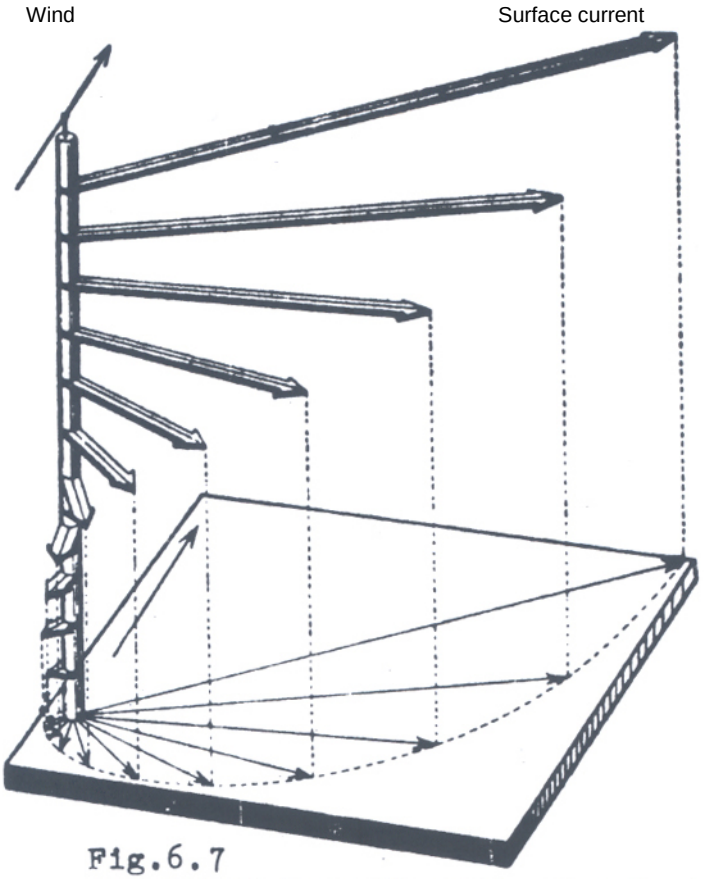

Fig.6.7
Vertical structure of a pure drift current (according to Ekman).

If a wind is blowing towards the north along the west coast of Norway, the water will be carried partly in the northern direction, and partly piled up against the coast (to the right of the wind's direction). One the other hand, if the wind is blowing towards the south, then the water will be transported partly southwards and partly away from the land (to the right of the wind). In order to replace the surface water that has been transported away from the coast, water will stream up from the layer below the surface layer (Fig. 6.8).

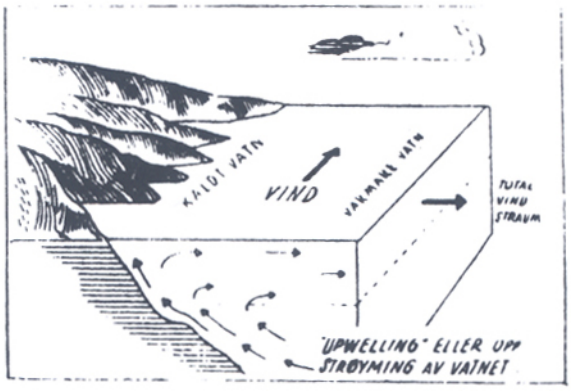

Fig. 6.8. When the wind current transports the surface waters away from the coast, upwelling from deeper layers will occur close to the coast.

This phenomenon, which is called *upwelling*, is quite important in many areas. For example, it determines fish and guano production outside Peru and Chile, where the upwelling water contains large amounts of nutrients for plankton, which in turn is the basis for fish and bird life.

While a geostrophic current theoretically can extend from the surface down to the ocean bottom, a wind current is limited to a top layer, and the thickness of this layer (defined as the depth where the current has turned 180° from the surface current) will depend on the wind force, the latitude, and the density stratification. Near the equator the wind currents can be 100 -200 m deep, at our latitude they can be maybe 50 m deep. Still, the wind currents may have indirect effects that are just as important as the direct ones:

We have said that the wind sets up a surface current which in the northern hemisphere is directed 45° to the right of the wind. Apparently this is not in agreement with Figs. 7.1, 7.2, and 7.3 in the next chapter, where it is seen that the currents and winds are moving in the same directions. However, we have to remember that the simple model for wind current that has been presented presumes that there are no pressure forces present. When the wind generates a current, after awhile this often results in a piling up of water in one place and a loss of water in another. This again can create new pressure forces that start up new currents, and when all of this has stabilized we can often end up with a current system that runs much deeper than the original wind current. The direction of the current can become more like the direction of the wind, while the energy used will be supplied by the wind as before.

The circulation in the world’s oceans is controlled by a complicated system of pressure, friction, and Coriolis forces, as well as "inertial forces". The large current systems, which make up the horizontal circulation, will for the most part be maintained by the large wind systems.

7 CIRCULATION OF THE OCEANS

7.1 Oceanic Gyres

We have already looked at an idealized picture of the pressure and wind systems. Reality is somewhat different. While the sea acts as an equalizing factor for the climate, the effect of land is to increase the differences. In Oslo, for example, the difference between the extreme air temperatures in the summer and winter can be 50°, while the same difference out in the Norwegian Sea is 20°. Therefore, in the course of a year, the pressure and wind conditions change more over land than over the sea. Fig. 7.1 and 7.2 show the most prevailing surface winds in January and July. For example, in January, cold and heavy air will create an anticyclonic gyre over Central Asia, while in July the air is warm and light and the wind system is cyclonic. However, over the ocean the characteristic features will be much more the same throughout the year. The most important exception is the Indian Ocean where the monsoon and the resulting currents change direction from summer to winter. If we look at Fig. 7.3 and compare it to Fig. 7.1 and 7.2, we can see that the major gyres in the world oceans mirror similar gyres in the wind system. Around the high pressures at 30°N and S, there are anticyclonic circulations. In the low pressure zone at 60°S there is an unbroken belt of westerly wind and a similar west wind drift in the ocean. The same type of west wind drift can be found in the oceans at 60°N, but the continents prevent a continuous circulation. We are now going to take a closer look at the different sea areas.

Atlantic Ocean

The current system in the Atlantic Ocean is for the most part made up of two large anticyclonic gyres, with their centres in the high pressure zones at 30°N and S. Near the equator runs the *South Equatorial Current* towards the west until it hits the South American continent (Fig. 7.4). At this point it breaks off into two branches, one that goes north and one that goes south as the *Brazil Current*. Outside of Uruguay, the Brazil Current is forced away from the coast by a branch of the West Wind Drift which is moving north and is called the *Falkland Current*, and it moves eastward toward the Cape of Good Hope. There the *Benguela Current* continues northward along the African west coast and the gyre is closed again near the equator with the *Guinea Current*.

The northern branch of the South Equatorial Current runs together with the *North Equatorial Current* and form the *Guiana Current*, which goes into the Caribbean Sea and the Gulf of Mexico, and the *Antilles Current* that runs north from the Antilles. The easterly winds

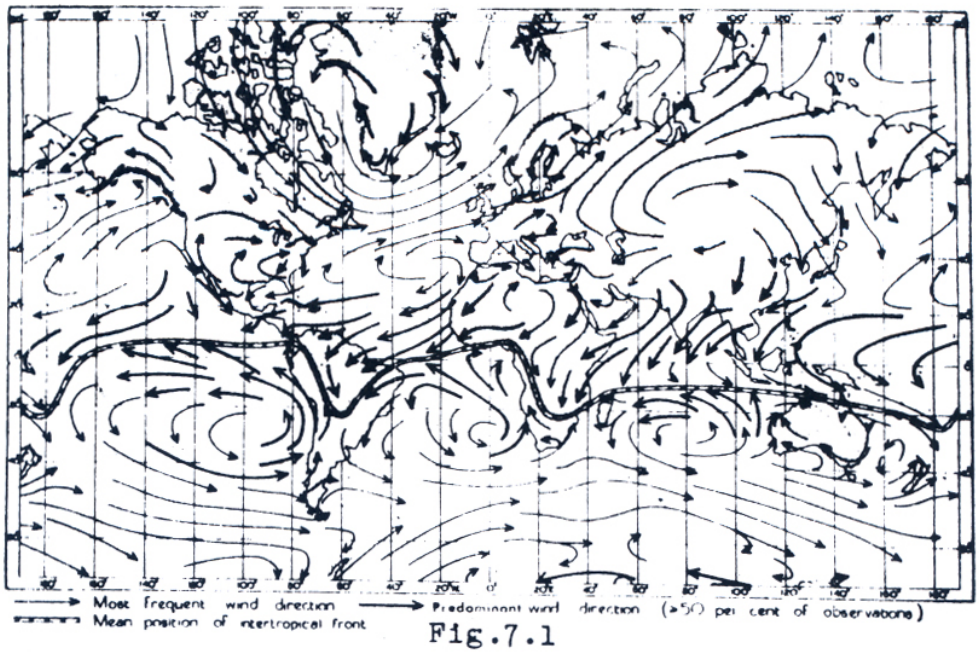

Fig.7.1

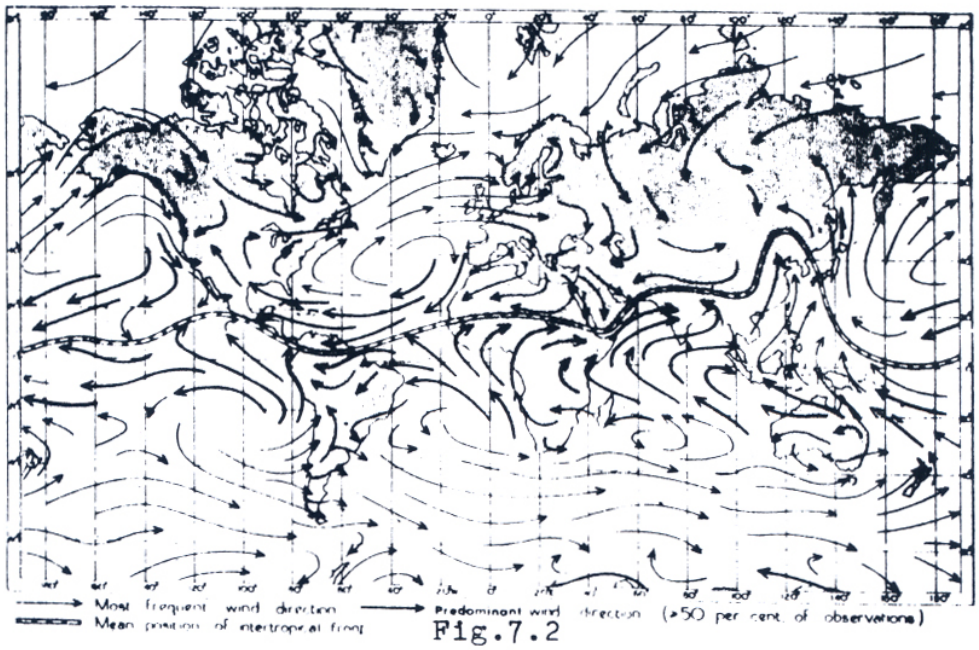

Fig.7.2

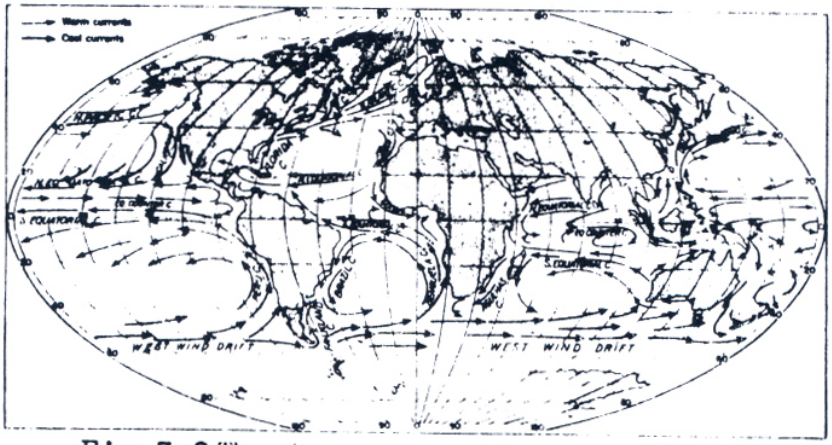

Fig.7.3 The main ocean currents of the world. (*After Schott.*)

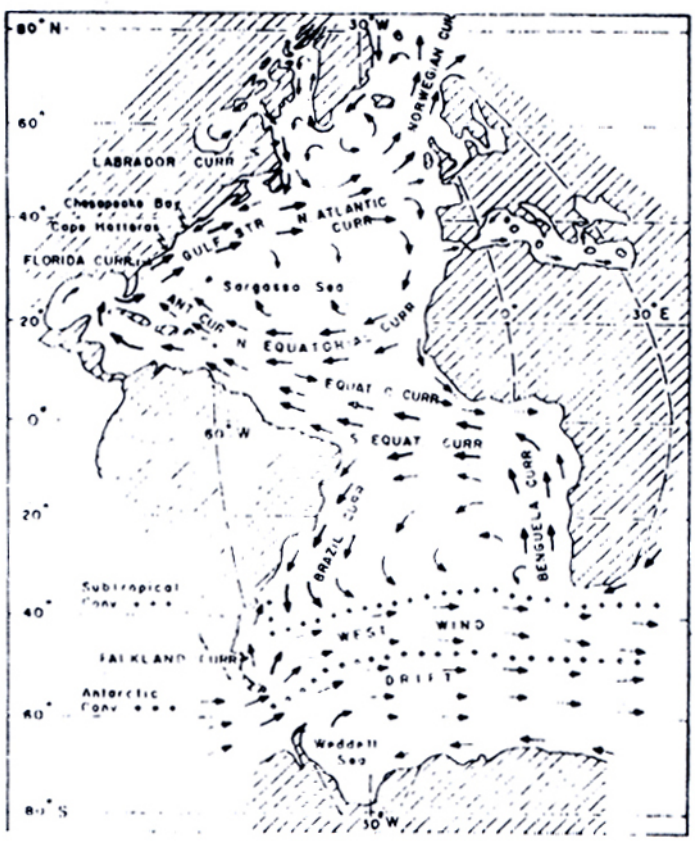

Atlantic Ocean— surface circulation.

Fig.7.4

in the area drive the Guiana Current into the Gulf of Mexico, where water is piled up. This excess of water can only escape through the Florida Strait as the *Florida Current*. Outside the strait, this current runs together with the Antilles Current and is then called the *Gulf Stream*. This follows the coast up to Cape Hatters where it begins to run northeast away from land. Up near Newfoundland, the Gulf Stream meets the cold *Labrador Current* and moves further northeast as the *North Atlantic Current*. (In everyday language, it is usually called the Gulf Stream all the way up to Svalbard, even though there is certainly very little left of the original water from the Mexican Gulf.) The North Atlantic Current again divides into two branches, one that continues towards the northeast and the Norwegian Sea, the *Norwegian Atlantic Current*, and one that turns south and runs along Portugal and Africa as the *Canary Current*. A small branch breaks off into the Mediterranean through the Gibraltar Strait. Outside of Africa the Canary Current closes the gyre with the North Equatorial Current. Between the two equatorial currents there is a smaller current moving eastward: the *Equatorial Countercurrent*.

The speed of the currents varies with the seasons and is influenced by the local pressure and wind variations. Even in the Florida Strait, there are days when the current goes in the opposite direction. This occurs when there is strong local low pressure over the Gulf of

Mexico. The depths of the currents not only vary, but they are difficult to estimate because there is a gradual transition of speed and characteristics in the water mass. Still, we will try to estimate some numbers. The gyre in the South Atlantic will be 200 m deep near the equator and 800 m deep further south. The greatest speed is found in the South Equatorial Current with 70 cm s^{-1}. The North Equatorial Current goes about as deep as the southern but it only runs about half as fast with 35 cm s^{-1}. The Florida Current is both faster, 160 cm s^{-1}, and it reaches deeper, to about 800 m. The Gulf Stream has speeds of up to 250 cm s-1, which is among the fastest found in the oceans. The mean speed, however, will be about 150 cm s^{-1}. The Gulf Stream goes deep, down to 1000 m. In Table 7.1 some transports are estimated. The + sign means that the transport is calculated in to the centre of the gyre. The table indicates that the transport around the centre of the gyre is about 4 times greater in the North Atlantic than in the southern part.

Table 7.1	
South Equatorial Current +	**23 Sv**
Brazil Current +	**17 Sv**
Benguela Current +	**23 Sv**
Florida Current	**26 Sv**
Antilles Current	**12 Sv**
Gulf Stream +	**80 Sv**
Canary Current +	**60 Sv**

The transports in the table are based on a mixture of direct current measurements and geostrophic calculations. The surface of the sea does not need to slope much in order to cause strong geostrophic currents. Outside of Cape Hatteras, the Gulf Stream can obtain speeds of 250 cm s^{-1} if the surface slopes 2 cm per km across the current (Fig. 7.5).

The interior of the gyre in the North Atlantic is called the *Sargasso Sea*. According to old superstitions, this area was full of drifting seaweed, *sargassum*, which would fasten itself to the ships and keep them back, often causing a starving to death of the crew. In reality, this stagnant area is biologically almost a desert, free of nutrients and particles; making these waters some of the clearest in the world. A curious fact is that the Sargasso Sea is the spawning grounds of the European eel. There is seaweed here, but often so scattered that one has to search in order to find some of it. But we do know that this is a high pressure area with little wind, and that is the reason why so many ships came to their tragic end here.

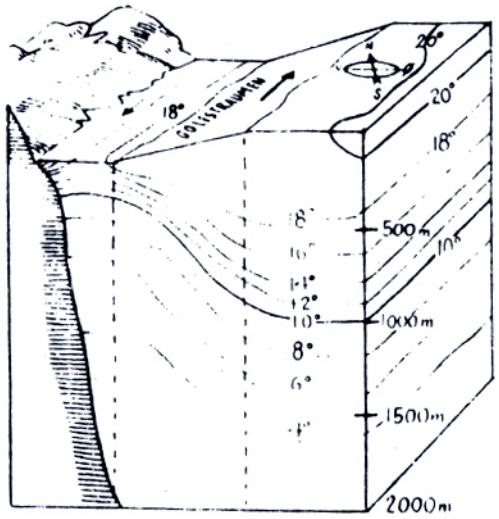

Fig. 7.5. Temperature conditions and surface slope across the Gulf Stream outside Cape Hatteras. The slopes of isotherms and surface are greatly exaggerated.

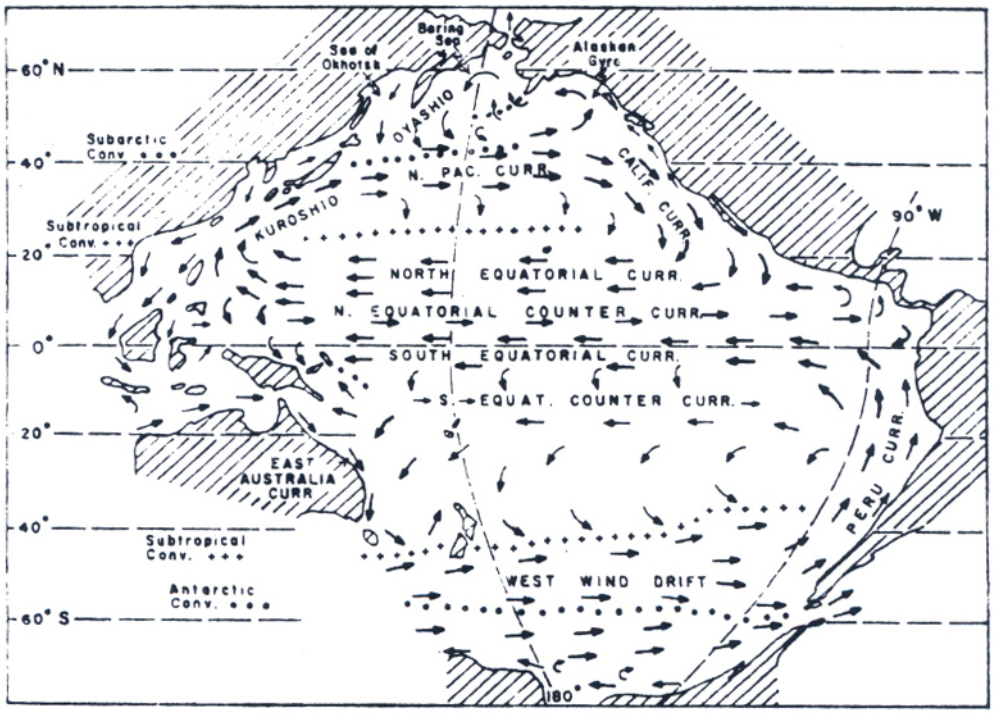

Pacific Ocean—surface circulation.

Fig. 7.6

Table 7.2	
Kuroshio	**65 Sv**
North Pacific Current (west wind drift)	**35 Sv**
California Current	**15 Sv**
North Equatorial Current	**45 Sv**
North Equatorial Countercurrent	**25 Sv**
Antarctic Circumpolar Current	**100 Sv**
Peru Current	**18 Sv**
Equatorial Undercurrent	**40 Sv**

Pacific Ocean

The patterns of the surface currents in the Pacific Ocean are very similar to those in the Atlantic Ocean (Fig. 7.6). In the southern part the anticyclonic gyre consists of the *South Equatorial Current*, the *East Australia Current*, the *West Wind Drift*, and the *Humboldt* or *Peru Current* which closes the circulation. In the northern part the gyre consists of the *North Equatorial Current*, the dark blue *Kuroshio* (Japanese for "black current"), the *North Pacific Current*, and the *California Current*. The Labrador Current has its parallel in the greenish *Oyashio* (Japanese for "fertile current" or "parent current"). In contrast to the Atlantic Ocean there are two equatorial countercurrents: The *North Equatorial Countercurrent*, which has its parallel in the Atlantic Ocean and is the strongest, and the *South Equatorial Countercurrent*, which is much weaker.

At the equator, between 70 and 200 m depth and with a width of 300 km there is a strong countercurrent that was not discovered until 1952. It is called the *Equatorial Undercurrent* or the *Cromwell Current* and has speeds up to 150 cm s^{-1} and a transport of 40 Sv, making it one of the larger ocean currents. Similar currents were later found in the Atlantic and Indian Oceans.

The North Equatorial Current is wide and slow with speeds usually below 20 cm s^{-1}. The Kuroshio is about 400 meters deep, with speeds up to 150 cm/s. The speeds of the Peru Current and the South Equatorial Current are up to 30 and 100 cm s^{-1}, respectively. Several transport values are presented in Table 7.2.

Indian Ocean

The Indian Ocean is different from the Atlantic and Pacific in that at 20°N it is bordered by the Asian continent. Therefore the wind conditions and resulting surface currents will be partly dominated by the "land climate". From November to March cold air sinks down from the Himalayas as the *Northeast-Monsoon*. It functions in the same way as the northeast trade wind in the other world oceans, and therefore we also have an equatorial current system here with one equatorial current in the north and one in the south, as well as an equatorial countercurrent and undercurrent (Fig. 7.22). The difference is that the system has its centre south of the equator. The *North Equatorial Current* is usually called the *Northeast Monsoon Drift*. The anticyclonic gyre in the southern half of the ocean consists of the *South Equatorial Current*, the *Agulhas Current*, the *West Wind Drift* and the *West Australian Current*.

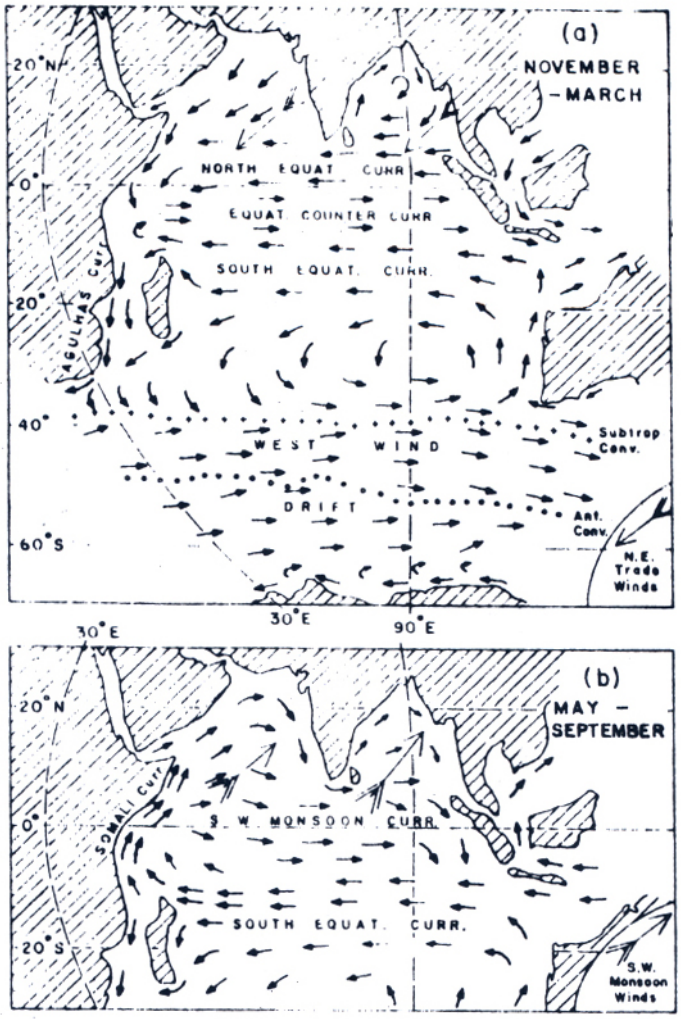

Indian Ocean—surface circulation.

Fig. 7.7

In April the continent begins to warm up, the warm air rises along the mountainsides and draws with it the air from the ocean, creating the *Southwest Monsoon*. The picture of the surface circulation is now significantly changed (Fig. 7.7). The Northeast Monsoon Drift towards the west is replaced by the *Southwest Monsoon Drift* towards the east, and the *Equatorial Countercurrent* disappears or cannot be distinguished from the Monsoon Drift. Along the African coast a strong north-going current is created, the *Somali Current*. In the period between May and September we have two opposing gyres in the Indian Ocean, but the centre of the northern one lies at 5°S, and there is only one equatorial current. Except for the Agulhas Current and the Somali Current, where the transports have been calculated to be about 50 and 65 Sv, respectively, we do not know enough about the Indian Ocean to estimate the different transports. However, the table below presents some numbers for the highest speeds in the major currents.

Table 7.3	
Somali Current	**250 cm s^{-1}**
Southwest Monsoon Drift	**150 cm s^{-1}**
Equatorial Countercurrent	**80 cm s^{-1}**
South Equatorial Current	**50 cm s^{-1}**
Agulhas Current	**200 cm s^{-1}**
West Wind Drift	**50 cm s^{-1}**
West Australia Current	**25 cm s^{-1}**

7.2 Surface Currents in Other Areas

Southern Ocean

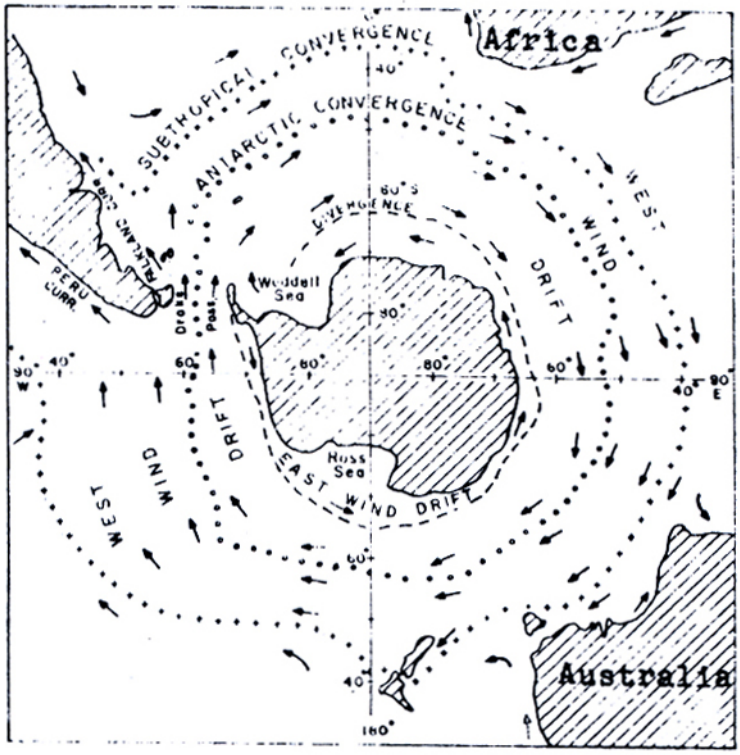

Southern Ocean surface circulation and mean positions of the Antarctic and Subtropical Convergences (Adapted from Deacon, "Discovery" Reports, by permission).

Fig. 7.8

The Southern Ocean is often not considered a proper ocean in itself, but is distributed on the other three great oceans: the Atlantic, the Pacific and the Indian Ocean. However, when we are looking at the surface currents, it is practical to regard it as a separate ocean of its own. It is bordered on the south by the Antarctic continent, and in the north the border can be set at the *subtropical convergence* around 40°S (Fig. 7.8). Over the South Pole there is a

cold high pressure that generates an anticyclonic wind, that is from east to west. The resulting current, which moves in a narrow belt around the ice cap, is called the *East Wind Drift*. (It moves towards the west). Further north we have the *West Wind Drift* in a considerably wider belt.

The speed in the West Wind Drift is not particularly high, lying between 4 and 15 cm s^{-1}. However, because the current runs so deep (even at 2000 m the speed is approximately 3 cm s^{-1}) it transports a very large quantity of water, up to 150-190 Sv (1 Sv = 1 Sverdrup = 1million m^3 s^{-1}, the unit is named after the Norwegian oceanographer Harald Ulrik Sverdrup), and this makes it the world's most powerful ocean current.

Mediterranean Sea

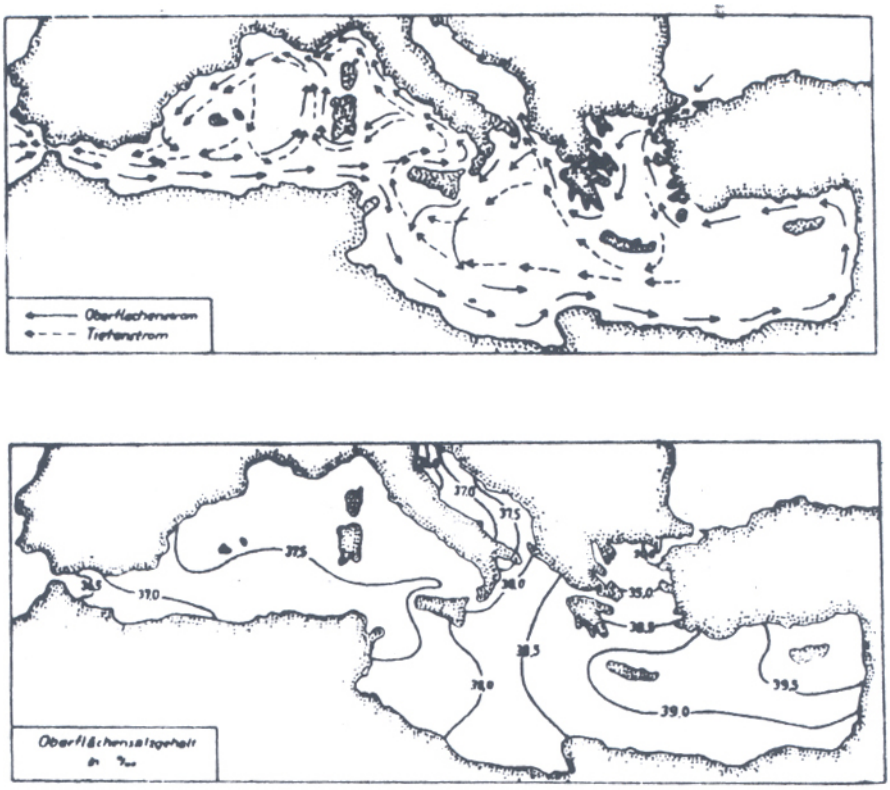

Fig. 7.9

Despite the large rivers that empty into the Mediterranean, there is still a net loss of fresh water due to the great amount of evaporation. If the water level is to remain constant, the loss needs to be compensated for by a current entering the Mediterranean through the Strait of Gibraltar. However, this implies that there is always more salt being added, and if the salinity shall remain unchanged, then it is necessary that some salt is taken out again through the Strait. That means that there must be two currents in this strait: One inwards with a certain volume and a certain salinity and one outwards with a somewhat less volume but a higher

salinity. By means of the volume and salt budgets, we can calculate these volumes if the fresh water loss and the salinities of the currents in the Strait are known. As the Atlantic surface water moves into the Mediterranean, its salinity increases (Fig. 7.9).

The connection between the Black Sea and the Mediterranean, which is called Bosporus, is both narrow and shallow. There only comes very little saltwater through the 30-40 m deep strait, and that is why the deep water in the Black Sea is stagnant with hydrogen sulphide from 200 m and downwards, and has a salinity about only 22.3.

Norwegian Sea

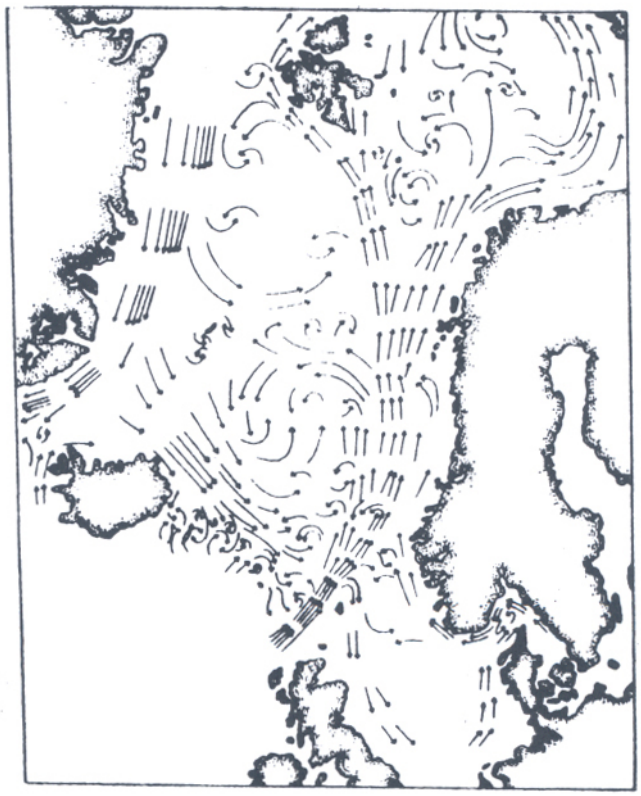

Fig. 7.10

According to the monograph "The Norwegian Sea", published by Nansen and Helland-Hansen in 1909, the *Norwegian Sea* is bordered in the north by the ridge between Greenland and Spitsbergen, in the east by Spitsbergen, the continental shelf along the Bear Island and the Barents Sea, and the Norwegian coast, in the south by the North Sea Plateau and the line Shetland - Faroes - Iceland - Greenland, and in the west by Greenland. Not all nations have accepted this definition, and often the area north of Jan Mayen is called the *Greenland Sea*, the areas around Iceland the *Iceland Sea*, and the rest the *Norwegian Sea*. The

sum of these areas then naturally becomes the *GIN Sea*. Lately the term the *Nordic Seas* has often been used for the same areas.

It was mentioned earlier that the North Atlantic Current splits into two branches, one going south and gradually becoming the Canary Current, and one going northeast towards the Norwegian Sea. The latter branch continues to divide into several branches, one being the *Irminger Current* which moves towards Iceland and there partly turns southeast until it is parallel with the East Greenland Current, and partly follows Iceland's west coast (Fig. 7.10). Another branch, and the most important one, is the *Norwegian Atlantic Current*, which enters the Norwegian Sea through the *Faroe-Shetland Channel*. This current is 600 m deep, the water has an average temperature of 7-9 °C and a salinity of 35.3-35.4, and the average speed of the surface current is about 30 cm s^{-1}. Transport estimates vary, and while 3 Sv was the established value 40 years ago, today a wider range from of 3 to 9 Sv seems to be reported.

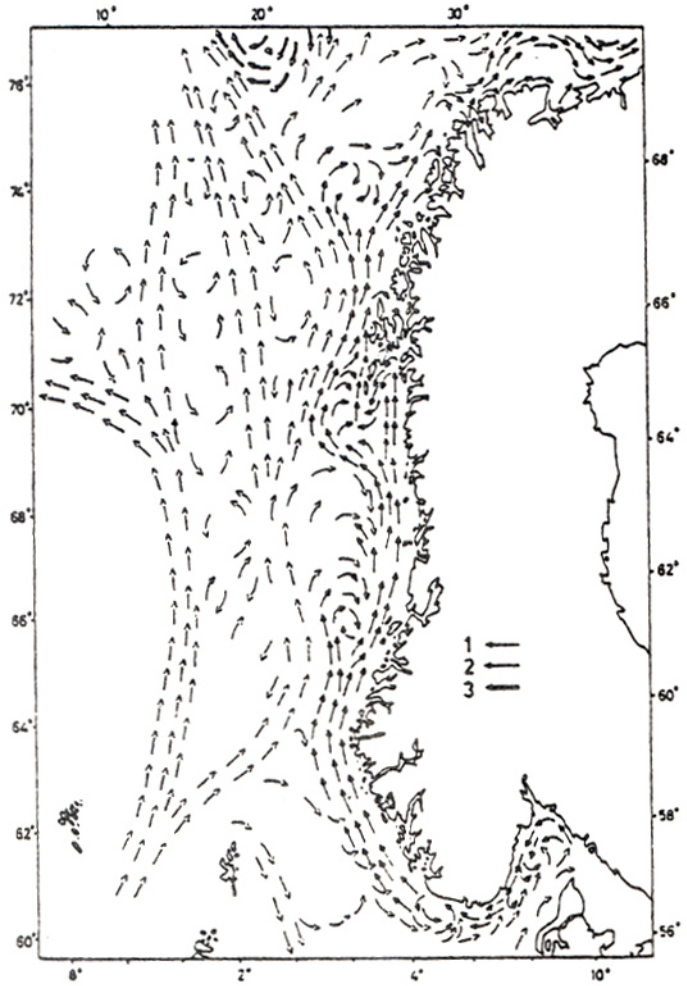

Fig. 7.11. Water types and currents. 1) Coastal water, 2) Atlantic water, 3) Polar water.

Some of the water transported through the Faroe-Shetland Channel spreads in over the North Sea banks, some water branches off and continues to the north towards the Jan Mayen

area (Fig. 7.11), while the main current follows the continental slope towards the north along the continental shelf as the *Norwegian Atlantic Current* (Figs.7.10-11). Gradually its water becomes colder and less saline. Outside of West Finnmark it splits in two: One branch continues eastward along the coast and into the Barents Sea as the *North Cape Current*. The other continues along the slope of the continental shelf west of Bear Island and Svalbard as the *West Spitsbergen Current* (Fig. 7.10, 7.21). The temperature is now below 5°C and the

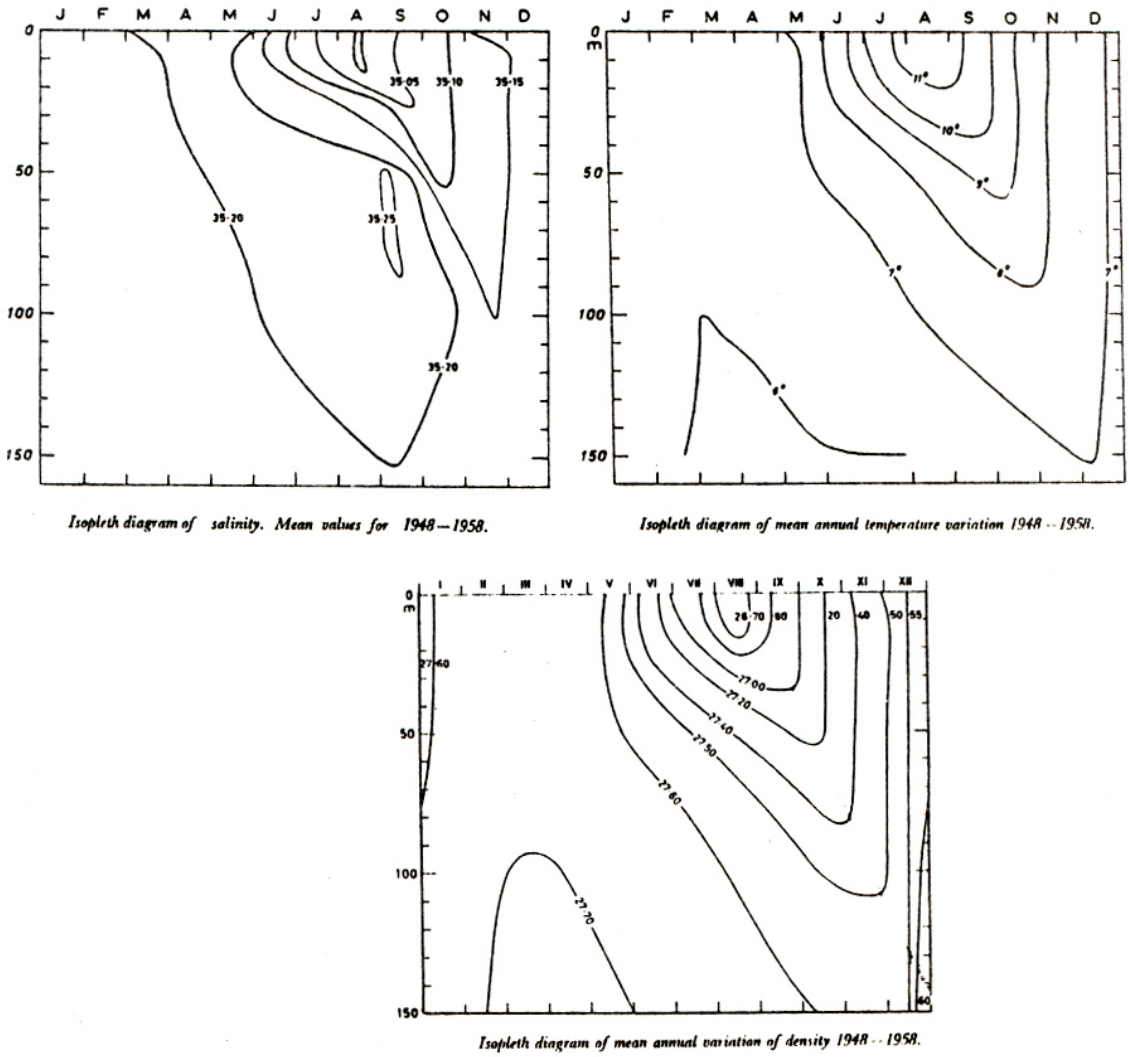

Fig. 7.12a, b, c

salinity below 35.15. North of Svalbard the current dives down under colder and less saline Arctic surface water and continues as an intermediate current across the Arctic Sea. In return comes the cold and less saline *East Greenland Current* which follows the coast of East Greenland down to Cape Farewell, turns around it and then continues northwards as the *West Greenland Current* (Fig. 7.22).

At the weather ship Polarfront (I and II) at 66°N, 2°E (Station M), diurnal oceanographic observations were made from 1948 to the end of 2009, making the series the longest in the world at a weather ship. Figs. 7.12a, b and c show the mean value of the observations from the first decade. We see how the upper mixed layer is hardly 20 m deep in August, while the thickness in January may be 10 times this value.

At other locations in the Norwegian Sea the vertical convection in winter may reach far deeper, and at a few places perhaps even down to the bottom. The gyre between Jan Mayen and Svalbard is such a place where the conditions for deep water formation are very favourable. By repeated coolings and ice freezings the surface water becomes so cold and saline, and thereby heavy, that it can sink to depths below 1500 m. It will then have a salinity of 34.92 and a temperature around -1 °C.

Baltic Sea

The Baltic Sea, like the Black Sea, only has a narrow connection to the oceans on the outside. The sill depth of the Sound and the Belts is 18 m, the average depth of the Baltic Sea is 65 m, and the maximum depth 460 m. The salinity is low, less than 16, and the surface salinity is usually below 10. However, unlike the Black Sea the Baltic does not have a stagnant water mass beneath the surface layer. This is due to the Baltic being so shallow, enabling tides and winds to stir up and mix the waters. Because the sea in addition to its shallow waters also has a low salinity, it freezes easily in the winter, especially in the northern part. On average there is 0.015 Sv (15000 $m^3\ s^{-1}$) of freshwater entering the Baltic Sea, and the double amount of seawater, 0.03 Sv, flowing out to the Kattegat. The *Baltic Current* follows the Swedish coast up to the Færder Lighthouse at the border between the Skagerrak and the Oslofjord, where it turns southwest along the Norwegian coast.

Norwegian Coastal Current

The extension of the Baltic Current is the *Norwegian Coastal Current* which follows the Norwegian Skagerrak coast from Færder to Lista, the southernmost point of Norway, turns gradually to the west and north and continues up along the West Coast to Stad where it meets the Norwegian Atlantic Current. From Stad and up to the Barents Sea the two currents run parallel to each other. The richest fishing in Norway takes place in the transition layers and mixing zones between the Atlantic and coastal waters.

At the Grip Bank just north of Stad the current splits into two branches: one following the coast and another following the continental slope. A similar splitting takes place south of

Lofoten (Fig. 7.11). North of Finnmark there are practically no differences between the Atlantic and coastal waters any more. The average speed in the coastal current is about 25 cm s^{-1}, but speeds of up to 1 m s^{-1} are sometimes measured. The transport of the current out of the North Sea is believed to be about 1 Sv.

The Norwegian Coastal Current is broad and shallow during summertime and narrow and deep during wintertime. Fig. 7.13 shows the mean monthly variation of salinity along the ferry route from Bergen to Newcastle. We see that coastal water with a salinity less than 32 extends farther to the west in May-June than in December. This movement, called the *lateral oscillation* by Nansen and Helland-Hansen, is very marked on the West Coast, but is thought to be smaller outside Northern Norway.

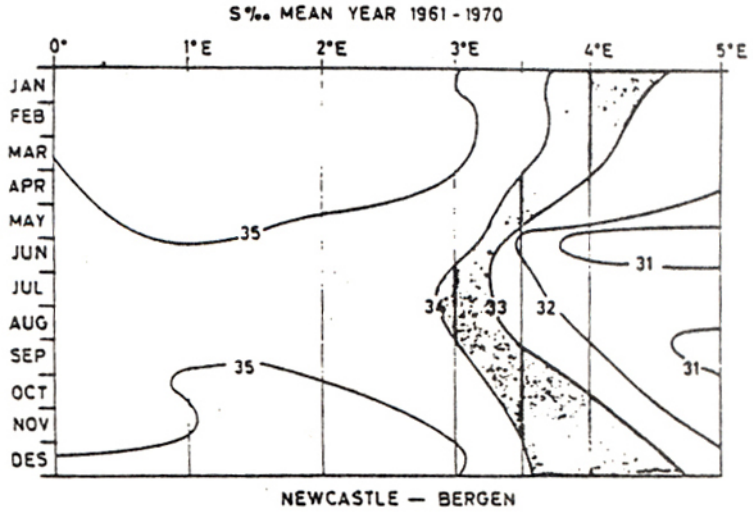

Fig. 7.13

In general the oceanographic conditions will vary significantly along the coast from Southern to Northern Norway. In the south the water masses will be clearly layered with water of low salinity at the surface lying over more saline and heavy water. The vertical differences of salinity and density are here so great that not even during the coldest winters will the surface layer become heavy enough to sink down and start a *vertical convection*. Only a thin upper layer (25 m) will soon obtain a temperature which is close to the air temperature (Fig. 7.14).

In Northern Norway, however, the water masses are far more homogeneous, and the vertical circulation caused by the winter cooling will reach deeper. Consequently the temperature may become almost constant from the surface down to more than 100 m depth (Fig. 7.15), implying that information about the temperature of the deeper layers can be obtained from the surface temperature.

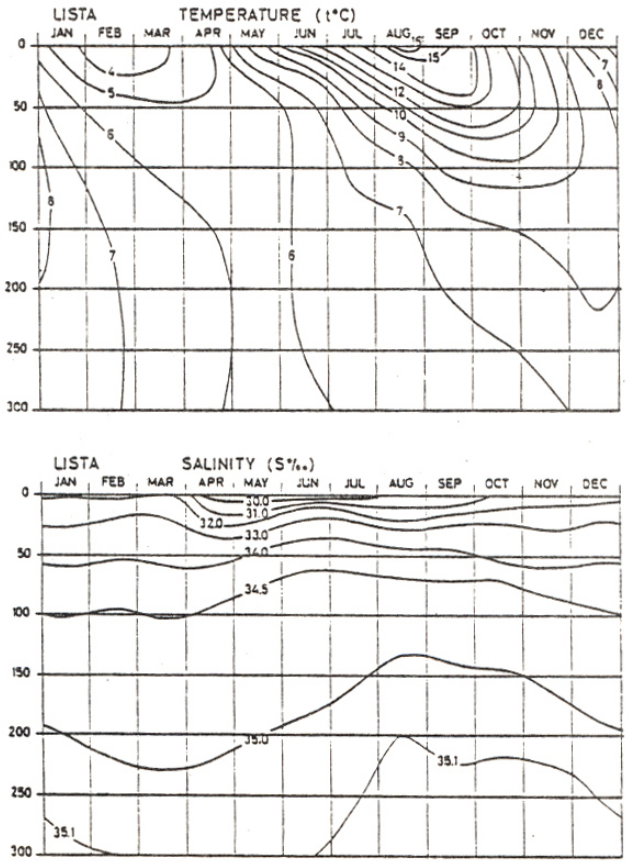

Fig. 7.14

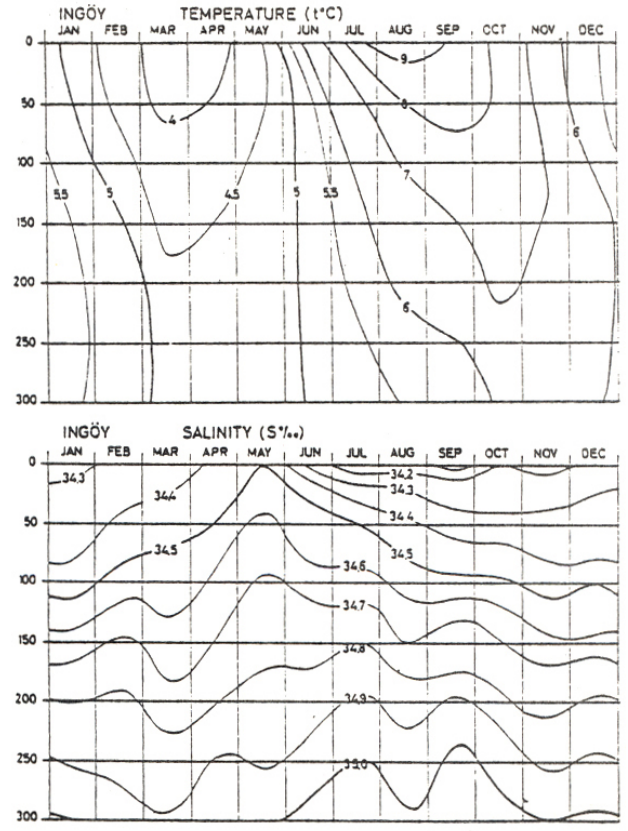

Fig. 7.15

The great vertical gradients of salinity observed in the southern part of the coastal current, have disappeared at Ingøy outside Finnmark. Fig. 7.15 shows that the salinity difference between 0 and 300 m has a maximum value of 1, while the same difference is obtained between 0 and 25 m at Lista (Fig. 7.14). Fig. 7.16 displays how the annual temperature difference decreases with depth at four stations along the coast. The stations having the greatest surface differences (creating larger vertical stability) also have the smallest differences at 300 m depth (due to the stability).

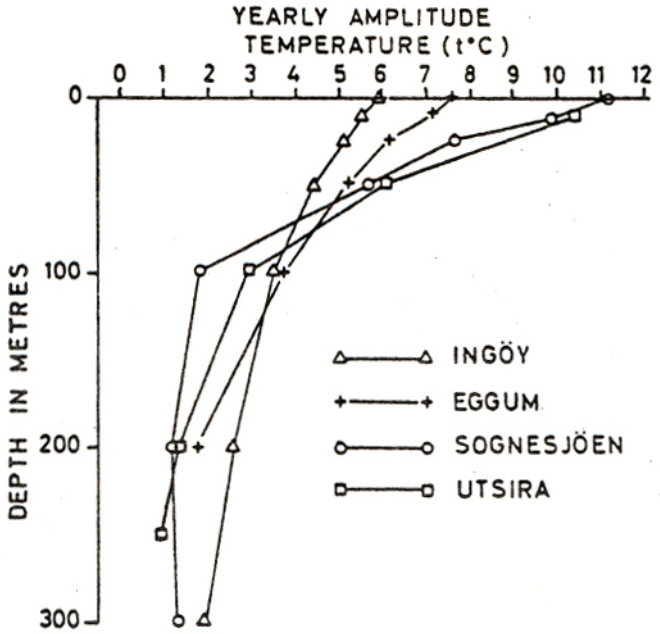

Fig. 7.16

North Sea

The depths conditions of the North Sea vary from 700 m in the Norwegian Trench to 10 m at the Dogger Bank (Fig. 7.17). The average depth is close to 100 m, and that means that the changing winds will have a great influence on the currents. The tides are also an important factor for the currents, especially near the English Channel, and they may contribute even more to the mixing than the wind-induced currents. Fig. 7.18 shows that the upper mixed layer in the central North Sea has a thickness of about 20 m in August. In the winter season, however, the conditions may be rather homogeneous from top to bottom. In the English Channel the strong tidal currents will create a vertical mixing that is almost independent of the season.

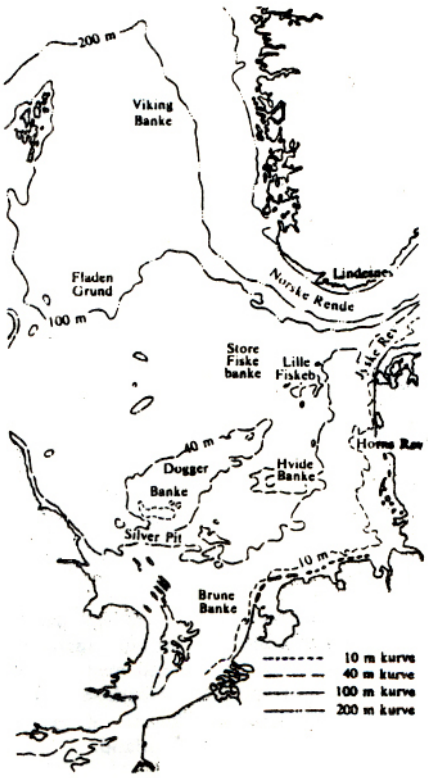

Fig. 7.17. Map of the most important fishing banks in the North Sea

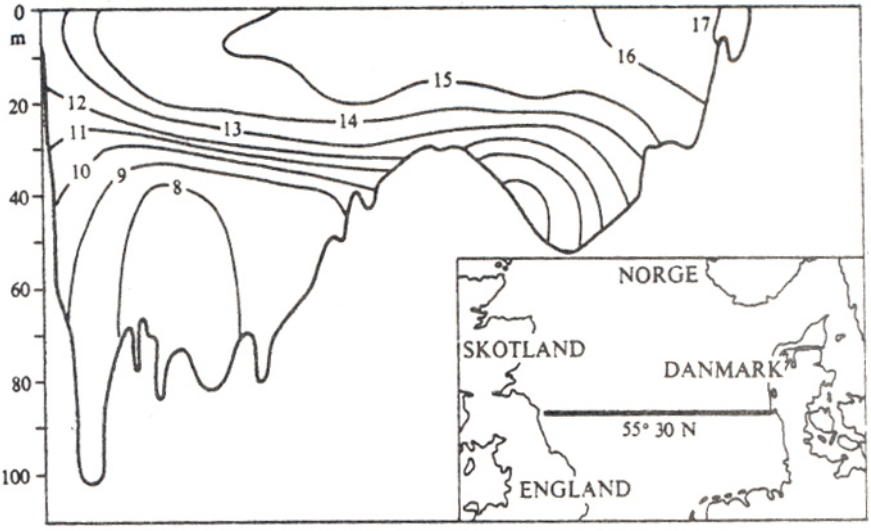

Fig. 7.18. Sea temperature in August in a vertical section from England to Denmark.

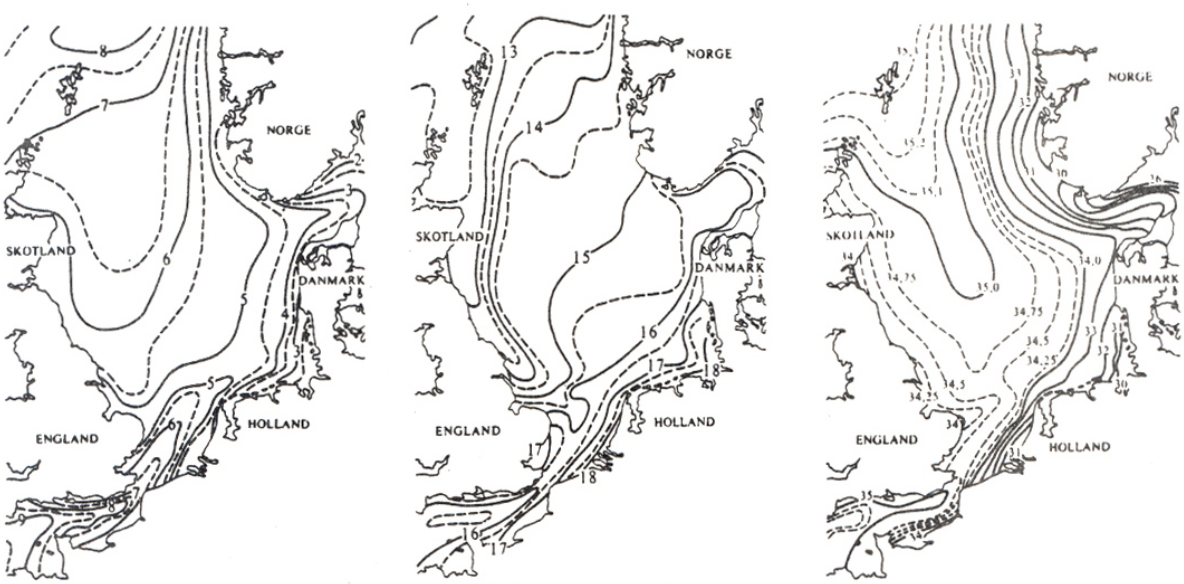

Fig. 7.19. (Left) Mean surface temperature of the North Sea in February.
(Middle) Mean surface temperature in August.
(Right) Mean surface salinity in June.

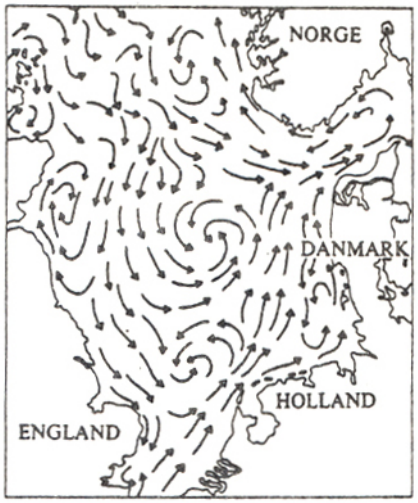

Fig. 7.20. Average pattern of surface currents in the North Sea.

North of Shetland a branch of Atlantic water seems to be entering the North Sea (Fig. 7.11, 7.19 and 7.20) and moving south along the outside of the Norwegian Coastal Current. Fig. 7.20 should be observed with a certain amount of scepticism, but what is correct is that the North Sea has many great and small vortices, and some of them are more stationary than others.

Barents Sea

The Barents Sea, like the North Sea, lies on the continental shelf, but the average depth is somewhat deeper - 150 m. The Barents Sea can be seen as a mixing area between warm and nutrient-poor Atlantic water and cold but nutrient-rich Arctic water (Fig. 7.19). In the transition zones between the two water types there are good conditions for plankton growth, and thus also for fish. The Barents Sea is the growing grounds for the Norwegian pelagic cod.

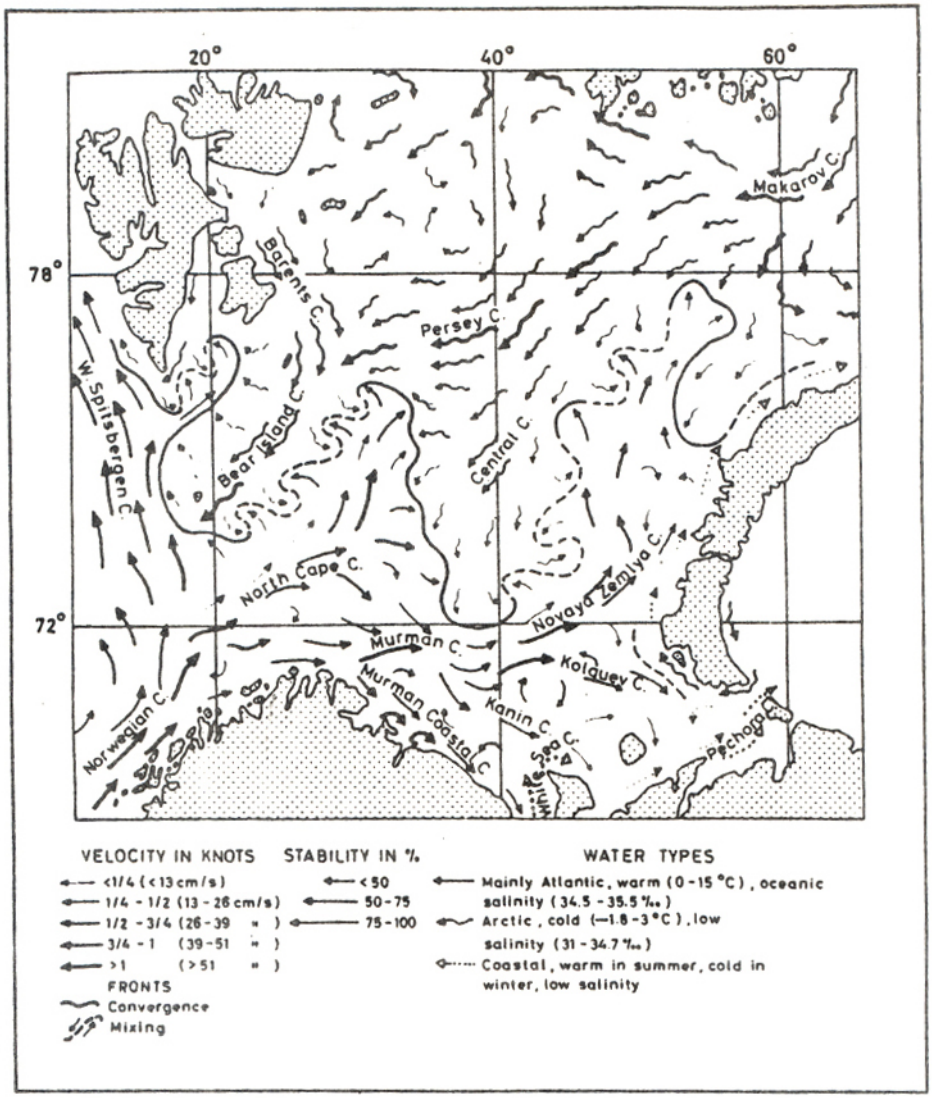

Fig. 7.21

The North Cape Current and the Norwegian Coastal Current will gradually become the *Murman Current* and the *Murman Coastal Current* (Fig. 7.21). The first of these will later on turn northwards and follow the west coast of Novaya Zemlya as the *Novaya Zemlya Current*. The cold and less saline *Bear Island Current*, *Persey Current* and *Central Current* come

down from the Arctic Sea, and in the zones where they butt against the warmer Atlantic water, numerous irregular vortices are created (Fig. 7.21).

Arctic Sea

Large parts of the Arctic Sea are covered with ice. This will slow down the surface currents, which may have speeds up to 4 cm s^{-1} (=1200 km/year). This is also why it took "Fram" 3 years to move from the New Siberian Islands to Spitsbergen (3000 km).
The Arctic Sea receives large amounts of freshwater from Siberia and Alaska. This surplus of volume is carried out by the Labrador Current west of Greenland and by the East Greenland Current between Greenland and Svalbard (Fig. 7.20, Table 7.2). There are three characteristic water types in the Arctic Sea:

Arctic Sea and North Atlantic adjacent seas, bathymetry and surface currents.

Fig. 7.22

- Polar or Arctic water (0-200 m), which is a mixture between the freshwater and the underlying more saline waters, clockwise circulation, $T < 0°C$, $S < 34.0$,
- Atlantic water (200-900 m), a continuation of the submerged West Spitsbergen Current, anticlockwise circulation, $T > 0°C$, $S > 34.8$,
- Deep and bottom water (900 m - bottom), from the deep waters in the gyres north and south of Jan Mayen, $T < 0°C$, $S = 34.90$-34.99.

Table 7.4. *Water Budget of the Arctic Ocean (average values)*

IN		**OUT**	
From Atlantic	3.5 Sv	East Greenland Current	3.7 Sv
From Pacific	1 Sv	Through Canadian Archipelago	0.9 Sv
From rivers and precipitation	0.1 Sv		

7.3 Upwelling

In Chapter 6.6, it was explained that when the wind in the northern hemisphere blows along a coast with land on its left, then water from the deeper layers will be brought up to the surface near the coast. In the southern hemisphere the same with happen when land is to the right of the wind. If we return to Fig. 7.1 and 7.2 and search for areas with strong winds that fulfil these criteria, we find that the trade winds on the west coast of the continents stand out. These coincide with the upwelling areas in Fig. 7.23, which are marked with dots. The Canary and Benguela currents in the Atlantic Ocean, the California and Humboldt currents in the Pacific Ocean and the West Australian Current in the Indian Ocean are all examples of west coast currents with upwelling of colder water from the deeper layers near land. An exception is the east coast upwelling inside the Somali Current, but this is not found the entire year, only in the period of the Southwest Monsoon. The upwelling inside the West Australian Current also only takes place during this period, but the other examples mentioned can be observed all year round.

In these examples of upwelling on a large scale, the cold water comes from depths typically between 100-200 m (Fig. 7.24). Upwelling can also take place on smaller scales, like for example in the Oslofjord during summer, where we notice how winds from the north can lead to clearer but also colder water. This water may be coming up from a depth of 5-10 m.

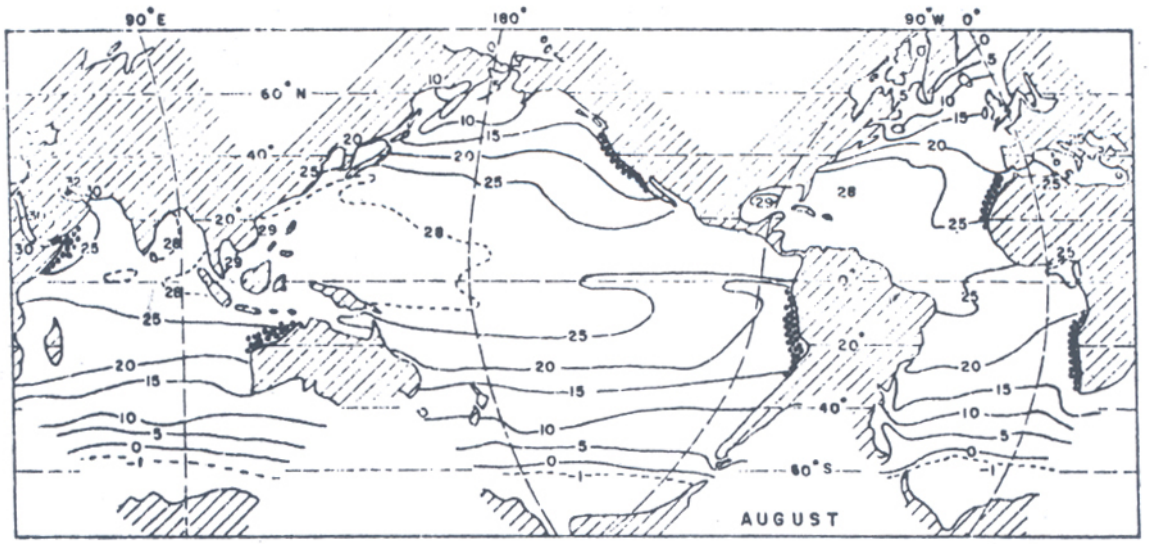

Fig. 7.23

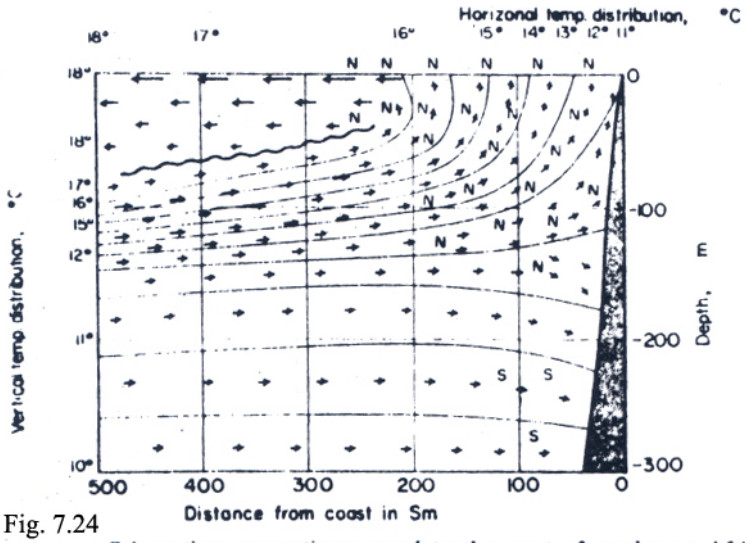

Fig. 7.24

Schematic cross-section normal to the coast of south-west Africa. *Full lines*, isopycnals; *arrows*, zonal and vertical velocity components (the length of the arrows can be taken approximately as a measure of the speed); *letters*, meridional velocity components and in special; *N*, parallel to the coast towards north; *S*, parallel to the coast towards south (the size of the letters can be taken approximately as a measure of the speed); *wavy lines*, axis of the vertical current vortex (vertical exaggeration 1:2300).

At intervals of a few years comes a type of natural catastrophe outside of Peru called *El Niño*. The name, Spanish for "the little boy", refers to the Christ child, since this phenomenon often has been noticed around Christmas time, but it may also start between January and April. It is caused by changes in the wind conditions that lead to the cold water in the Peru Current being replaced by warmer water. The result is that the fish disappears, seabirds die, rainfalls

increase and floods cause heavy regional damage. The opposite anomaly - an excess of cold water in the surface layer - is called *La Niña*. The Atlantic tropical cyclone activity usually increases during a La Niña event.

7.4 Vertical Circulation

We have now looked at the horizontal circulation in the top layer, namely the surface currents, as well as the vertical circulation called upwelling within the same layer. However, there are also horizontal circulations in the deeper layers as well as vertical circulations extending from the surface to the ocean bottom.

Earlier, it was believed that the currents in the deeper layers and near the bottom were weak, although rather constant in their direction and speed. However, as more observations have become available, it seems that these currents can have speeds at least up to 50 cm s^{-1}, and that they can be just as variable as the surface currents.

We shall just take a brief look at some examples of the vertical circulation. It was mentioned in Chapter 5.3 that deep and bottom water could only be formed in areas where the thermocline is little developed, and such areas are found at higher latitudes. In an idealized picture of the vertical circulation, there will go a net transport on the surface from the equator to the poles, where water will sink to the deeper layers and to the ocean bottom, and then there will be a current in the deeper layers from the poles to the equator while water diffuses from this current and back up to the surface currents again. The topography of the world ocean and the local climates make this picture considerably more complicated.

In Fig. 7.25 a schematized picture of the surface currents and the vertical circulation in the Atlantic Ocean is shown. In the Weddel Sea the heavy water sinks down the slope from the continental shelf and constitutes the bottom water (T = -0.5°C, S = 34.6) in the western Atlantic trough. The Walvis Ridge acts as a block for this bottom water in the eastern trough. South of Greenland, the winter-cooled saline Atlantic water sinks down and forms the deep water, which lies above the bottom water.

In the Norwegian Sea there are no typical differences between the deep and bottom water. North of Jan Mayen the East Greenland Current and the Spitsbergen Current create a cyclonic gyre. In the winter, the constant freezing of ice and cooling at the surface makes this water so saline (S = 34.92) and cold (T < -1°C) that it sinks and forms the deep and bottom waters of the Norwegian Sea.

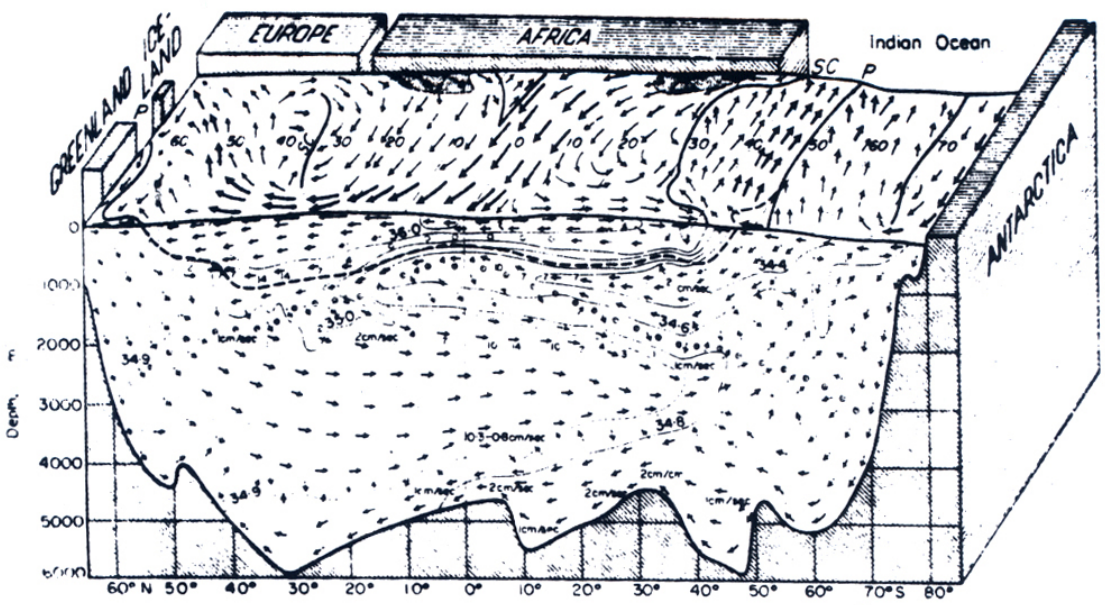

Schematic block-diagram of the surface currents and of the deep sea circulation of the Atlantic Ocean (according to Wüst).

Fig. 7.25

8 WAVES

8.1 Generation of Waves

When the wind scratches a still ocean surface, it creates ripples and small waves (wavelets), and as the wind friction continues to work on the surface these waves will grow. As a rule, the wind is uneven and turbulent, and therefore it creates small waves of many different sizes. After awhile the wavelets become bigger waves, which have a longer lifespan than do the small. At the same time new small waves are being created. The mechanisms behind the creation of waves are complex and not completely understood, but the wind's turbulent character is of essential importance. In an area that is being influenced by strong wind systems the waves will appear chaotic and without order. An example of a topographic picture of the ocean surface is shown in Fig. 8.1.

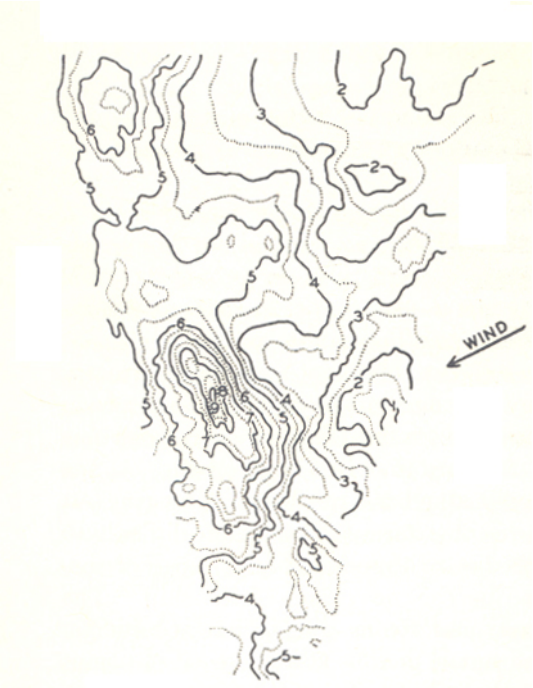

Topography of the sea surface derived from stereophotogrammetric pictures of the sea surface taken on board the *Meteor* on January 23, 1926, in lat. 59°S, long. 63°4′W. The state of the sea was recorded as 6, waves as advancing from WSW, wind WSW 7 (Beaufort).

Fig. 8.1

In order to make sense of this chaotic phenomenon, we need to analyze the *wind waves*, which are made up of many smaller waves. One then uses spectral analysis in order to separate the most important components, which are the ones containing the greatest energies. Statistical methods are necessary for describing a chaotic wave area. Often the sea state is characterized by the *significant wave height*, defined as the average height of the highest third

of the waves. The maximum wave height is often much higher than this and is the result of coincidental meetings (interference) between high waves. The significant wave height in an area will depend on: (1) the force of the wind (*speed*); (2) the time the wind has been blowing (*duration*); and (3) the length of the area the wind is blowing over (*fetch*). There are methods for making wave forecasts based on the observed and predicted wind fields. Wave forecasts of this kind are given out regularly by the Meteorological Institute.

When the wind dies out, or the waves move out of the wind field, the lesser waves will quickly calm down and the sea will become more orderly. The big and long waves that remain, and which can propagate a long distance away from the wind field, are called *swells*. For example, with a wavelength of 200 m the swell will move at an effective speed (group velocity) of almost 10 m s^{-1} (20 knots), and it will often hit land before the storm centre that has created it.

8.2 Wave Theory

In order to understand waves better, we shall simplify the phenomenon. We will look at simple, orderly waves (swells can often be close to this), and choose to investigate a wave that moves in direction x with a constant speed and with a cosine form (*harmonic wave*). For the vertical coordinate ζ of the surface we can write

$$\zeta = A\cos\left(\frac{2\pi}{L}x - \frac{2\pi}{T}t\right) \ . \tag{8.1}$$

Here x is the horizontal coordinate along the direction of the wave, and t is the time. A is the *amplitude*, and the *wave height* H - the distance between bottom of wave trough and top of wave crest - is $H = 2A$. At a particular place (x = constant) $\zeta(t)$ will vary periodically. There will go an amount of time T between each time there is a wave top at that place. T is called the period. At a particular time (t = constant) the surface $\zeta(x)$ will have a cosine form and a distance L between each wave top. L is then called the *wavelength*. The wave shape will move in the x direction with the velocity

$$c = \frac{L}{T} \ . \tag{8.2}$$

This is the speed of propagation or phase velocity. The movement of the individual water particles is completely different. In order to calculate their movement, one needs to use the hydrodynamic equations of motion and the equation of continuity. Under the simplifying assumption that the amplitude is small compared to the wavelength, it is relatively easy to solve these equations, and it is found that the phase velocity is related to the water depth *h* by the general equation

$$c = \sqrt{\frac{g\,L}{2\pi}\tanh\left(\frac{2\pi h}{L}\right)}, \tag{8.3}$$

where *g* is the gravity force. For waves where the ratio between wavelength *L* and depth *h* lies in the interval from 2 to 20, the particles will move in ellipses with a long horizontal axis.

If $L/h < 2$, the waves are called *short waves* or *deep-water waves*, and equation (8.3) can be simplified to

$$c = \sqrt{\frac{g\,L}{2\pi}} = 1.25\ [\mathrm{m}^{0.5}\ \mathrm{s}^{-1}]\sqrt{L} = 1.56[\mathrm{m\ s}^{-2}]\ T \tag{8.4}$$

Wind waves at open sea, such as we have looked at so far, often have a wavelength that is short compared to the bottom depth. When this is the case, the water particles will move in circles with a radius that decreases exponentially with increasing depth. At the surface the radius is the same as the amplitude of the wave. In Fig. 8.2 the unbroken line connects a number of particles on the surface at a certain time. The dotted line shows their position a moment later. The particles at the top of the wave move in the direction of the wave, in the trough they move in the opposite direction.

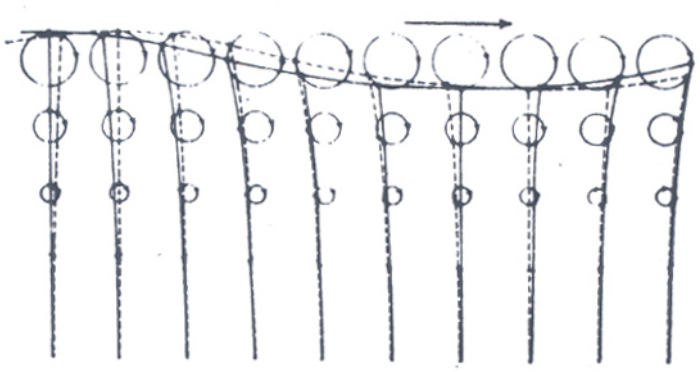

Fig. 8.2

The ratio between the particle speed and the wave speed is:

$$\frac{2\pi A}{T} : \frac{L}{T} = \frac{2\pi A}{L} \tag{8.5}$$

This ratio is seldom greater than 1/10. The impression that an observer may have at a beach, namely that the water of the wave is rolling towards him at great speed, is therefore just an illusion. It is the wave shape that is moving quickly, the water is moving considerably slower and in a circle (Fig. 8.2).

Equations (8.3) and (8.4) show that the phase velocity increases with the wavelength. Therefore, when waves from a storm area, where the sea is made up of waves with many different wavelengths, propagates out of the area as swells, the longest swell will hit land first.

When the ratio $L/h > 20$, equation (8.3) can be approximated by Lagrange's simple formula for the phase velocity of *long waves* or *shallow water waves*:

$$c = \sqrt{gh} = 3.15\sqrt{h} \quad [\mathrm{m^{0.5}\ s^{-1}}] \quad . \tag{8.6}$$

In this case the speed of the wave is not dependent on the wavelength but on the depth. For example, if $h = 100$ then $c = 31.5$ m s^{-1}. At great ocean depths we find great speeds. For example, if $h = 4000$ m then $c = 200$ m s^{-1}. In long waves the particle orbits are neither circles nor ellipses but straight horizontal lines; the particles are moving back and forth, and the orbits are the same from top to bottom of the water column.

It should be noted that while the *shape* of the wave propagates with the phase velocity, the *energy* of the wave propagates with the so-called *group velocity*. For long waves the group velocity c_g is identical with the phase velocity c, but for short waves the group velocity is related to the phase velocity by $c_g = 0.5\ c$.

The most important of the long waves may be the *tidal wave*, which we will get back to in the next chapter. An example of a more dangerous long wave is the so-called *tsunami* that originates with earthquakes. This happened, for example, on April 1, 1946, with an earthquake in the Aleutian Islands of Alaska. It took the wave 4 hours to reach Hawaii, corresponding to a wave speed of 220 m s^{-1} (800 km hr-1). According to equation (8.5) the average sea depth should then be 4900 m, which is similar to the observed depth. It was observed that the wave had a period of 15 minutes, which makes the wavelength 200 km. At open sea, with such a long wavelength, it must have been almost unnoticeable. However, in

more shallow waters it towered and wreaked havoc on Hawaii. A far more disastrous tsunami occurred in the Indian Ocean on December 26, 2004. After the catastrophe an international network for detection and warning of tsunamis has been organized.

Wind waves and swells that come closer to land and into shallower waters will gradually become long waves, and in accordance with the equation (8.6) the speed will decrease when the depth decreases. When a long wave goes over a slanting ocean floor, the speed of the wave crest will decrease towards the shallower areas. Since the period is the same along the wave crest, the wavelength must also decrease towards shallower waters, making the crest steeper. As the wave propagates along the coast, the direction of the wave will be deflected more and more towards land (Fig. 8.3), until the front is parallel with the bottom contours. This deflection is predicted by the general wave theory stating that waves will be refracted towards the areas of minimum wave speed.

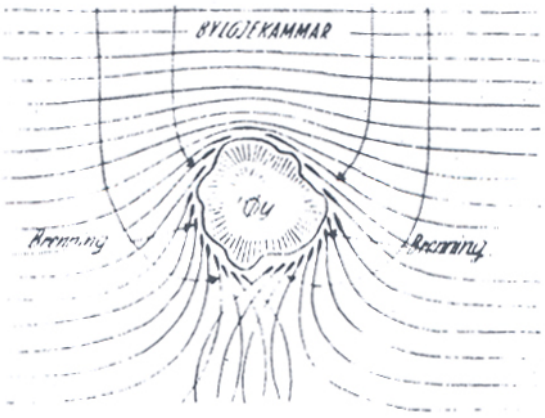

Fig. 8.3

When the water becomes very shallow, then the difference between the depth in the wave crest and wave trough becomes noticeable. The top of the wave will travel faster than the bottom of the wave, the wave crest will continually become steeper, and finally the wave will break. We get breakers or surf. If the bottom topography is known, then we can calculate the generation of the breakers. These types of calculations are done routinely in countries that have problems with big breakers. With the help of the bottom contours and weather forecasts, one can calculate where the waves will hit the hardest and give out the necessary warnings.

8.3 Wave Observations

The visual observation of waves is very unreliable, especially from boats, because boats do not always stand horizontally (Fig. 8.4). This is especially true of wave height, while the period can be measured more easily as long as the sea is not too chaotic. If the water is not too deep, one can measure the wave height as a function of time by mounting pressure sensors at the sea bottom. Otherwise one can use accelerometers that measure the vertical acceleration of the wave. These instruments can be mounted on a boat, or an anchored buoy, where the recordings are sent via radio to a computer on land. The wave height is then found by integrating the acceleration two times along the time axis.

Fig. 8.4

8.4 Internal Waves

When we discuss waves, we normally mean surface waves. However, there is also a different type of waves that occurs in water masses where density varies with depth. These waves are called *internal waves* because the amplitude is greatest where the density varies the most, for example at the interface between brackish surface water and seawater, while the amplitude will be quite small at the surface. In contrast, surface waves had maximum amplitude at the surface. Internal waves can be of both the short and long wave type. In both cases it is characteristic that they travel much more slowly than surface waves.

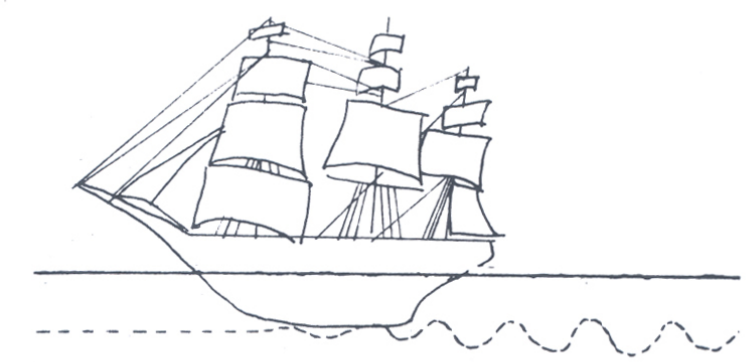

Fig. 8.5. The dashed line is the interface between brackish and saline waters.

Long ago, big sailboats could experience this phenomenon when they sailed with weak wind in brackish water in a fjord or outside large river mouths. If the keel of the boat reached down to the *pycnocline* (the transition layer between brackish and more saline water), this could create large internal waves. The energy for these waves came from the movement of the boat, and there appeared to be an invisible force holding back the boat. The phenomenon was called *dead water*. Only when the boat was able to go faster than the speed of these internal waves could the boat pull itself free.

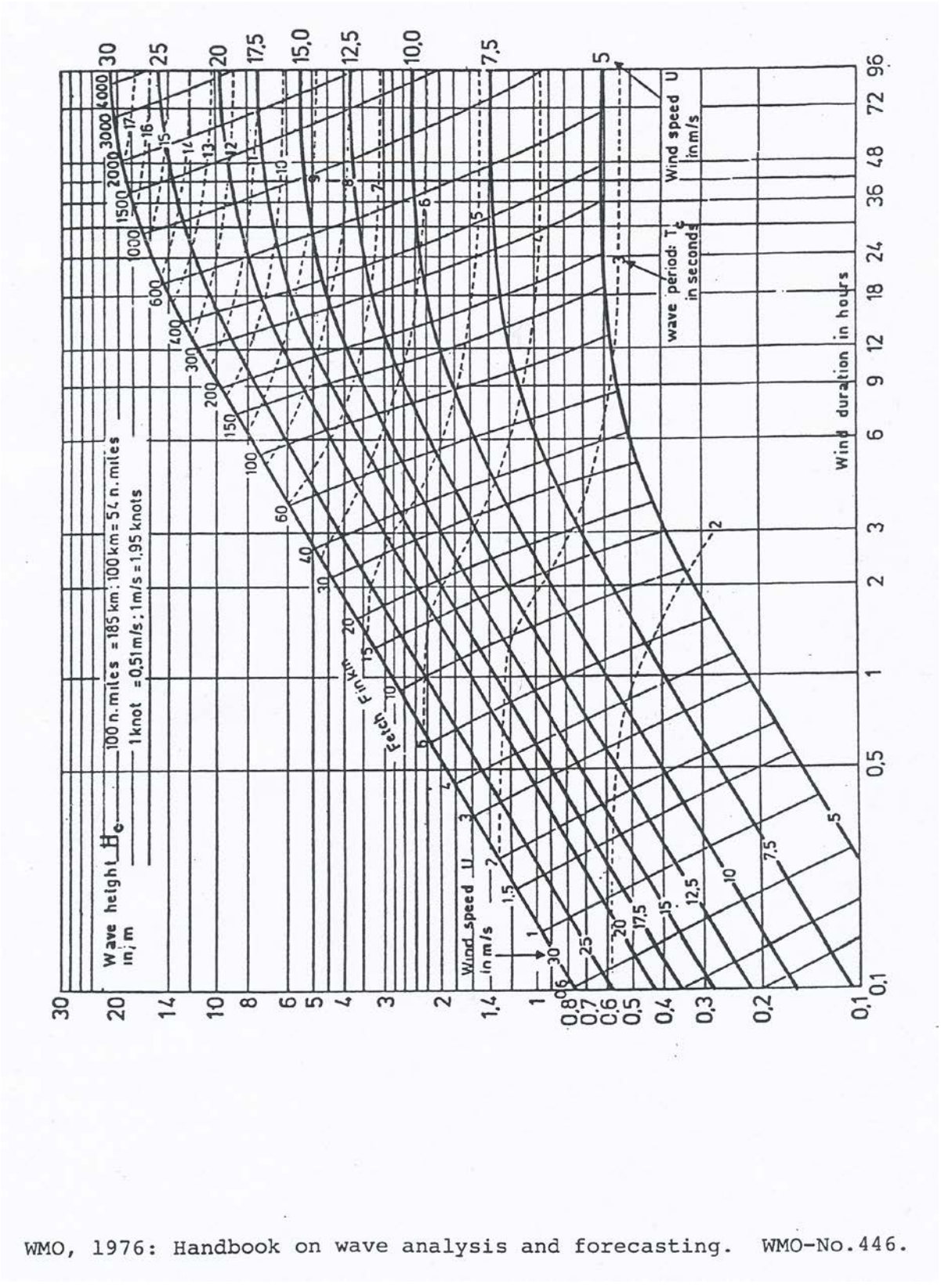

WMO, 1976: Handbook on wave analysis and forecasting. WMO-No.446.

9 TIDES

9.1 Tidal Force

The tides are the most powerful of all wave movements in the sea. There can be thousands of kilometres between the crest and trough of the wave. The period is also very long, normally about 12 hours but in some places 25 hours. The phenomenon has been known about and studied since the beginning of time. Innumerable attempts have been made to describe and explain the phenomenon. The periodic change between high tide and low tide is obvious to anyone, and that the tides are controlled by cosmic powers seems to be evident. The normal period of 12 hours and 25 minutes, which is half a moon day (the time between two following moon culminations), shows that the tides is more dominated by the moon than by anything else. Nevertheless, it is also clear that the sun plays a role as well because the magnitude of the tide varies with the phases of the moon, that is with the relative positions of moon and sun. When the two celestial bodies are in a straight line with the earth, at full and new moon, the tide is at its highest, *spring tide*. One week later when we have a half moon and the tide is at its lowest, *neap tide*. It was impossible to come up with a reasonable explanation for the tides before the laws of mechanics and the laws of the movements of the planets were known. It was Newton who found the principally correct explanation.

In order to simplify the problem, we will first only look at the system of the moon and the earth and their interactive movements. The moon exercises an attraction force (gravitation) on every water particle in the ocean. According to Newton's law of gravitation this force is inversely proportional to the square of the distance from the moon. The force is then at its greatest at the point that lies directly under the moon (zenith) and least at the point that lies the furthest from the moon (nadir). At these two points the force is directed along the line of connection between the centres of the moon and earth. If the earth had stood still in space, then the gravitational force would be the only effect creating a tide. However, in the earth-moon system, both celestial bodies move around a common central point of mass, which in this system lies inside the earth. Now Newton's second law on the simple form $\vec{k} = m\vec{a}$ is valid only in a coordinate system that is in rest relative to space, while we are primarily interested in the water's movement relative to a coordinate system fixed to the earth. Still we can use Newton's second law for this motion if we introduce an *inertial force* - the centrifugal force - generated by the acceleration of the earth's centre around the common central point of mass, and with a direction opposite to the acceleration of the earth centre. This centrifugal force is balancing the moon's gravitational pull in the earth centre, but while this gravitational

pull varies for each mass point of the earth, the centrifugal force due to the movement of the earth centre remains constant. The difference between the vector of the gravitational pull and the vector of the centrifugal force is what we call the *tidal force*. Fig. 9.1

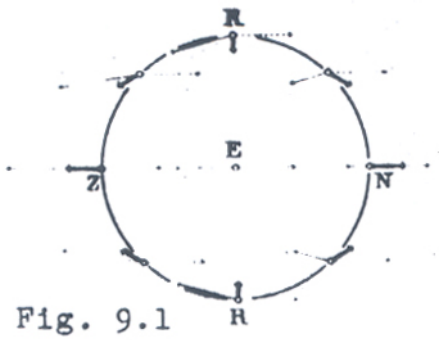

Fig. 9.1

In Fig. 9.1 the thin arrows are the moon's gravitational pull and the dotted arrows are the centrifugal force. The thick arrows describe the resulting tidal force. The moon is standing directly over point *Z* (zenith). The figure exaggerates the angles between the gravitational pull and the centrifugal force. In reality these angles never exceed 1°. The pull in *Z* is 3 % greater than the centrifugal force and in *N* (nadir) 3 % less. That means that the tidal force in reality is only 3 % of what it would have been if the earth's centre had stood still in space. We should be happy about this; anything else would have meant very uncomfortable consequences for us.

In Fig. 9.1 we see that the tidal force is pointed perpendicularly out and away from the earth in both Z and N. In the points *R* and on a circle between these points right between *Z* and *N* the tidal force is pointing perpendicularly inwards. All other places have a horizontal component.

9.2 Equilibrium Theory

Newton asked himself the following question: If the whole earth were covered by ocean, what would the ocean surface have to look like in order to have equilibrium between the earth's gravity and the tidal force? This can also be formulated such that we try to shape the ocean surface so that the resultant of the above-mentioned forces stands perpendicular to the surface everywhere.

However, gravity is so powerful (about 10 million times greater than the tidal force) that it only takes a very small tilt of the ocean surface to make the component of the gravity

along the surface balance the corresponding component of the tidal force. The desired equilibrium surface will therefore differ little from the almost perfect spherical shape the oceans would have in the absence of tidal forces. Still this very small difference is responsible for the tides. Calculations show that the equilibrium surface will be an ellipsoid with the long axis pointing towards the moon. Deviations from the spherical shape vary between an elevation of 36 cm in zenith and nadir, and a sinking of 18 cm in a circle midway between these two points. So we have high tide both at the point that lies nearest the moon and at the point that lies furthest from the moon. This provides us with two high tides (and low tides) a day.

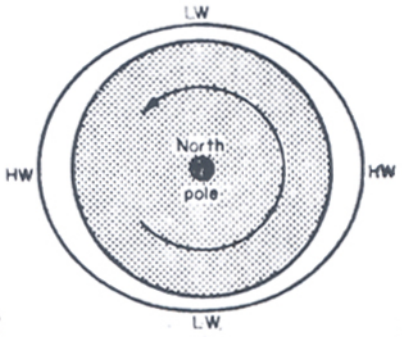

Fig. 9.2
The rotating earth in a water-jacket with high water (HW) and low water (LW).

Let us imagine, just to keep things simple, that the moon is positioned in the plane of the equator (the paper's plane in Fig. 9.2). Now let the earth rotate around its axis under the oval water profile. The water of course rotates along with the earth, but the form keeps its position with the long axis pointing towards the moon. If we are sitting on a little island in the high water on the left side of Fig. 9.2, then after about 12 hours we will be in the high water on the right, and after a little more than a whole day we will be back again in the high water on the left. In the meantime we have also had two low waters. The reason it will not be exactly 24 hours between the high waters on the left, is that while the earth had rotated the moon had also moved a little, so it will take 24 hours and 50 minutes in order to reach the high water on the left the second time.

Now the moon is in the equatorial plane only twice a month and this complicates things. When the long axis of the equilibrium ellipsoid lies tilted relative to the equator plane, then two high waters following one another will not be exactly the same (Fig. 9.3). This is

called the *diurnal inequality*. The angle δ (Fig. 9.3) between the position of the moon and the equator plane is called the *lunar declination*.

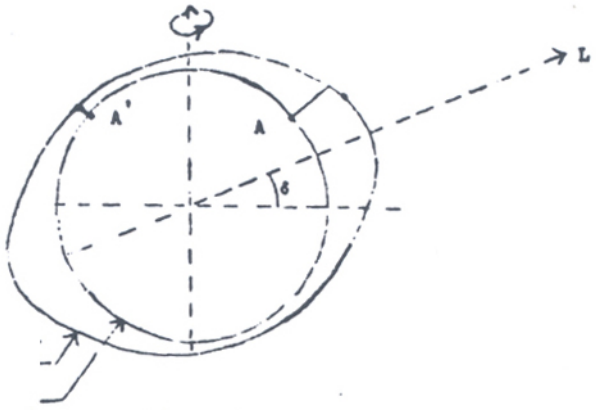

Fig. 9.3

Until now we have only looked at the earth-moon system, but the sun also plays a role. We can deal with the earth-sun system in the same way as we did for the moon and add up the effects. Despite the fact that the mass of the sun is 27 million times greater than the mass of the moon, the sun has less impact on the tides. This is because although the tidal force is proportional to the mass, it is also inversely proportional to the third power of the celestial body's distance from the earth, and the sun is 390 times further away from the earth than is the moon. It has also been shown that the tide is proportional to the magnitude of the tidal force. The ratio between the solar and lunar tides then becomes $27 \cdot 10^6/390^3 = 0.46$, meaning that the solar tide is less than half of the lunar tide. The combined tide is easily obtained by simply adding the two tides. According to the Equilibrium Theory we will then obtain maximum tidal effect (*spring tide*) when the long axes of the lunar and solar ellipsoids point in the same direction, or in other words when the sun and the moon lie in an almost straight line with the earth (- an almost straight line because the orbital planes of the sun and moon are at a 5° angle with one another). This occurs when the moon is new and full. If the two axes are standing perpendicular to one another, then the two tidal components will partly nullify one another and there will be minimum tidal effect (*neap tide*). This happens when we have a half moon. The phases of the moon have a period of 29.53 days, and during this period we have two springs and two neaps.

The tidal characteristics that have been mentioned - two high waters daily, diurnal inequality, spring and neap - can be explained both principally and qualitatively by the Equilibrium Theory. However, the real tides cannot be explained by this theory, precisely

because the theory is based on equilibrium. The tidal phenomenon results in a lot of water mass being moved, so we have tidal waves with accompanying tidal currents, and this is only possible if there is not equilibrium between the components of tidal force and gravity in the plane of the water surface. The tidal equations of motion have been set up by Laplace and are very complicated. This is due to the fact that the distances of the moon and sun from the earth vary, as well as their declinations. The phenomenon is complicated further by the varying topography of the ocean bottom and the irregular distribution of land and sea.

The tide may be predicted by advanced numerical models, but better predictions are obtained by a quasi-empirical method: We have to expand mathematically the tidal force into a long series of harmonic components (harmonic functions of the type $a_n \cos \sigma_n t + b_n \sin \sigma_n t$), and then assign a partial wave to each of these. For a specific place where we have observed

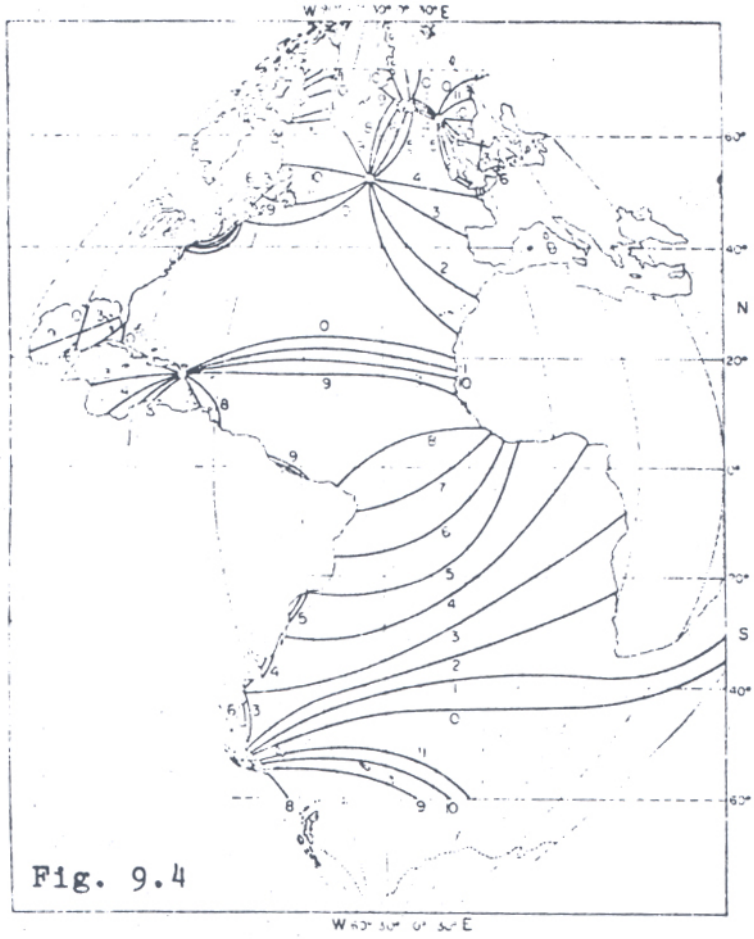

Co-tidal lines for the Atlantic Ocean for the semi-diurnal tides (M_2 and S_2 are together; referred to Greenwich) (STERNECK, 1920).

the tide over some time (preferably one year or more), we may separate and identify the partial waves that are present by *harmonic analysis*. The values of these can then be calculated and added together to predict the tide for whatever possible time in the future.

9.3 Presentation of Observed Tides

Observations of the tides usually come from the coast and ocean islands. How the tidal wave travels out in the open sea can only be calculated from what we know about the laws governing the tide. It is common practice to draw lines between places where the high tide occurs at the same time, these are called *cotidal lines*. Such a map for the Atlantic Ocean is given in Fig. 9.4. The numbers indicate the different hours (actually it is *moon hours*).

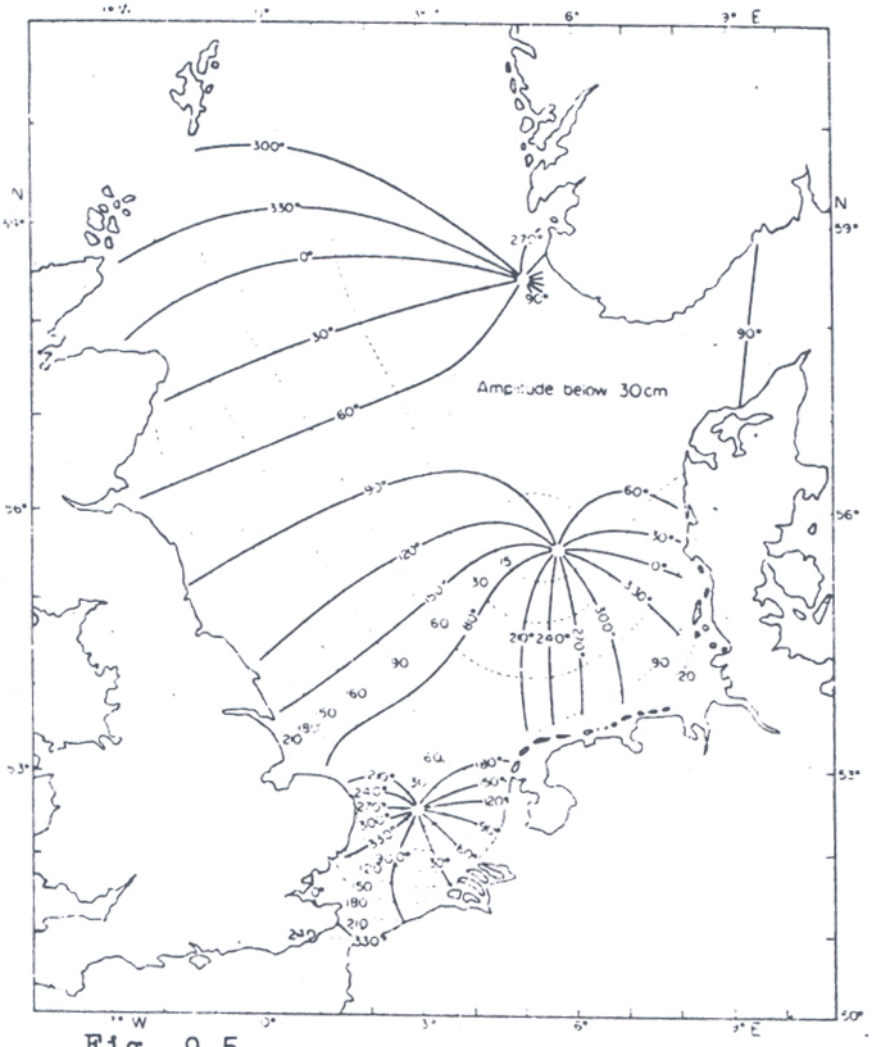

Fig. 9.5
Co-tidal lines (in degrees) and co-range lines (amplitudes in cm) of the M_2 tide in the North Sea (Proudman and Doodson).

The figure shows that the propagation of the tides is very irregular. This is not strange since we have a mixture of *forced waves* (the tides created directly by the tidal force), *free waves* (which run with the speed of $c = \sqrt{gh}$), *reflected waves* that create *standing waves*, etc. The influence of the Coriolis force on the horizontal movements is also involved. This force is responsible for the pattern we see in the middle of the North Atlantic (Fig. 9.4), where the cotidal lines come out from a centre point like the spokes of a wheel. The phenomenon is called *amphidromy*; the centre is called an *amphidromic point*. Fig. 9.5 shows the conditions in the North Sea, where the tides are dominated by such amphidromic systems.

Along the Norwegian coast the tide moves northward from Jæren like one free progressive wave, with an amplitude that increases from about a meter outside of Bergen up to 2-3 meters in Finnmark. Along the southern Norwegian coast, even the spring tides are under a half meter, in Oslo the spring tide is about 40 cm. The extremely large tidal amplitudes that one can find at some places in the world are due to resonance phenomena. A difference of 18 m at spring tide can be found in Fundy Bay between Nova Scotia and New Brunswick.

9.4 Tidal Types

We mentioned earlier that tides at a specific place can be described as a sum of oscillations with different amplitudes and phases:

$$\sum_n a_n \cos \sigma_n t + b_n \sin \sigma_n t$$

It is obvious that the results can be very different from place to place. Most often tides are *semidiurnal*, with half a day between the high tides. Some places (for example the Mexican Gulf) have *diurnal* tides, with an entire day between the high tides. And finally, there are also tides that are mixed, with a combination of both types. In Fig. 9.6 we see some observed tidal patterns from different places.

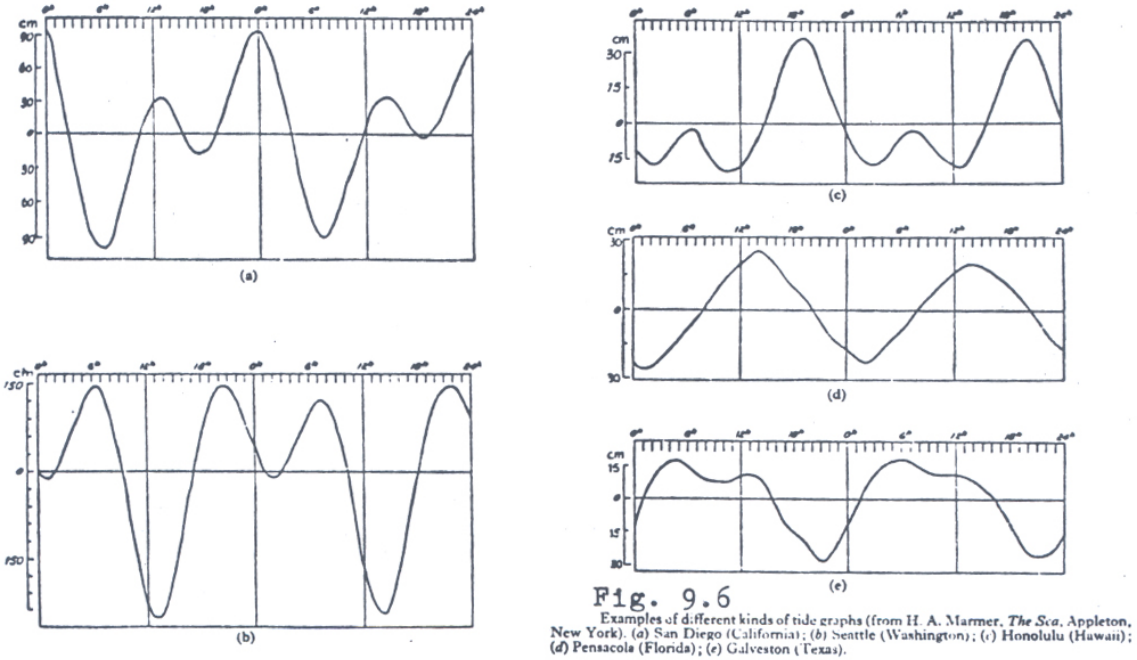

Fig. 9.6
Examples of different kinds of tide graphs (from H. A. Marmer, *The Sea*, Appleton, New York). (*a*) San Diego (California); (*b*) Seattle (Washington); (*c*) Honolulu (Hawaii); (*d*) Pensacola (Florida); (*e*) Galveston (Texas).

9.5 Tidal Currents

As mentioned earlier, the movements of the particles in long waves are for the most part horizontal. In narrow sounds and straits the tidal current will go approximately 6 hours each direction. Out in the open sea, the tidal current will normally not have only two directions but instead will gradually turn 360°. If one draws the velocity as an arrow from a fixed point, during the course of a tidal period the point of the arrow would in the ideal case describe an ellipse (the *tidal ellipse*). This is due to the earth's rotation. The presence of more than one tidal component will however complicate the picture.

10 FJORDS AND ESTUARIES

10.1 Characteristics of Estuaries and Fjords

The expression *estuary* is often loosely used to describe the outermost part of a river where the river water and the seawater meet one another. It is difficult to find a perfect and precise definition for our purposes, but we can use Cameron's definition: "An estuary is a half enclosed inlet, which has a free connection to the open sea, and where the seawater is clearly influenced by the freshwater from land." With such a wide definition, we find that we have many types of estuaries with different physical characteristics. In river mouths where the slant of the bottom out towards the sea and is gradual and small, we have the so-called *salt wedge* estuaries. Here the seawater penetrates up the river along the bottom like a wedge. The seawater often extends a long distance. The Mississippi River is a typical example where the salt wedge goes 20 km upstream. In the Glomma River the seawater also goes quite far up, and we find this phenomenon in some of our other big rivers. If the water movements are strong (for example due to tidal currents), we can get different degrees of mixing instead of the sharp separations observed in the salt wedge.

However, of special interest to us is the *fjord* type of estuaries. It is characterized by being comparatively deep and it stretches out longer than is normal for a river mouth. The fjords are found along the coasts at higher latitudes, both in the south and the north. They are found in Canady, Alaska, Greenland, Norway, Chile, New Zealand, etc. According to geologists they are primarily the result of glacial erosion. The majority of fjords have a deep basin and a shallower sill (however, some fjords do not have a sill, for example the fjords in Finnmark). Most of them also have fresh water supply from one or more rivers. The circulation in their surface layer will therefore have characteristics similar to those of the estuarine river mouths. A "real" estuary (river mouth) is simpler because it receives its freshwater from a concentrated source (a river), while fjords and other estuaries often receive their freshwater from many rivers. Both in fjords and other estuaries the fresh water, mixing with seawater, streams out in the surface layer, with a compensating current moving inwards in a deeper layer. In addition the fjords have deeper down a third layer of water with its own specific processes.

10.2 Seasonal Changes

Due to the geographical position, the run-off from rivers (in unregulated water systems) to most fjords is rather small during the winters. Instead the water is saved on land in

the form of ice or snow. The result is a typical seasonal variation with the top in the spring and early summer. This in turn provides seasonal variations in the hydrographical conditions of the surface layer (Fig. 10.1).

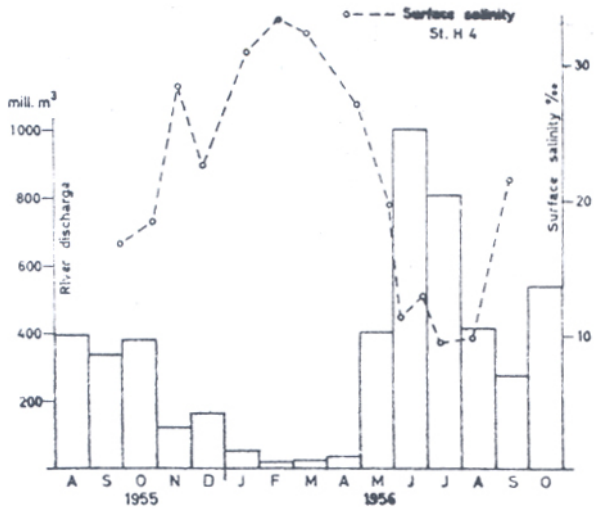

Discharge of Eio, Kinso, Opa, and Tysso Rivers into the innermost areas of Hardangerfjord, and surface salinity at station H4. Fig. 10.1

In the winter time, the effects of reduced freshwater run-off and lower temperatures combine to create a higher density and therefore reduced stability in the surface layer, which again results in vertical convection in some fjords. However, deep-reaching convection is only found in fjords with very severe climatic conditions. In the western Norwegian fjords convection, when it occurs, may reach down to a maximum of only 20 -30 meters.

In the summer we have a warm surface layer with a low salinity. The average salinity in the Hardangerfjord from August (Fig. 10.2) and February (Fig. 10.3) illustrates the difference between the two seasons. The typical estuarine condition is found in the summer. However, the top low salt content layer is not particularly thick and the structure varies.

10.3 Estuarine Circulation

The type of circulation which is normally called *estuarine circulation* is dependent on a noticeable freshwater supply. In the winter, this is almost completely nonexistent in many fjords. A simplified graph of the estuarine circulation is shown in Fig. 10.4. In principle it is a two-layer circulation but the border between the layers is not as sharp as in the salt wedge estuary. The freshwater supply streams out in the surface layer, continually mixing with more saline water from below, so that the surface salinity increases as the water moves outward. At

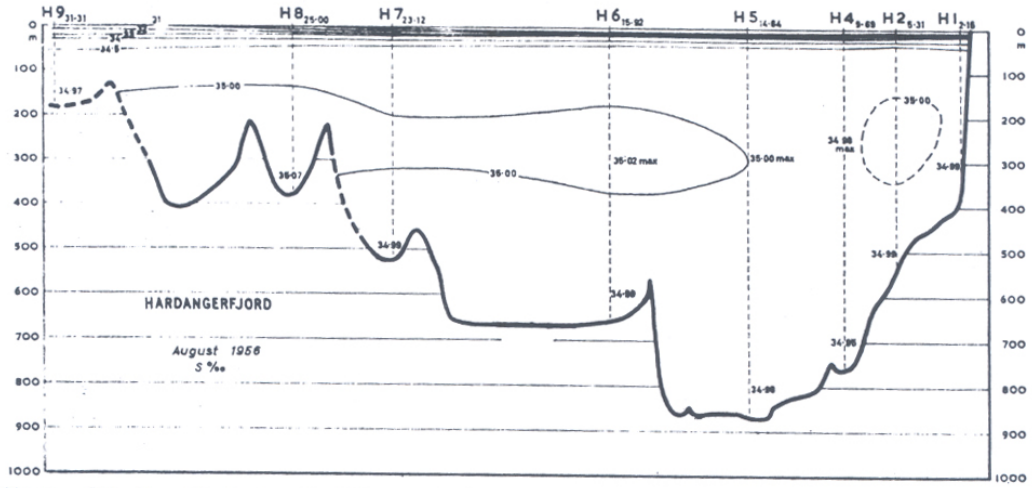

Fig. 10.2 Distribution of salinity in a longitudinal section of the Hardangerfjord, August, 1956.

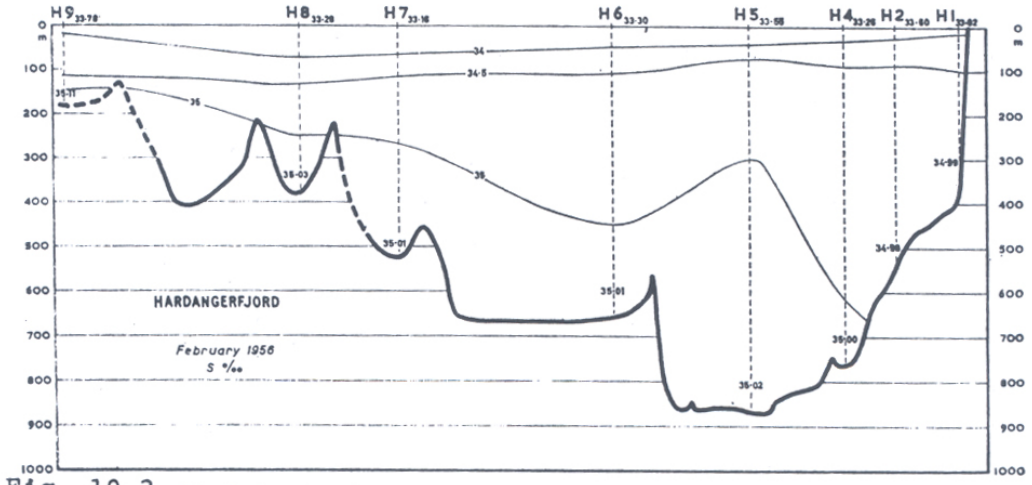

Fig. 10.3 Distribution of salinity in a longitudinal section of the Hardangerfjord, February, 1956.

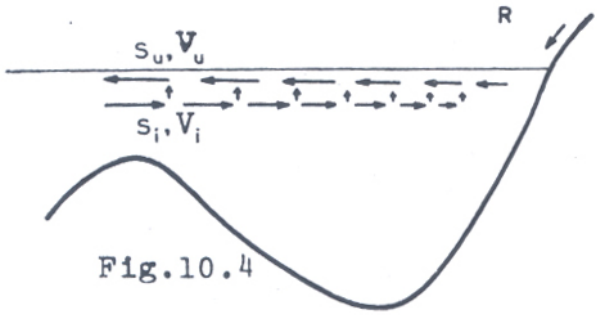

Fig.10.4

Upper fjord circulation, schematically.

the same time the volume transport increases. Continuity (or the volume budget) will require a compensation current moving inward under the outward moving layer, as well as a vertical transport from the lower to the upper current. This vertical transport is called *entrainment*. The surface current moving outwards is capturing and enclosing water from below.

As long as the conditions are stationary, it is possible to set up continuity conditions for volume and salt for the entire fjord in a random cross section (Fig. 10.4):

Volume budget: $V_o = V_i + R$

Salt budget: $V_o S_o = V_i S_i$

V_o is outward volume transport of water

V_i is inward volume transport of water

R is freshwater supply inside the cross section

S_o is salinity of water moving outwards in the cross section

S_i is salinity of water moving inwards in the cross section

It has been estimated here that $|P\text{-}E| \ll R$, or in other words that precipitation minus evaporation can be left out compared to the other terms.

From the equations above we obtain the so-called *Knudsen's relations*:

$$V_o = \frac{S_i R}{S_i - S_o} \qquad \textit{and} \qquad V_i = \frac{S_o R}{S_i - S_o}$$

Here it is always true that $S_i > S_o$. S_i will most likely not vary much along the direction of the fjord, but S_o will increase evenly outwards. This is clearly seen in Fig. 10.2 where the surface salinities are marked at the top. When S_o increases, V_o increases as well, and therefore the surface transport will increase outwards in the fjord. At the mouth of the fjord the transport can be many times larger than the freshwater supply. At station H8, which lies near the sill of the fjord, S_o=25, and by estimating S_i as 33 we obtain

$$V_o = \frac{33R}{33-25} \approx 4R \qquad \textit{and} \qquad V_i = V_o - R \approx 3R$$

As seen in Fig. 10.1, R was for the same month (August) $400 \cdot 10^6$ m^3 month^{-1}=150 m^3 s^{-1}. Then V_o becomes 600 m^3 s^{-1} and V_i=450 m^3 s^{-1}. As mentioned, this is a very simplified

method. Current systems can be more complicated than assumed here, and the tides can complicate the picture. The assumption of stationary conditions also needs to be checked. If necessary the equations should have a term added, taking into account the temporary changes of the salinity. For example, the salinity in a fjord will most certainly not remain constant during the first phase of melting snow in spring; it will decrease. However, later in the summer the salinity often becomes stationary (end of June until August), as shown by Fig. 10.1.

The processes we have discussed until now take place in the top layer of the fjord. There is reason to believe that the compensating current moving inwards lies quite closely under the outward moving current, although we must admit to having too few measurements of this in order to give an accurate depth.

10.4 Deeper Layers in the Fjord

It was earlier mentioned that deep-reaching convection (vertical exchange) could occur in fjords having extreme weather conditions. For most Norwegian fjords it is safe to say that the deeper layers have relatively little communication with the top layers and that they are more influenced by the depth of the sill and the characteristics of the waters outside the sill. In some fjords, especially those with very shallow sills, deep water may remain isolated for years. Oxygen is continually being used in the deep water, especially if there is a lot of organic material at the bottom. Finally a time may come when all oxygen has been consumed, and at that point hydrogen sulphide will begin to be produced. This destroys all life. Kaare M. Strøm published in 1936 an overview of all Norwegian fjords that were like this and called them land-*locked waters*. An extreme example of such waters is shown in Fig. 10.5, the small fjord Framvaren close to Lista. Here we have large amounts of H_2S from 20 m down to the bottom. The fjord is isolated from the sea by a series of very shallow sills. The stagnating condition within this fjord is due to natural causes and not to pollution.

However, in many other fjords, the *anoxic* conditions are the result of human activity with a great supply of organic materials. The Oslofjord is a classic example. This was earlier a clean fjord, with an interesting community of animals, especially in the deeper layers of Bunnefjorden. With increasing organic burden, from time to time hydrogen sulphide has been produced in the deeper layers, and then all life at the bottom and close to it is extinguished. In the Oslofjord there is often an annual exchange of deep water, so that

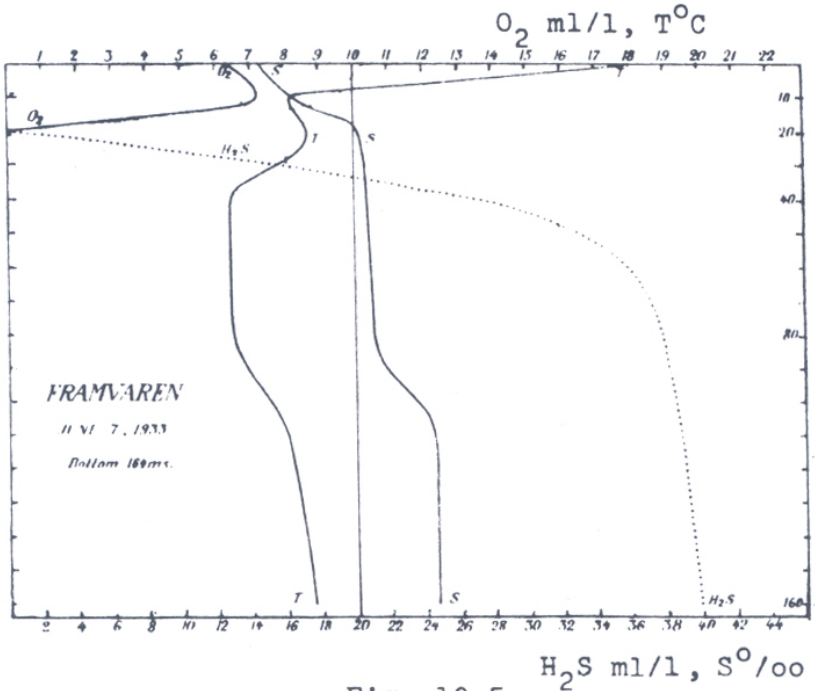

Fig. 10.5

Longitudinal section. March 30, 1951
Distribution of oxygen. ml/L.

Fig. 10.6

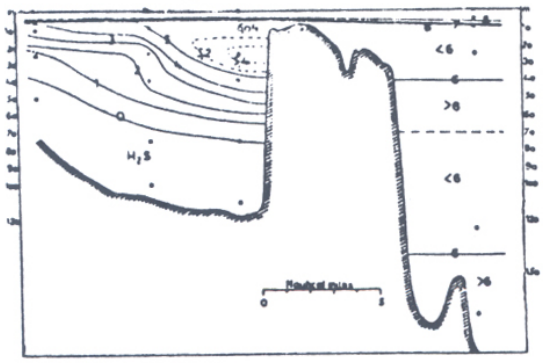

Longitudinal section. April 23 - 24, 1951.
Distribution of oxygen. ml/L.

Fig. 10.7

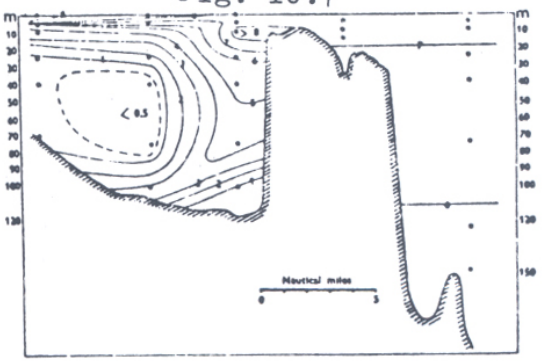

Longitudinal section. June 21 - 22, 1951.
Distribution of oxygen. ml/L.

Fig. 10.8

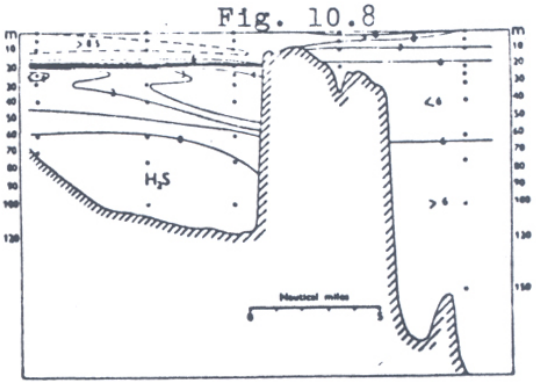

oxygen-rich water comes down to the deeper layers. However, the oxygen can be used up quickly due to the large organic burden.

The Drammensfjord is another example of an overly burdened fjord. Figs. 10.6-8 feature a series of vertical cross sections presenting the content of O2 and H_2S, and these show how quickly the rotting process can go. Within the sill (8 m depth) on March 30th (Fig. 10.6) there was H_2S below 80 m. At the next observation on April 23rd, an inflow of oxygen-rich water had obviously taken place and there was no longer any H_2S in the water (Fig. 10.7), only in the ground sediments. Two months later (Fig. 10.8) the sediments and the oxygen consumption have managed to fill the entire deep-water mass with H_2S again.

Still, such stagnating conditions are not normal in Norwegian fjords. Most of our fjords have a deep enough sill and are not overly polluted, so that the communication with the outside sea is enough to maintain a good level of oxygen. This occurs with a more or less regular inward moving transport across the sill. Such transports require that the outside water at sill depth is heavy enough, because if the water shall be able to sink down from the sill to the deeper parts of the fjord, then it should have a higher density than the water it is to replace. Such deep-water renewals can be recognized by sudden changes in the deep-water temperature or salinity, but often the increase of the oxygen content is the best indicator.

In Figs. 10.9-10.10 an example of deep-water renewal is offered by two temperature sections from the Hardangerfjord. The courses of the isotherms (especially the 6.5°C isotherm) give the striking impression that a colder water mass has pressed itself in along the bottom in the period between April and June.

The deep-water exchange in most Norwegian fjords seems to be closely related to the properties of the water mass outside the coast. Light coastal water lies in a wedge form over the heavier and more saline Atlantic water. The rising of this wedge may sometimes permit the heavier Atlantic water to rise enough so that it may flow over the sill and into the fjord (Fig. 10.11). In some cases it looks as if an annual pulsation of coastal water creates a parallel annual deep-water exchange. In other cases the renewals are less regular, and it seems that the wind may provide the final impulse to the deep-water inflow. This has been demonstrated in the Oslofjord, for example.

On average, the gradients of temperature and salinity are small in the deep water, both horizontally and vertically. The salinity will for the most part be determined by the depth of the sill. In the Norwegian fjords the salinity of the deep water will be approximately 35, as long as the sill is not too shallow. In the fjords of Alaska and British Columbia the salinity

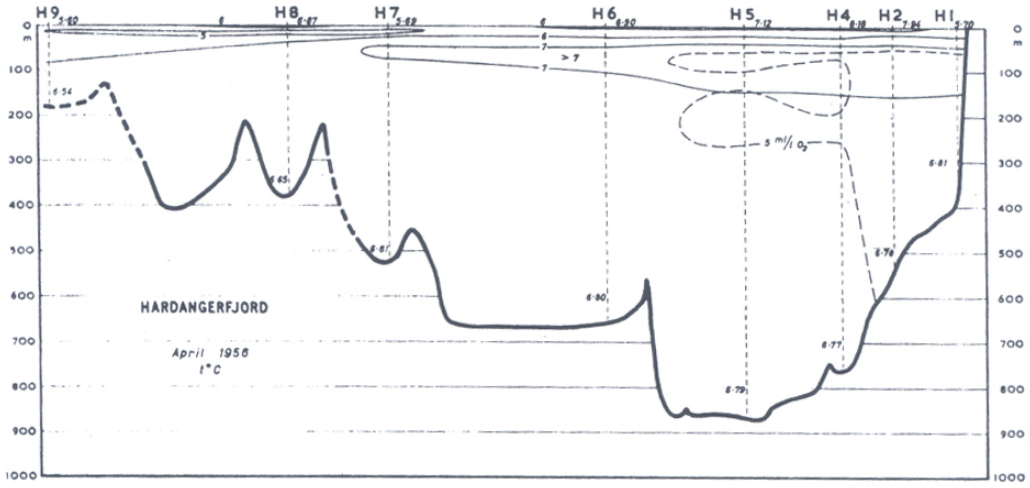

Fig. 10.9 Distribution of temperature in a longitudinal section of the Hardangerfjord, April 25, 1956.

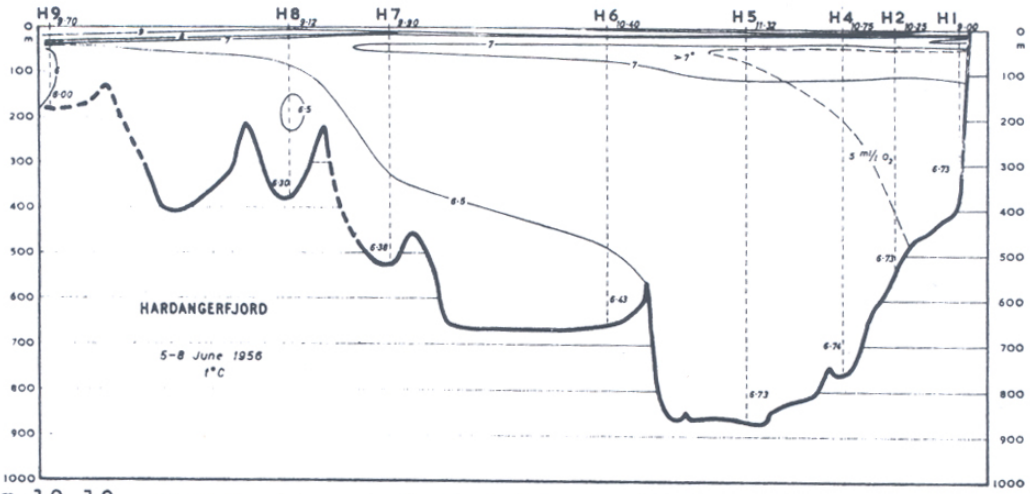

Fig.10.10 Distribution of temperature in a longitudinal section of the Hardangerfjord, June 6, 1956.

will be significantly lower (less than 34), as a direct consequence of the generally lower salinity of the Pacific Ocean.

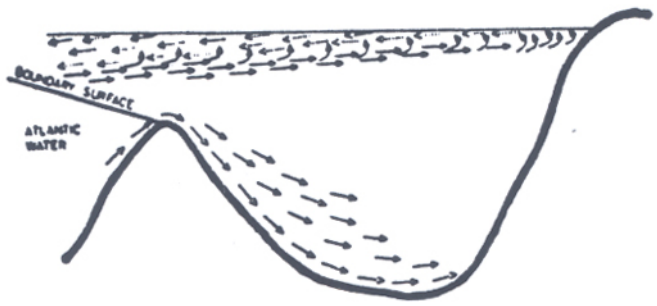

Fig. 10.11

REFERENCES

The figures in these lecture notes have been borrowed from the following sources:

Anikouchine & Sternberg: *The World Ocean*: Fig. 2.1-2, 3.1

Beyer: *Studies of a Threshold Fjord - Dramsford - in Southern Norway*: Fig. 10.6-8

Braaten & Sætre: *Oppdrett av laksefisk i norske kystfarvann. Miljø og anleggstyper*: Fig. 7.9, 10.11

Brun: *Ozeanologie*: Fig. 7.7-8

Defant: *Physical Oceanography*: Fig. 1.1a, 1.5-6, 3.7, 6.7, 7.24-25, 9.4-5

Dietrich et al.: *General Oceanography*: Fig. 3.8

Groen: *Waters of the Sea*: 9.2, 9.6

Helland: *Temperature and salinity variations in the upper layers at Ocean Weather Station M (66°N, 2°E)*: Fig. 7.10

Hermann: *Hydrografi.* I "Danmarks natur. Bind. 3. Havet": Fig.7.15-18

Hess: *Introduction to Theoretical Meteorology*: Fig. 6.5

Ingmanson & Wallace: *Oceanology: An Introduction*: Fig. 1.8

Jerlov: *Marine Optics*: Fig. 3.9

Lamb: *Climate: Present, Past and Future*: Fig. 7.1-2

Midttun: *Long term observation series of surface temperature and salinity in Norwegian coastal waters*: Fig. 7.12-13

Neumann & Pierson: *Principles of Physical Oceanography*: Fig.1.1b, 3.2-5, 3.9-13

Pettersen: *Introduction to Meteorology*: Fig. 4.1, 4.3, 7.3

Petterson: *Oceanografi*: Fig. 8.2, 9.1

Pickard: *Descriptive Physical Oceanography*: Fig. 1.4, 4.2, 5.1-4, 5.7-9, 7.4-5, 7.20-23

Stene & Dannevig: *Meteorologi og Oseanografi*: Fig. 8.4

Strøm: *Land-locked Waters*: Fig. 10.5

Sverdrup: *Havlære*: Fig. 1.2, 5.4, 6.8, 7.6, 8.3, 11.1

Sverdrup, Johnson & Fleming: *The Oceans*: Fig. 8.1

Sælen: *Some Features of the Hydrography of Norwegian Fjords*: Fig. 10.1-4, 10.9-10

Sætre & Ljøen: *The Norwegian Coastal Current*: Fig. 7.11, 7.14

Tantsyura: basis for Fig.7.19

Turekian: *Oceans*: Fig. 1.3, 1.7

Wüst: *Gesetzmässige Wechselbeziehungen zwischen Ozean und Atmosphäre*: Fig. 5.6